SERI/STR--211-3525

DE89 009436

Research on Amorphous Silicon-Germanium Alloys for Tandem Solar Cells

Annual Subcontract Report 1 September 1987—31 August 1988

W. Paul, Principal Investigator
Division of Applied Sciences
Harvard University
Cambridge, Massachusetts

June 1989

SERI Technical Monitor: B. Stafford

Prepared under Subcontract No. XB-7-06071-1

Solar Energy Research Institute
A Division of Midwest Research Institute
1617 Cole Boulevard
Golden, Colorado 80401-3393
Prepared for the
U.S. Department of Energy
Contract No. DE-AC02-83CH10093

NOTICE

Printed in the United States of America
Available from:
National Technical Information Service
U.S. Department of Commerce
5285 Port Royal Road
Springfield, VA 22161

Price: Microfiche A01
Printed Copy A07

Codes are used for pricing all publications. The code is determined by the number of pages in the publication. Information pertaining to the pricing codes can be found in the current issue of the following publications which are generally available in most libraries: *Energy Research Abstracts (ERA)*; *Government Reports Announcements* and Index (*GRA* and I); *Scientific and Technical Abstract Reports (STAR)*; and publication NTIS-PR-360 available from NTIS at the above address.

PREFACE

This report covers the second year of a two-year project to attempt to improve further the properties of amorphous silicon-germanium alloys for solar energy applications. In our report of the first year's operations, we explored the reasons for the inferior properties of the alloys compared with those of amorphous hydrogenated silicon (a-Si:H), and also the reasons why alloys prepared from fluoride gases instead of hydrides showed superior photoconductivity. Evidence from structural, electrical and optical measurements was assessed which concluded that the fundamental reasons for the deterioration and relative improvement lay in the structure of the films on a scale of the order of 100 Å.

The present year's work has carried this research further by first completing the study of a-$Si_{1-x}Ge_x$:H and a-$Si_{1-x}Ge_x$:H:F alloys. This has included more extensive structural examination by transmission electron microscopy (TEM), gas evolution (GE) and differential scanning calorimetry (DSC) and also a measurement of the dependence of the mobility-lifetime ($\mu\tau$) product for electrons in the two types of alloy. It has also included the completion, for the moment, of a project to deposit a-Si:H and its alloys by photo-CVD. which will also be described.

In the second part of the current period we have begun to concentrate on the end-component, a-Ge:H, of the a-$Si_{1-x}Ge_x$:H alloy series, operating under the philosophy that it would be best to understand the deposition conditions optimizing that end-component before choosing conditions to optimize an intermediate alloy. Therefore, the second part of this report will discuss experiments directed to that end, as well as discussing subsidiary collaborative projects.

The work performed at Harvard is a collaborative effort of postdoctoral fellows and graduate students. A list of group members is given below.

Professor William Paul

Professor Choochon Lee

Dr. Kenneth D. Mackenzie

Mr. Bruce Bateman - technical associate

Mr. Scott Jones - graduate student: gas evolution studies

Ms. Susanne Lee - graduate student: differential scanning calorimetry, transmission electron microscopy

Mr. Yuan-min Li - graduate student: optical measurements including photoconductivity

Mr. Warren Turner - graduate student: preparation of samples by glow discharge; optical and electrical measurements

Mr. Paul Wickboldt - graduate student; new methods of deposition of amorphous Si and Ge films.

SUMMARY

Objectives

The objectives of the second year of this study were (1) to carry out additional measurements on the structure of a-Si:H, a-Ge:H, a-$Si_{1-x}Ge_x$:H and a-$Si_{1-x}Ge_x$:H:F by DSC, TEM and GE, to complete measurements on the $\mu\tau$ product and to write up and publish a full archival account of this research; (2) to prepare films of a-Si:H and a-Ge:H by photo-CVD, and to find out if such films are comparable in properties to those of films prepared by conventional r.f. glow discharge; (3) to initiate a detailed study of a-Ge:H prepared by r.f. glow discharge, varying all relevant deposition parameters, so as to discover the parameter values optimizing this end-component of the a-$Si_{1-x}Ge_x$:H alloys series; (4) to continue a collaboration with Professor Richard Norberg of Washington University to prepare films of a-Si and a-Ge containing deuterium, so that the Norberg laboratory can study deuteron magnetic resonances, which may be interpreted to give information on the microstructure of films on a 100 Å scale; (5) to continue a collaboration with Dr. M.L. Theye of the Laboratoire d'Optique, University of Paris, to explore low photon energy absorption spectra determined either by photothermal deflection spectroscopy (PDS) or by steady-state photoconductivity (PC); (6) to continue a collaboration with Dr. K.L. Narasimhan of the Tata Institute, Bombay, India, to study the properties of Schottky barriers on amorphous hydrogenated SiGe alloys.

Discussion

These objectives have been met. The work on SiGe alloys has been published in an article in the Physical Review which is included here as Appendix A. The second objective, to prepare films by photo-CVD in a new apparatus which incorporated a windowless hydrogen discharge lamp, has been pursued, with the particular focus to discover whether, in this arrangement, the photo-excitation can be differentiated from other causes of deposition such

as d.c. glow discharge attributable to the lamp power. The study of a-Ge:H is now the central concern of this laboratory, and the initial experiments on optimization of deposition temperature and H_2 dilution will be reported in what follows. Films of a-Si:F,D, a-Si:H,D, a-Ge:H,D, and a-SiGe:F,D have been produced for the Norberg laboratory at Washington University according to their requirements, and the detailed results of deuteron magnetic resonance measurements performed there will be reported by them. Codeposited or identically-prepared films were characterized by us, not only through measurements of conductivity versus temperature, optical absorption edge and infrared vibrational absorption, but also by TEM, DSC and GE. The structural measurements are of particular importance as will be detailed below. We have continued to produce samples for our collaboration with Dr. M.L. Theye. This research has concentrated on the development, with Dr. Claude Boccara, of a new method designed to establish the source of the low photon energy absorption in PDS measurements, specifically whether it occurs at the front surface of the samples, in the sample bulk, or at the rear surface. Such studies have obvious importance for the discovery of poor surfaces and poor interfaces in device structures. Our collaboration with Dr. K.L. Narasimhan, which will be continued, has resulted in a paper accepted for publication in the Journal of Applied Physics, which is included here as Appendix B.

Conclusions

The work done at the beginning of this second year on the structure of films of a-$Si_{1-x}Ge_x$:H and a-$Si_{1-x}Ge_x$:H:F has confirmed our conclusions that microstructure on a scale of 100 Å is an important determinant of film properties. It is our view that an important ingredient in the improvement of certain photoelectronic properties when films are produced from fluorine-containing gases are the processes at the growth surface and the resultant film structure. This structure can also be modified by alteration of the proportions of SiH_4, GeH_4 and H_2. We have therefore added to the above-described objectives and experiments a study by combined DSC, TEM and GE measurements of differences in a-Si:H films produced with

and without dilution of the SiH_4 plasma by H_2, and correlation of these differences with differences in the photoelectronic properties. This study is also significant for our collaboration with the Norberg group since our deuterated a-Si films are usually produced from a plasma of (SiH_4 + D_2).

From our study of films of a-Si:H and a-Ge:H produced in our photo-CVD apparatus, we have concluded that a very significant proportion of the deposition is caused by d.c. glow discharge in the environs of the lamp. As a result, we have decided to build a modified apparatus to study "pure" photo-CVD by using an external ultraviolet lamp and suitable windows, but without the mercury sensitization currently being explored by the group at the Institute of Energy Conversion.

Finally, our collaborations with the French and Indian groups are proceeding systematically. While it is too early to report conclusions from our collaborative study on PDS, it can be said that the methods used should be capable of differentiating absorption at the front surface of samples of a-Si:H from absorption at the back interface with a substrate. Our collaborative effort on Schottky barriers has proceeded to the next stage of exploring potential barrier heights and band offsets.

TABLE OF CONTENTS

PREFACE iii

SUMMARY v

Objectives v

Discussion v

Conclusions vi

TABLE OF CONTENTS viii

LIST OF FIGURES ix

LIST OF TABLES xii

LIST OF APPENDICES xiii

I *Introduction* 1

II *Amorphous Si-Ge Alloys Produced by Glow Discharge from Hydrides and Fluorides of Si and Ge* 2

III *Production of a-Si:H and a-Ge:H by Photo-CVD* 4

IV *Amorphous Hydrogenated Germanium Prepared by R.F. Glow-Discharge* 6

V *Collaborative Research* 37

(1) Professor Richard Norberg, Washington University: *Deuteron Magnetic Resonance Studies* 37

(2) Dr. M.L. Theye, Laboratoire d'Optique, Paris: *Determination of Sub-Band-Gap Absorption by Photothermal Deflection Spectroscopy and Steady-State Photoconductivity* 40

(3) Dr. K.L. Narasimhan, Tata Institute, Bombay: *Studies on a-Si/a-Si$_{1-x}$Ge$_x$ Heterojunctions* 45

REFERENCES 47

LIST OF FIGURES

Figure 1. Changes of the optical gaps, E_{04} and E_{03}, and of the refractive index, of a-Ge:H as a function of the substrate temperature T_s. The open and closed symbols refer to samples made in the same run at different points on the substrate platform. 17

Figure 2. Infrared vibrational absorption spectra of films of a-Ge:H prepared at low and high substrate temperatures T_s, illustrating O-related absorption in the 1000 cm^{-1} region for the low T_s deposition. 18

Figure 3. Infrared vibrational absorption spectra of a capped film of a-Ge:H prepared at 150°C, illustrating the growth of O-related absorption in the 1000 cm^{-1} region as a function of time. 19

Figure 4. TEM micrograph of a sample of a-Ge:H prepared at the low substrate temperature of 200°C, illustrating distinct island and tissue material. 20

Figure 5. TEM micrograph of a sample of a-Ge:H prepared at the high substrate temperature of 300°C, illustrating the reduction in tissue material compared with Figure 4. The large area of white is an artifact of the reproduction process. 21

Figure 6.	Gas evolution as a function of heating temperature for a representative sample of a-Ge:H.	22
Figure 7a,b,c.	DSC spectra of samples of a-Ge:H prepared at substrate temperatures of 100°C, 150°C, 250°C, 300°C and 350°C.	25,26,27
Figure 8.	Room temperature conductivity and quantum efficiency-mobility-lifetime product ($\eta\mu\tau$) for samples of a-Ge:H prepared at different substrate temperatures.	29
Figure 9.	Room temperature conductivity and quantum efficiency-mobility-lifetime product ($\eta\mu\tau$) for samples of a-Ge:H prepared at different substrate temperatures, with and without "capping" layers of a-Si:H.	30
Figure 10.	Changes of the optical gaps, E_{04} and E_{03}, and of the refractive index, of a-Ge:H prepared with different amounts of dilution of GeH_4 by H_2 in the preparation plasma. The open and closed symbols refer to samples made in the same run at differents points on the substrate platform.	33

Figure 11. Transport properties of a-Ge:H prepared with different amounts of dilution of GeH_4 by H_2 in the preparation plasma. 34

Figure 12. TEM micrograph of a 500 Å thick film of a-Ge:H prepared from undiluted GeH_4. 35

Figure 13. TEM micrograph of a 500 Å thick film of a-Ge:H prepared from a plasma of one part of GeH_4 to 40 parts of H_2. 36

Figure 14. PDS spectra for three samples of a-Si:H:P made under the same conditions but of different thicknesses. 42

Figure 15. CPM spectra for four samples of a-Si:H:P made under the same conditions but of different thicknesses. 43

Figure 16. Comparison of PDS and CPM spectra for a sample of a-Si:H:P. 44

LIST OF TABLES

Table 1. Deposition conditions for the films referred to in this Report. 8

Table 2. Optical and transport properties for films of a-Ge:H prepared at different substrate temperatures. 16

Table 3. Optical and transport properties for films of a-Ge:H prepared with different degrees of H_2 dilution in the GeH_4 preparation plasma. 32

Table 4. Properties of samples prepared for DMR measurements by Professor Norberg's group at Washington University. 38

LIST OF APPENDICES

A. "Comparison of the structural, electrical and optical properties of amorphous silicon-germanium alloys produced from hydrides and fluorides" by K.D. Mackenzie, J.H. Burnett, J.R. Eggert, Y.-M. Li and W. Paul, Phys. Rev. *B38*, 6120 (1988).

B. "Current transport in a-SiGe Alloy Schottky Barriers" by D.K. Sharma, K.L. Narasimhan, S. Kumar, B.M. Arora, W. Paul and W.A. Turner, accepted by the Journal of Applied Physics.

C. Abstract of paper on "Comparison of the structural properties of a-Si:H prepared from SiH_4 and $SiH_4 + H_2$ plasmas, and correlation of the structure with the photoelectronic properties" by S.M. Lee, S.J. Jones, Y.-M. Li, W.A. Turner and W. Paul, accepted for publication in the Philosophical Magazine.

D. Abstract of presentation on "Rotating Silyl Groups in a-Si:D,H Films" by P. Santos, M.P. Volz and R.E. Norberg, at the American Physical Society Meeting at New Orleans, March, 1988.

E. Abstract of a presentation by Dr. M.L. Theye at the Chelsea Amorphous Semiconductor Conference, December 1987.

F. Abstract of a presentation by Dr. M.L. Theye at the Chelsea Amorphous Semiconductor Conference, December 1987.

I. *Introduction*

In section II, we discuss our conclusions from our work on a-$Si_{1-x}Ge_x$ alloys and introduce new projects suggested by our studies.

In section III, we describe our interim conclusions from our attempt to develop a windowless H_2 lamp for production of samples by photo-CVD, and introduce a new project being developed as a result.

In section IV, we discuss the next phase of our study of unalloyed a-Ge:H which has involved the variation of the substrate temperature and the dilution of GeH_4 by H_2.

In section V, we discuss three continuing collaborative projects: the first with Professor Richard Norberg on deuteron magnetic resonances in the class of materials represented by a-Si:H; the second with Dr. M.L. Theye on a study of sub-band-gap absorption by photothermal deflection spectroscopy and steady-state photoconductivity; and the third with Dr. K.L. Narasimhan on the properties of Schottky barriers on SiGe alloys.

II. *Amorphous Si-Ge Alloys Produced by Glow Discharge fom Hydrides and Fluorides of Si and Ge*

Our work on these alloys was essentially completed at the time of the last Annual Report. However, at the beginning of the current report period more measurements were done of the variation of the mobility-lifetime product with composition, and of the changes in microstructure with preparation conditions as revealed by studies of DSC, GE and TEM. The results served to amplify and confirm our conclusions regarding the central role microstructure on a 100 Å scale plays in the properties of the alloys. They also de-emphasized the importance of F *incorporation* in the alloys, and suggested that there might be a number of different plasma conditions leading to optimized properties of a-Si:H.

Our article on this subject, published in the Physical Review, is included as Appendix A. Partly as a result of this work, we have devoted considerable time to the study of the photoelectronic properties and the microstructure (as revealed by TEM, DSC and GE) of samples of a-Si:H prepared with and without dilution of the plasma by H_2. There have, in fact, been a number of reports in the literature concerning improvement of the properties of a-$Si_{1-x}Ge_x$:H alloys when H_2-diluted plasmas are used. Our results on unalloyed a-Si:H indicate that the structure of these films is also changed by H_2 dilution of the plasma, but the effect on the as-deposited photoelectronic properties is considerably less marked. A paper on this subject is in course of preparation at the time of writing, and its Abstract is included as Appendix C.

In our published paper, we referred to the possibility of small-scale phase separation in the 50:50 alloys. Unsuccessful attempts were made to demonstrate this on samples $Si_{0.5}Ge_{0.5}$:H 441 and a$Si_{0.5}GE_{0.5}$:H:F 436. Using the Harvard TEM (Philips 420T High Resolution Electron Microscope) no phase separation was seen using EDS (x-ray analysis) on a scale of 400 Å. Areas which showed different contrast in the TEM micrographs were examined. The MIT machine (Vacuum Generators HB501 STEM) has a nominal spatial

resolution of 40 Å for x-ray analysis, but again no phase separation was found between the islands (apparent high density) and the connecting tissue between islands (apparent low density). Thus, the contrast in the transmission micrographs appears to be caused by a difference in atom density (but not composition) or by a difference in local thickness.

Our work on the alloy system led us to the conclusion that the usual approach to their optimization, involving minor alterations of the plasma conditions used to deposit as-Si:H, was inappropriate. It seemed to be possible that the optimization conditions on substrate temperature, gas flow and electrical powers could not be met simultaneously for Si and Ge. Separate Si and Ge plasmas might be required. Thus, concentration on optimization of the conditions of preparation of a-Ge:H was judged to be a good alternative approach, it being known that the properties of that substance were much inferior to those of a-Si:H, and that much less work had been done to improve them. In last year's report we described our results on a-Ge:H prepared at a substrate temperature of 260°C while the r.f. power was systematically varied over an order of magnitude. Most of the samples were produced with H_2 dilution of the GeH_4 plasma. Besides the conventional measurements of optical and transport properties we carried out studies by GE, DSC and TEM. In the next Section, we extend these studies to include depositions of a-Ge:H with substrate temperature and H_2 dilution ratio as the principal variables.

III. *Production of a-Si:H and a-Ge:H by Photo-CVD*

During this report period, approximately fifty more runs were made to test the production of amorphous hydrogenated Si and Ge in a system incorporating a windowless H_2 discharge lamp. The rationale for trying such a system, a description of the experimental arrangement, and the optical properties of a-Si:H films produced, were described in the last Annual Report.[1] An unanswered question carried over from last year was the precise mechanism of the gas decomposition: whether photo-CVD, d.c. glow discharge, or hydrogen radical-enhanced CVD all contributed to the deposition, and in what proportion.

Most test runs were carried out with substrate temperatures near 200°C, pressure of SiH_4 of several torr and with variable flow rates of SiH_4 in the chamber and of H_2 in the lamp. To illustrate the sort of tests applied, we mention (1) runs with no H_2 in the lamp, to see if d.c. glow discharge of SiH_4 diffusing into the lamp would lead to a deposit, (2) runs with D_2 instead of H_2 in the lamp, to see if atomic D would be incorporated in the film (3) different pumping schemes for the two gases, (4) installation of LiF or MgF_2 windows, to permit light to reach the volume occupied by SiH_4 while preventing gas molecules from doing so, and (5) installation of deflecting baffles which permitted the flow of gas molecules to and from the lamp, but blocked the ultraviolet radiation.

When deposits of a-Si:H and a-Ge:H were obtained their photoelectronic properties were comparable to those of our r.f. glow discharge material, as was related in last year's report.[1] However, the totality of the experiments done - particularly those where either the light or the gas molecules from the lamp were blocked, suggested that the main deposition process was d.c. glow discharge. We have therefore decided to redesign our system to use an external light source for direct photo-CVD. A more conventional UV light source will be used (an H_2 or He arc lamp). A new chamber has been commissioned with ports which are more accessible to the deposition area than our present chamber, as it is necessary to bring the light source as close as possible to the substrates. Also, a load-lock system has been bought to reduce

turnaround time. This system will be used to complement our r.f. glow discharge system in producing a-Ge:H.

It is appropriate to record here two other brief trials which were made. A temporary chamber was set up to make use of an excimer laser as a light source. The chamber was arranged with a "buffer" tube that was purged with H_2 gas to separate the UV window from the disilane deposition gas, and thus prevent deposition directly on the window. The laser was operated at the ArF line of 198 nm, with about 200 mJ/pulse, a pulse width of 20 ns and a repetition rate of 10 Hz. Deposits were achieved on the order of 500 Å over several hours of running time. While this may be termed a successful attempt, it is clear that the rate of deposition in much too low for practical use. The primary limitation is the low repetition rate of the laser. In such a system, also, the plasma generated never reaches a chemical steady state, and no doubt this would pose potential problems for a full analytical understanding.

Some attempts were also made to deposit germanium on silicon substrates when a GeH_4 atmosphere was bombarded with high energy He^{++} and H^+ particles from the Harvard accelerator run by Professor J. Golovchenko. The original motivation for this attempt was the observation by a number of workers that carbon films are formed when high energy particles are used in an atmosphere which contains hydrocarbons. However, we have to date not been able to successfully reproduce this result for GeH_4, even though very minute deposits were found in the few experiments done.

IV. *Amorphous Hydrogenated Germanium Prepared by R.F. Glow-Discharge*

For the sake of completeness, we begin this account with a brief summary of the results reported in the last Annual Report.[1] Samples prepared at 260°C with and without H_2 dilution of the preparation plasma were inferred to have different microstructures: the latter samples possessed infrared vibrational spectra including Ge-O lines; their gas evolution spectra showed much release of gas (H_2) at low temperatures (200-400°C); and their TEM micrographs confirmed a more open, low atomic density structure. These results suggested that better films of a-Ge:H were possible using H_2-diluted plasmas, and our more recent work has all been done with H_2 dilutions.

A systematic series of measurements was carried out on samples prepared at 260°C from a plasma of 1 sccm of GeH_4 and 40 sccm of H_2 at r.f. power densities ranging from 0.05 to 0.4 watts/cm^2 at the powered electrode. Except for the sample produced at the lowest power density, there was no evidence of O contamination in the infrared spectra. These spectra showed Ge-H stretching modes at 1875 cm^{-1} and 1975 cm^{-1} and wagging modes near 560 cm^{-1}. The optical absorption edge spectra were all consistent, and showed no evident dependence on the power density used in the preparation. Moreover, the absorption edge was at least as sharp (in energy) as for the best a-Si:H. The activation energies for transport all lay in the range of 0.51 ± 0.02 eV. These data suggest very good films whose properties are very little affected by the order of magnitude change in the power density used in their preparation. However, preliminary studies by GE, DSC and TEM gave consistent evidence for differences in the microstructure.

During the past year, 73 separate depositions of a-Ge:H or a-Ge:H:D have been carried out. Some of these have produced films approximately 1 μm in thickness, which were used primarily for measurements of transport as a function of temperature, photoconductivity, optical absorption edge spectra, infrared vibrational absorption spectra and other property measurements directed at optimizing the photoelectronic response. Other films were deposited on

Al substrates from which they could be removed for studies of gas evolution (GE) or for differential scanning calorimetry (DSC); these films were necessarily much thicker, between 5 and 10 μm. Yet others were prepared on C-coated Ni grids in 500 Å thicknesses for transmission electron microscopy (TEM). Finally, films were prepared for a collaboration on deuteron magnetic resonance studies with Professor R. Norberg of Washington University from plasmas of GeH_4 and D_2; all such films were characterized by a full complement of photoelectronic measurements as well as by GE and TEM. The deposition conditions for the selection of these films referred to in this report are given in Table 1.

An important parameter systematically varied while holding other deposition variables constant was the deposition temperature T_s. The changes in the principal properties are listed in Table 2, and the changes in the optical properties are illustrated in Figure 1. The roughly 10% decrease in the energy gap is clearly insufficient to explain the 40% increase in refractive index, and we infer that the higher T_s films have higher mass density. Films produced below about 250°C showed considerable infrared absorption attributed to oxygen which is inferred to have come from the atmosphere when the samples were removed from the deposition apparatus. Figure 2 illustrates infrared vibrational absorption spectra of films of a-Ge:H prepared at low and high T_s and measured immediately after preparation; the O-related absorption in the low T_s film is evident. Figure 3 illustrates the change in the absorption in a film produced at low T_s as a function of time; here the growth of the O-related absorption is clear. The TEM studies on five samples showed distinct island and tissue material for samples produced at 100°C, 150°C and 200°C. The sample produced at 250°C was more compact but still showed low-density tissue. A significant change occurred for the material produced at 300°C: it had very little tissue material. We conclude that there is a relatively sharp elimination (with increasing T_s) of a structural defect at 250°-300°C in our preparation regime. See Figures 4 and 5.

The gas evolution measurements , illustrated in Figure 6, usually show three evolution

Table 1
Deposition conditions for the films referred to in this Report

Sample	T_S	Power	Pressure	Flow SiH_4	Flow GeH_4	Flow H_2	Flow PH_3 *	Flow D_2	Time	Thick	Rate	C_H	Comment
	°C	Watts	Torr	sccm	sccm	sccm	sccm	sccm	mins	μm	Å/m	%	
SiGe 436	301	36	0.41			15.1			13				34.8 sccm SiF_4 +0.73 sccm GeF_4
SiGe 441	300	2.5	0.25	12.0	3.0				2.83				
SiHD 479	231	10	0.68	4.0				76.0	248	3.26	131		Norberg
SiHD 480	231	10	0.68	4.0				76.0	1019				Norberg
SiHP 496	230	2.5	0.20	20.0			$1.8\ E^{-4}$		630				Evolution
SiHP 503	230	2.5	0.20	20.0			$1.8\ E^{-4}$		630	5.67	90		Evolution
SiHP 504	230	2.5	0.20	20.0			$1.8\ E^{-4}$		1028	7–10	70–95		Theye
SiHP 505	230	2.5	0.20	20.0			$1.8\ E^{-4}$		214	1.5–1.9	70–90		Theye

Sample	T_S °C	Power Watts	Pressure Torr	Flow SiH_4 sccm	Flow GeH_4 sccm	Flow H_2 sccm	Flow PH_3 sccm *	Flow D_2 sccm	Time mins	Thick μm	Rate Å/m	C_H %	Comment
SiHP 506	230	2.5	0.20	20.0			$1.8\ E^{-4}$		7.25				T.E.M.
SiH(H) 507	230	10	0.70	4.0		76.0			5.25				T.E.M.
SiH(D) 508	230	10	0.68	4.0				76.0	5.25				T.E.M.
GeH(D) 510	261	8	0.95		1.01			40.0	70	1.2	170		Norberg
GeHD 511	260	8	0.95		1.02			40.0	807	12			Norberg
SiH 514	141	2.5	0.20	20					840	6–7	70–90	30	Theye
SiHP 515	230	2.5	0.20	20.0			$1.8\ E^{-4}$		55	0.3–0.4	55–70	14	Theye
SiHP 516	232	2.5	0.20	19.8			0.2		7.25				T.E.M.

Sample	T_S	Power	Pressure	Flow SiH_4	Flow GeH_4	Flow H_2	Flow PH_3 *	Flow D_2	Time	Thick	Rate	C_H	Comment
	°C	Watts	Torr	sccm	sccm	sccm	sccm	sccm	mins	μm	Å/m	%	
SiHP 517	232	2.5	0.20	19.8			0.2		630	3.1	49.2		G.E.
GeH(H) 518	102	8	0.95		1.01	40.0			50	0.75–0.85	150–170		
GeH(H) 519	151	8	0.95		1.01	40.0			50	0.7–0.8	145–160		
GeH(H) 520	200	8	0.95		1.01	40.0			50	0.65–0.75	130–150		
GeH(H) 521	250	8	0.95		1.01	40.0			60	0.75–0.85	120–140		
GeH(H) 522	298	8	0.95		1.01	40.0			60	0.7–0.85	120–140		
GeH(H) 523	348	8	0.95		1.01	40.0			60	0.75–0.8	120–140		
GeH(H) 524	53	8	0.95		1.01	40.0			70	1.2–1.35	170–190		

Sample	T_S °C	Power Watts	Pressure Torr	Flow SiH_4 sccm	Flow GeH_4 sccm	Flow H_2 sccm	Flow PH_3 sccm *	Flow D_2 sccm	Time mins	Thick μm	Rate Å/m	C_H %	Comment
GeH(H) 525	101	8	0.95		1.01	40.0			3.25				T.E.M.
GeH(H) 526	200	8	0.95		1.01	40.0			3.67				T.E.M.
GeH(H) 527	300	8	0.95		1.01	40.0			4				T.E.M.
GeH(H) 528	151	8	0.95		1.01	40.0			3.25				T.E.M.
GeH(H) 529	248	8	0.95		1.01	40.0			3.5				T.E.M.
GeH(H) 530	101	8	0.95		1.01	40.0			480				
GeH(H) 531	200	8	0.95		1.01	40.0			480				
GeH(H) 532	299	8	0.95		1.01	40.0			155				

Sample	T_S °C	Power Watts	Pressure Torr	Flow SiH_4 sccm	Flow GeH_4 sccm	Flow H_2 sccm	Flow PH_3 sccm *	Flow D_2 sccm	Time mins	Thick μm	Rate Å/m	C_H %	Comment
GeH(H) 533	249	8	0.95		1.01	40.0			480				
GeH(H) 535	100	8	0.95		1.01	40.0			70	1.1–1.2	155–175		
SiH(H) 536	230	10	0.70	4.0		76.0			2880				Norberg
SiH(H) 537	230	10	0.70	4.0		76.0			5.25				T.E.M.
SiH 538	230	2.5	0.20	20.0					2743				Norberg
SiH 539	230	2.5	0.20	20.0					6.25				T.E.M.
SiHD 540	230	10	0.70	4.0				76.0	5.25				T.E.M.
SiHD 541	230	10	0.70	4.0				76.0	2880				

Sample	T_S	Power	Pressure	Flow SiH_4	Flow GeH_4	Flow H_2	Flow PH_3 *	Flow D_2	Time	Thick	Rate	C_H	Comment
	°C	Watts	Torr	sccm	sccm	sccm	sccm	sccm	mins	μm	Å/m	%	
GeH(H) 546	150	12	0.95		1.01	40.0			200	4.55	228		
GeSi 547	150	8/2.5	0.95/0.20	/20.0	1.01/	40.0			75/10	1.21/1.33	143/156		**
GeH(H) 548	150	1	0.95		1.01	40.0			1080				**
Ge/Si 549	250	8/2.5	0.95/0.20	/20.0	1.01/	40.0			82/10	1.20/1.34	130/152		**
Ge/Si 550	200	8/2.5	0.95/0.20	/20.0	1.01/	40.0			76/10	1.12/1.31	124/147		**
Ge/Si 551	300	8/2.5	0.95/0.20	/20.0	1.01/	40.0			83/10	1.17/1.38	41/56		**
GeH(H) 561	250	8	0.95		1.00	30.0			75		122–142		
GeH(H) 562	249	8	0.95		1.01	20.0			90		135–163		

Sample	T_S	Power	Pressure	Flow SiH_4	Flow GeH_4	Flow H_2	Flow PH_3 *	Flow D_2	Time	Thick	Rate	C_H	Comment
	°C	Watts	Torr	sccm	sccm	sccm	sccm	sccm	mins	μm	Å/m	%	
GeH(H) 563	249	8	0.95		1.01	10.0			80	1.27–1.43	159–182		
GeH(H) 564	250	8	0.95		1.00	50.0			70	0.79–0.98	113–141		
GeH(H) 565	251	8	0.95		1.01	5.0			50	0.85–0.97	170–194		
GeH 566	247	8	0.95		1.01	0			50	1.04	208		
GeH(H) 567	250	8	0.95		1.00	20.0			3.36				T.E.M.
GeH(H) 568	251	8	0.95		1.00	10.0			2.94				T.E.M.
GeH(H) 569	251	8	0.95		1.01	5.0			2.75				T.E.M.
GeH 570	249	8	0.95		1.00				2.26				T.E.M.

Sample	T_S °C	Power Watts	Pressure Torr	Flow SiH_4 sccm	Flow GeH_4 sccm	Flow H_2 sccm	Flow PH_3 sccm *	Flow D_2 sccm	Time mins	Thick μm	Rate Å/m	C_H %	Comment
GeH(H) 571	250	8	0.95		1.00	20.0			270				
GeH(H) 572	249	8	0.95		1.01				180				
GeH(H) 573	349	8	0.95		1.01	40.0			480	5.7–6.1	119–126		
GeH(H) 574	349	8	0.95		1.00	40.0			3.85				T.E.M.
GeH(H)583	249	8	0.95		1.01	40.1			80	0.97	121.5		

* Samples prepared either from a flow of 2.5 sccm of 72 ppm of PH_3 in SiH_4 or of 20 sccm of 1% PH_3 in SiH_4

** Samples of GeH capped with a layer of SiH. Upper line refers to conditions for Ge deposition, lower line to Si deposition.

Table 2

Optical and transport properties for films of a-Ge:H prepared at different substrate temperatures. For other parameters of preparation, see Table 1.

Sample	T_s (°C	E_{04} (eV)	E_{03} (eV)	$n(2\mu m)$	E_σ (eV)	σ_0 $(\Omega\ cm)^{-1}$	$\eta\mu\tau$ (cm^2/V)
518	101	1.28	1.12	3.55	0.37	6.6E1	3.2E- 9*
519	151	1.24	1.06	3.80	0.41	1.2E2	9.3E- 9**
520	200	1.20	1.06	3.99	0.48	6.8E2	7.0E-10
521	250	1.16	1.01	4.16	0.55	4.9E3	1.7E-10
522	298	1.15	1.01	4.45	0.55	7.2E3	2.0E-10
523	348	1.15	1.00	4.43	0.50	2.8E3	9.7E-10
524	53	1.29	1.09	3.12	0.51	1.0E3	3.5E-11***

* $\eta\mu\tau$ was measured on an identically-prepared sample (530), after the sample had been annealed at 100°C for ~1.5 hours. The sample is not considered to be in a fully annealed state.

** Sample annealed at 148°C.

*** Sample not annealed.
All other samples annealed at 180° for $\geq$ 40 minutes, and measured in the Staebler-Wronski "A" state after many days of air exposure.

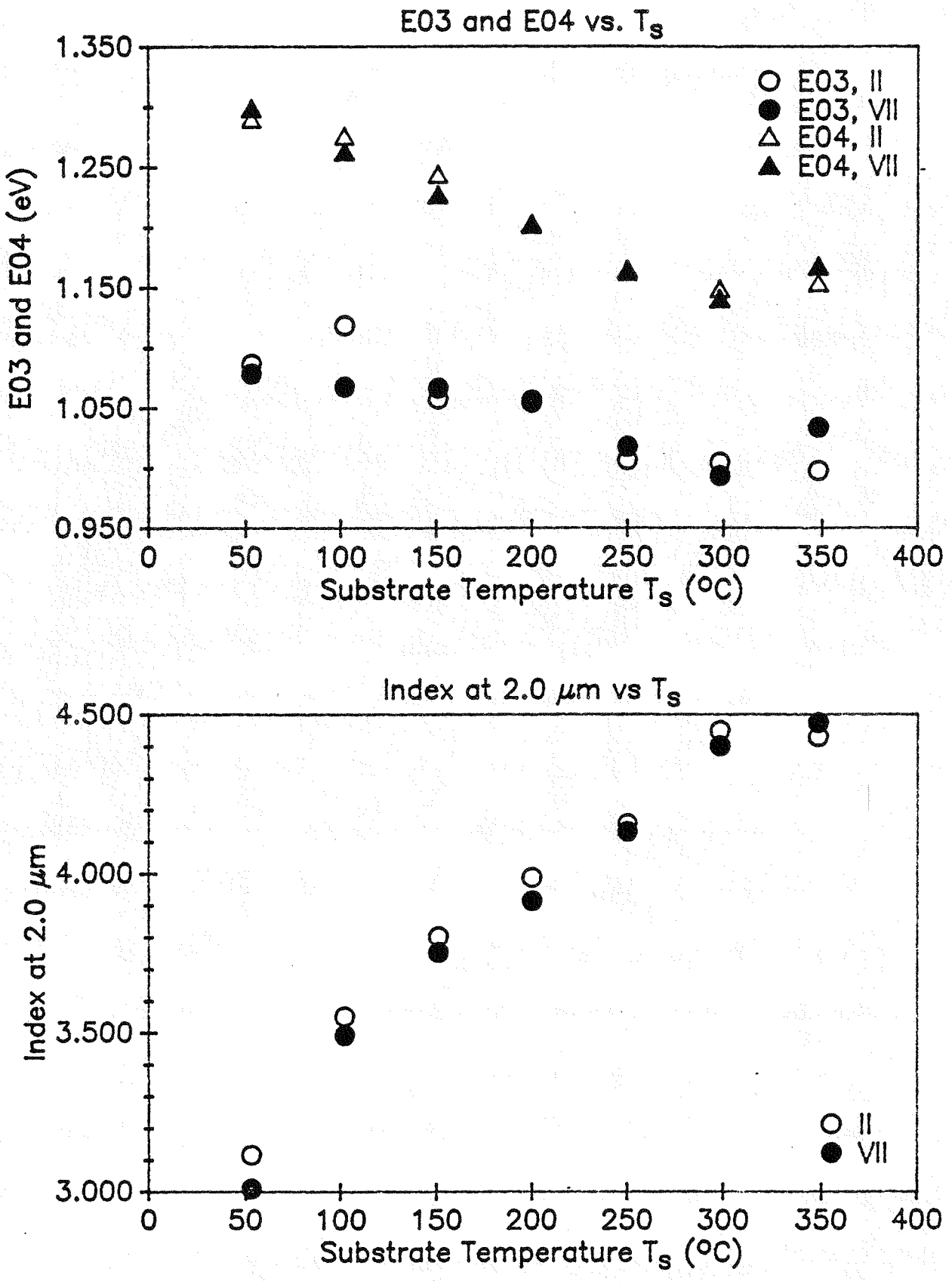

Figure 1. Changes of E_{03}, E_{04} and the refractive index of a-Ge:H with T_s.

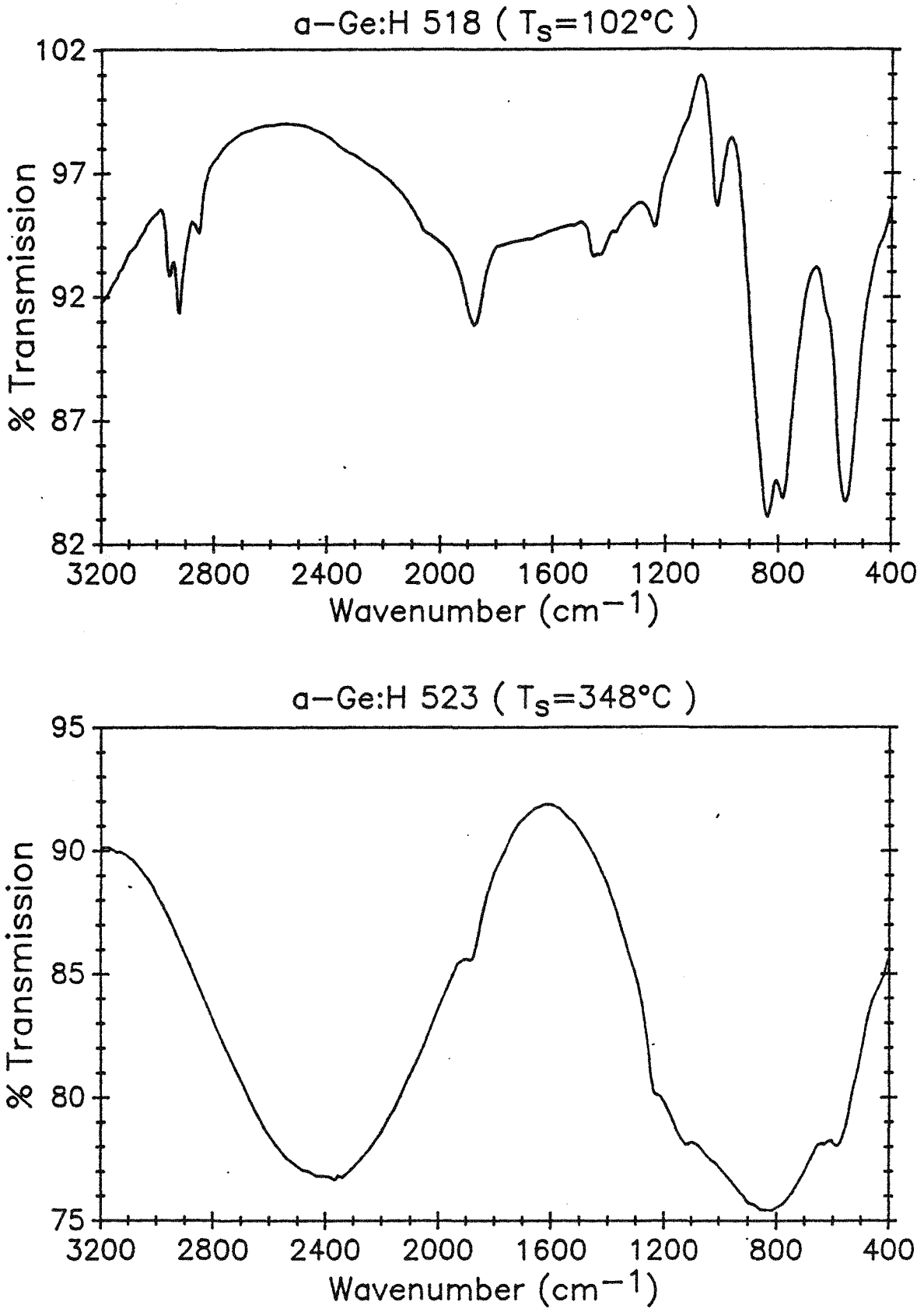

Figure 2. I.R. absorption of a-Ge:H, illustrating O-related absorption near 1000 cm^{-1}.

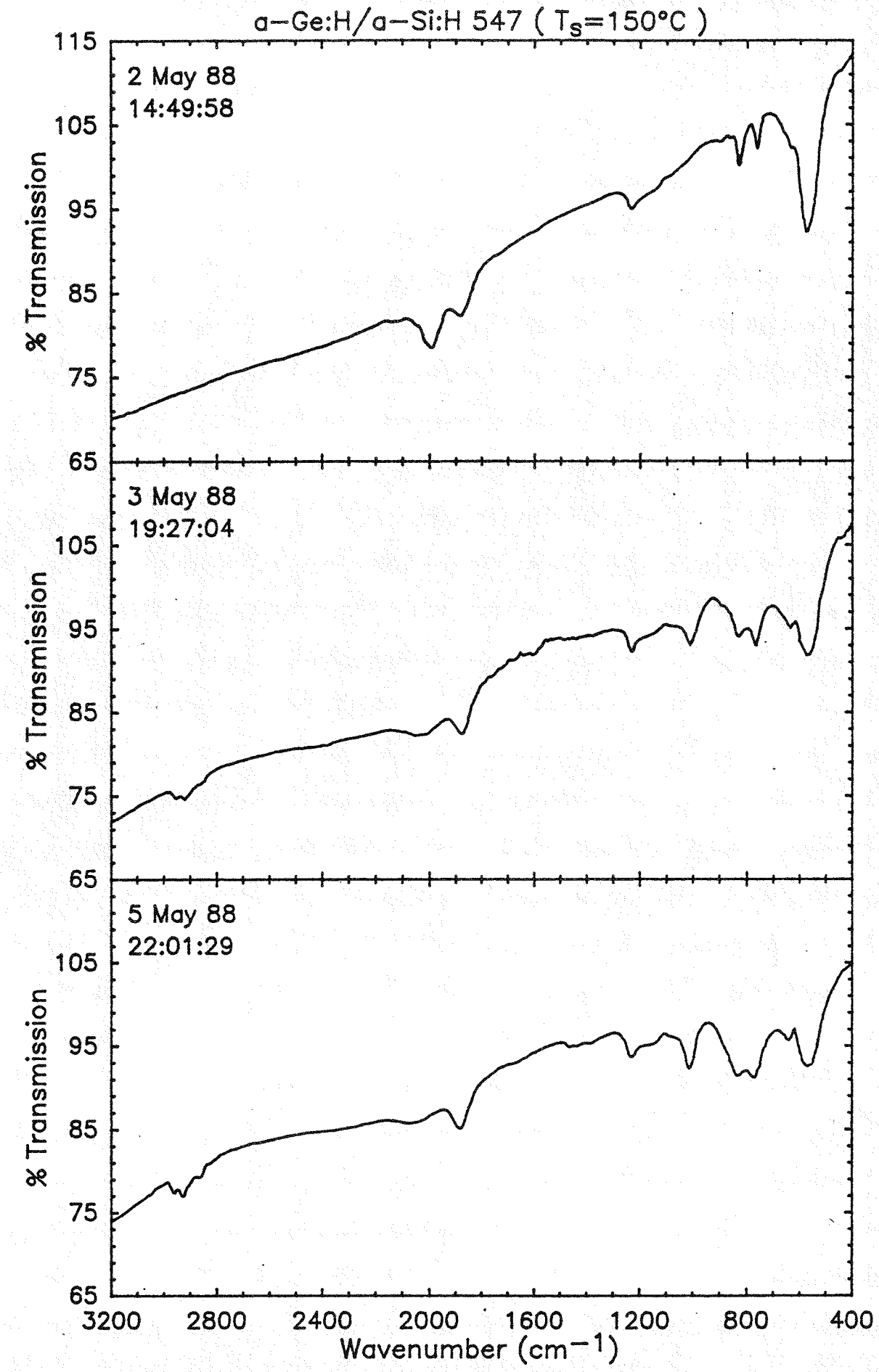

Figure 3. I.R. absorption of capped a-Ge:H at different times after deposition.

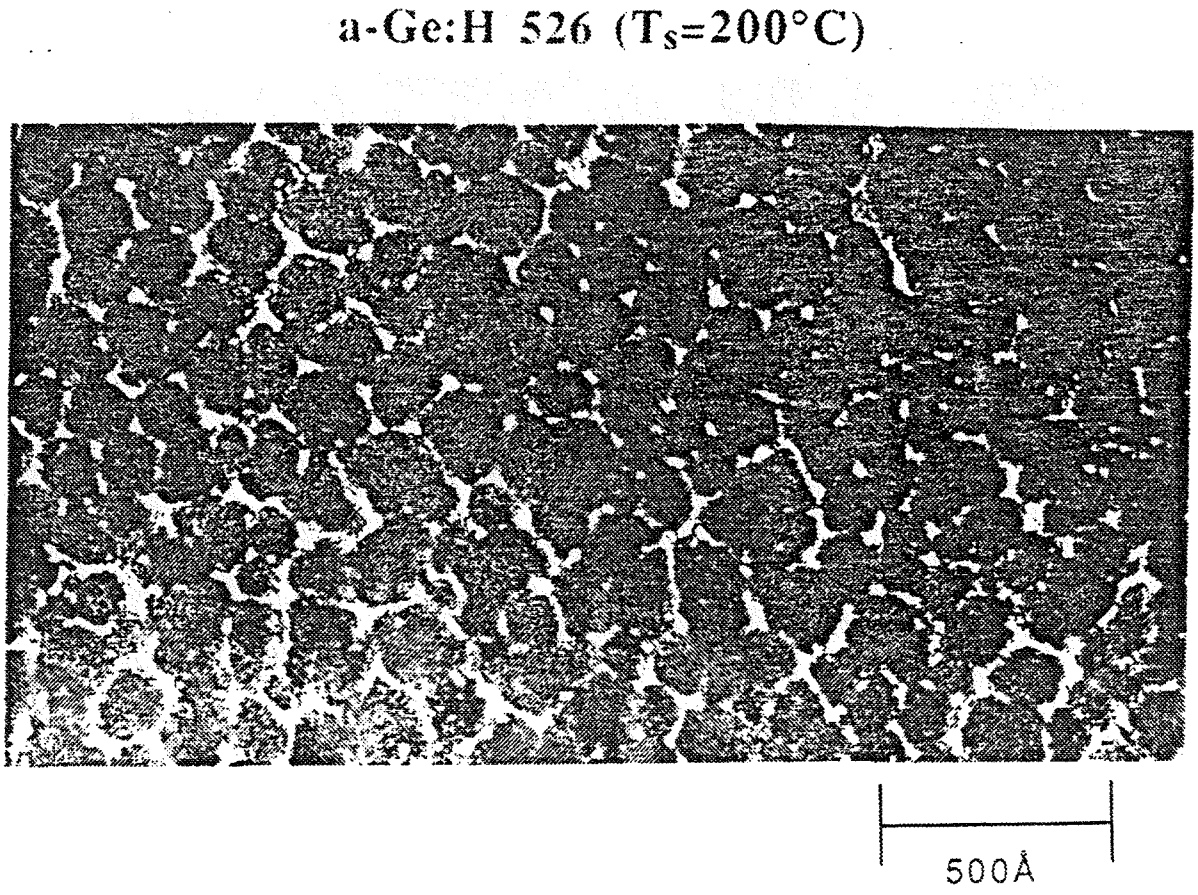

Figure 4. TEM micrograph of low T_s a-Ge:H.

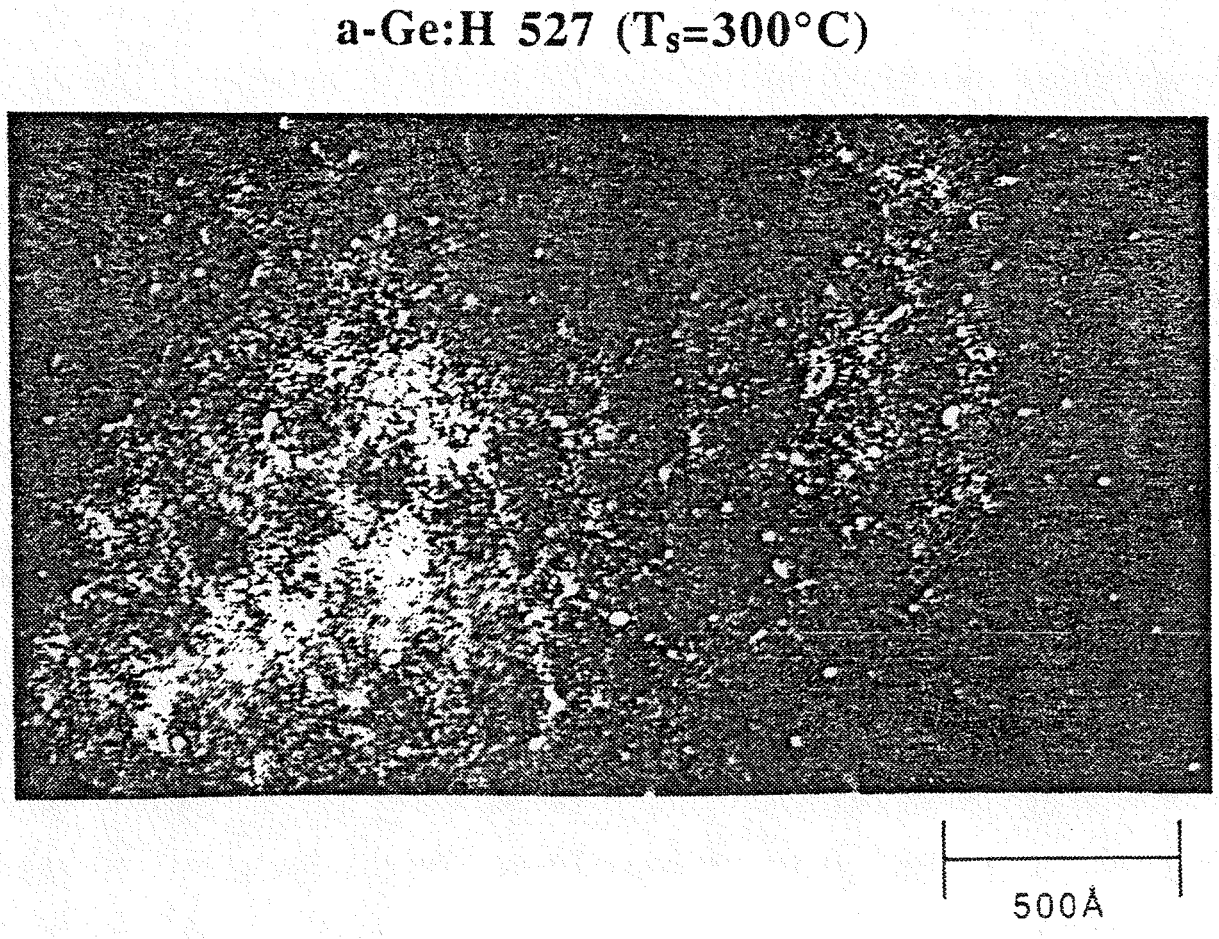

Figure 5. TEM micrograph of high T_s a-Ge:H.

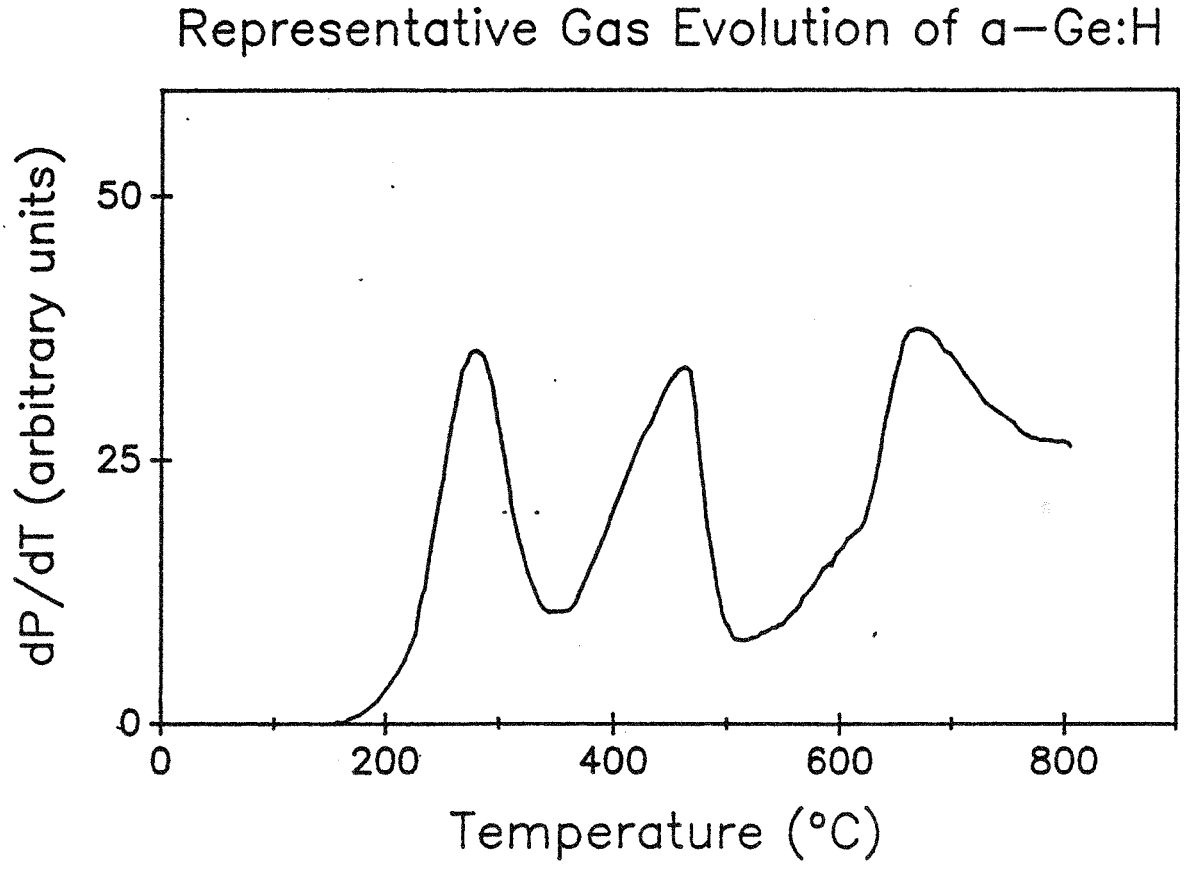

Figure 6. Gas evolution spectrum of a-Ge:H.

peaks.[2] It is notable that gas is always evolved at temperatures below the nominal substrate temperature. It is also notable that all of the samples show the evolution of CO and CO_2 as well as H_2 (from RGA traces) and that partial anneals followed by RGA examination prove that all of the CO and CO_2 is evolved in the lowest temperature evolution peak. After anneal to ~330°C, above the first evolution peak, a subsequent temperature scan over the full temperature range - *whether or not the sample is exposed to the atmosphere before the second scan* - shows no CO, CO_2 or H_2 evolved in the temperature region of the first evolution peak. The fact that no gas is evolved in the second scan after the sample has been exposed to air suggests that a reconstruction short of crystallization has taken place, without, of course, implying that the gas evolved during the first scan required reconstruction to facilitate its evolution. It is not surprising that the temperature necessary for the reconstruction is comparable to the (250-300°C) *substrate* temperature we suggest leads to the elimination of a basic structural defect.

As T_s is increased, the fraction of gas evolved in the first peak decreases dramatically (there is essentially none by T_s = 300°C) and the fraction in the second highest temperature peak increases slightly. We note that the temperature of this second peak correlates with the generally-accepted value (~ 500°C) of the crystallization temperature for a-Ge,[3] and that more specifically, most of the gas evolved in this peak does so before the change of phase takes place. We do not yet know if there is a cause and effect relationship.

The third evolution peak was described in a long reference 1 to our Report of last year.[1] It presents special difficulties of interpretation not encountered in the evolution of a-Si:H. As an introduction to these, we reproduce here the above-mentioned account:

> "The high temperature evolution is of particular interest, and concern, since it is observed that, at the temperature at which it starts, a black deposit is seen to form on the cooler portions of the quartz tube which contains the sample being heated. SEM x-ray analysis showed this deposit to be Ge. In one test, the evolution was stopped after the first peak at ~415°C, the sample cooled, and the apparatus opened for examination. A black deposit was then found on the sample holder for the Ge. This deposit was tentatively assumed to be Ge; at this stage no deposit was to be seen on the quartz tube

containing sample holder and sample. The sample was removed and the sample holder (with its black deposit) reinstalled in the quartz-containing tube. The sample holder was placed, first, away from the tip of the quartz tube while it (the tube tip) was baked above 800°C, and the system pumped down to 10^{-8} torr. The sample holder was then placed near the tube tip and heated to 800°C; after this, a black coating appeared on the quartz tube, while the coating on the sample holder had disappeared. Notably, no pressure rise, corresponding to gas evolution, was found as a result of the heating of the sample holder and its deposited film.

"In a different experiment, the sample was evolved through the first peak, and the evolved gas examined by an RGA: as expected, it proved to be hydrogen. After evacuation again to 10^{-8} torr, the sample was heated to 800°C; only the second peak was then found, and RGA examination confirmed that the gas evolved was also hydrogen. Again, a black coating was found on the quartz container after the 800°C evolution.

"It should be remarked that the evolution of gas in the temperature range of 700-800°C is much greater in a-Ge:H than in a-Si:H. This, and the peculiar appearance of Ge deposits, are being examined very carefully at the present time."

Probably the gas evolved is a molecule of Ge and H, incorporated during deposition or formed during the evolution run, which undergoes CVD at a sufficiently high temperature. Thus, the *observed* evolution spectrum may not accurately represent the gas released from bonding environments in the film. We propose infrared and Raman studies at different anneal temperatures in order to clarify the evolution process.

The DSC measurements made on samples prepared at different T_s are illustrated in Figures 7a, b, and c. It is notable that very weak exothermic effects are seen for T_s = 100°C and 150°C, in the range (470-600K) of the first gas evolution peak. We suppose that the weakness of the effect is the result of near-perfect cancellation of an exothermic reconstruction effect and the endothermic gas evolution. Samples produced at the higher T_s of 250°C, 300°C and 350°C (Figures 7b and 7c) show no effects in the temperature range of 470-600K, but neither do they show significant gas evolution there.

For samples produced at T_s below about 200°C, there are two clear exothermic peaks, while only one or a weakly-resolved doublet is seen for higher T_s. The first DSC exothermic peak is found near the *second* peak in the GE spectrum. At the temperature of the second exothermic peak, no gas is being evolved in the evolution experiment.

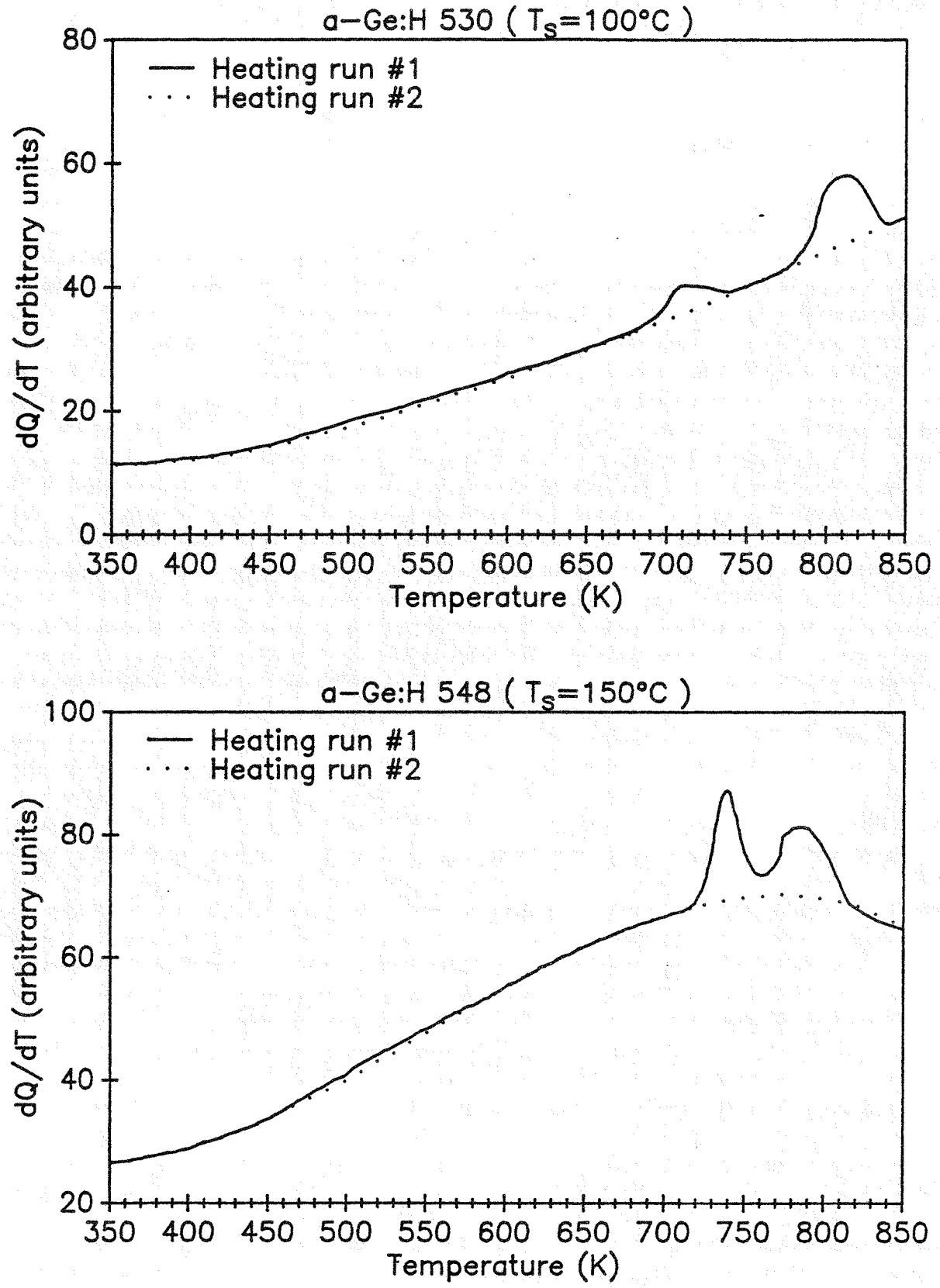

Figure 7a. DSC spectra of a-Ge:H for T_s of 100°C and 150°C.

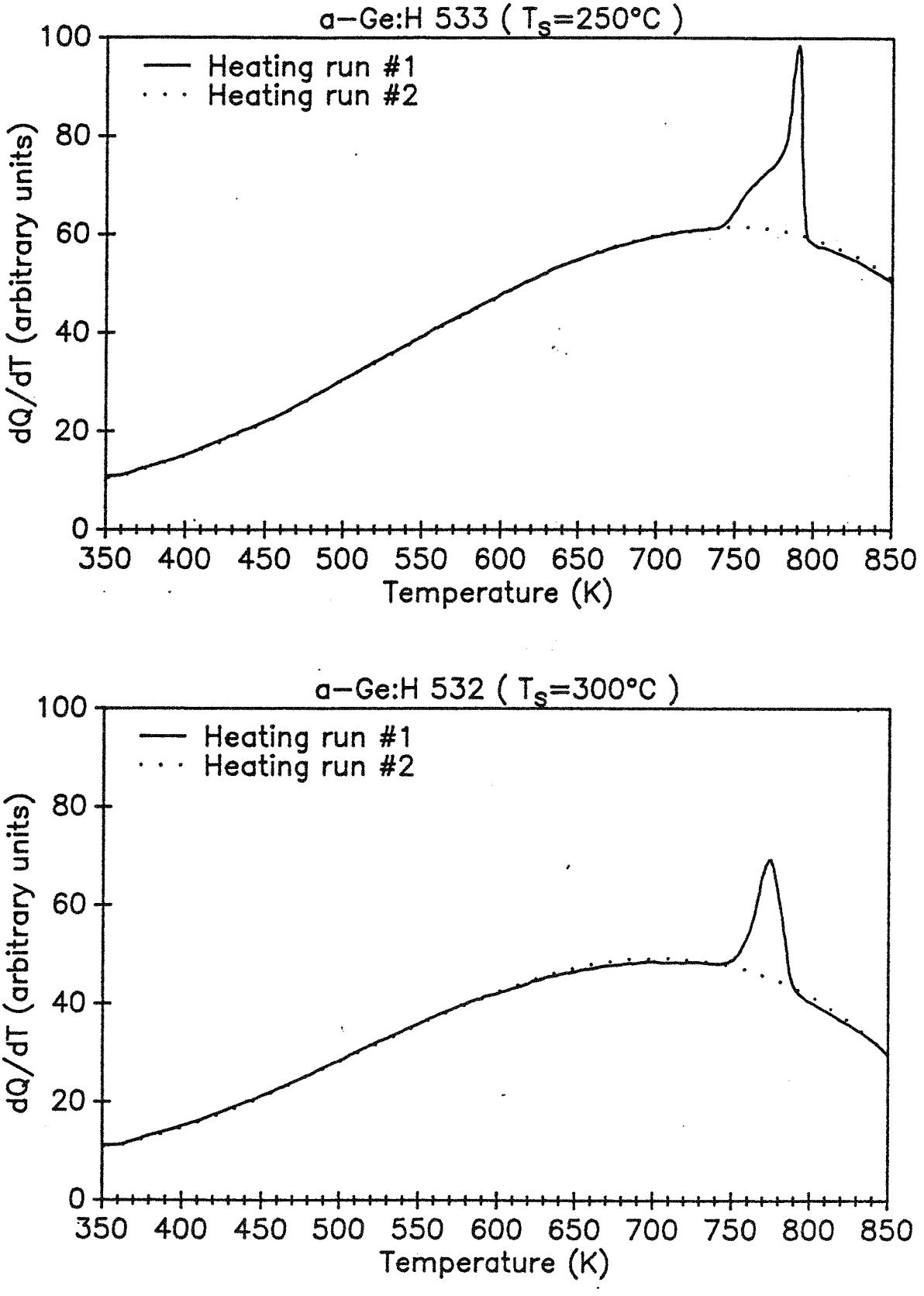

Figure 7b. DSC spectra of a-Ge:H for T_s of 250°C and 300°C.

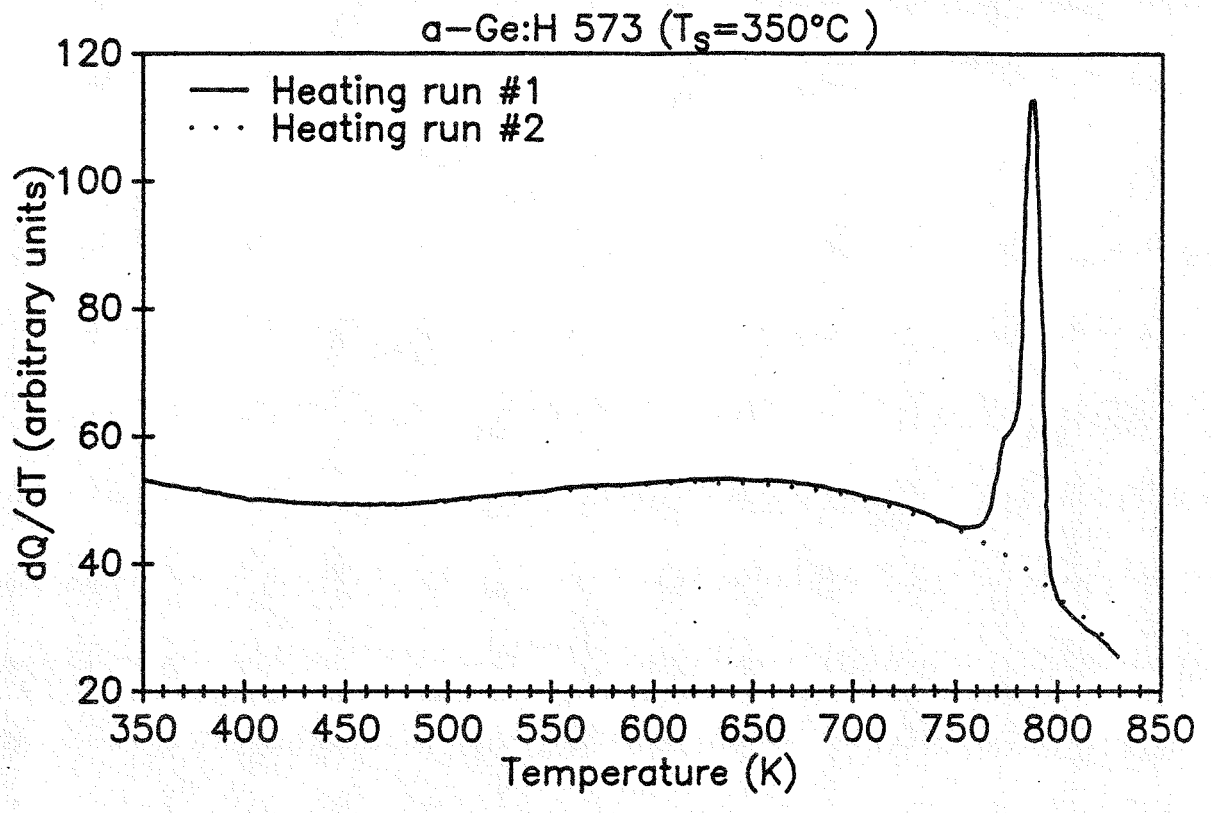

Figure 7c. DSC spectra of a-Ge:H for T_s of 350°C.

We conclude, from (1) the increase and asymptote of the refractive index with increasing T_s, (2) the observation of much tissue microstructure at low T_s which decreases and disappears at the higher T_s, (3) the observation of O pick-up with time for films produced at low T_s, absent in films produced at the higher T_s, (4) the gas evolution data, particularly the observation of evolution at temperatures below the substrate T_s and the observation of CO and CO_2 in RGA traces which is eliminated by 330°C anneal, and (5) the differences in DSC spectra for films made at different T_s, that the a-Ge:H prepared at or above 250°C is a more homogeneous, higher-density material with less void volume, that the samples produced at low T_s ($T_s < 250^{\circ}C$) pick up gases from the ambient atmosphere *after* film deposition is completed, and that deposition at $T_s \geq 300^{\circ}C$, or anneal in that high temperature range, leads to the elimination of a structural defect responsible for the open low-density structure. We now discuss results for the photo-transport which add supporting evidence for this model of our film fabrication procedure.

Figure 8 shows the results of measurements of the room-temperature D.C. conductivity and the $\eta\mu\tau$ as a function of substrate temperature T_s. One set of measurements was taken with the samples in air, in the Staebler-Wronski state B. The second set was taken after the samples were annealed *in vacuo* above 150°C, and held *in vacuo* while the measurements were taken. The photoconductivity data were taken both at 13 Hz and in the DC mode. There is a considerable difference in the dark conductivity and the $\eta\mu\tau$ for samples produced below 250°C under the two sets of measurement conditions. Both the dark conductivity and the photoresponse decrease by about an order of magnitude because of the anneal. By contrast, the dark conductivity and the $\eta\mu\tau$ remain unchanged with the anneal procedure when the deposition T_s was above about 250°C. These results are strikingly elaborated by measurements made on a-Ge:H films which were "capped" by ~1000 A of a-Si:H before removal from the deposition apparatus, and which were measured immediately afterwards. Figure 9 shows data for the dark conductivity and $\eta\mu\tau$ of the capped samples, and for the uncapped but annealed films already discussed under Figure 8. Differences of about 10^3 in dark

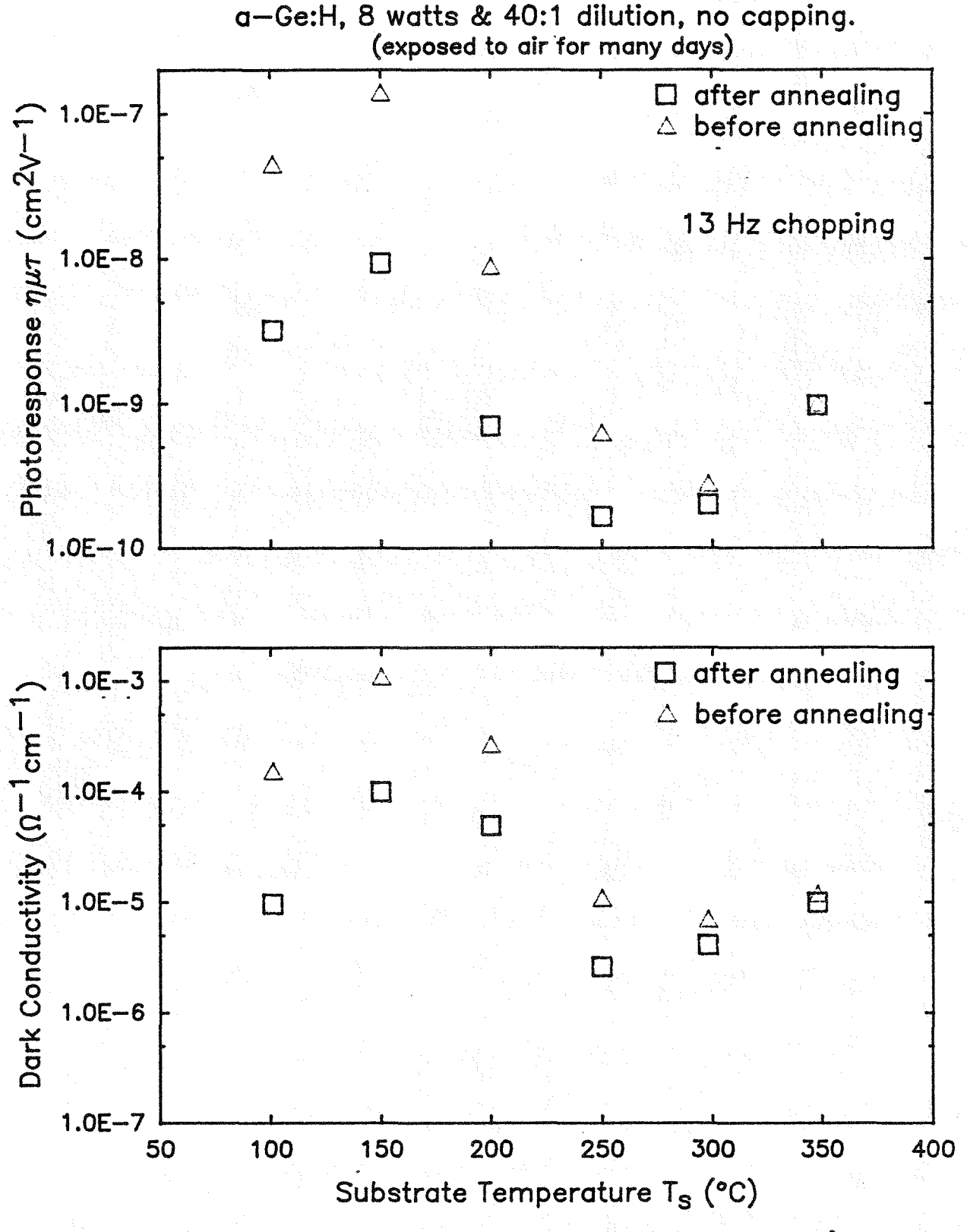

Figure 8. Dark and photoconductivity of a-Ge:H *versus* T_s.

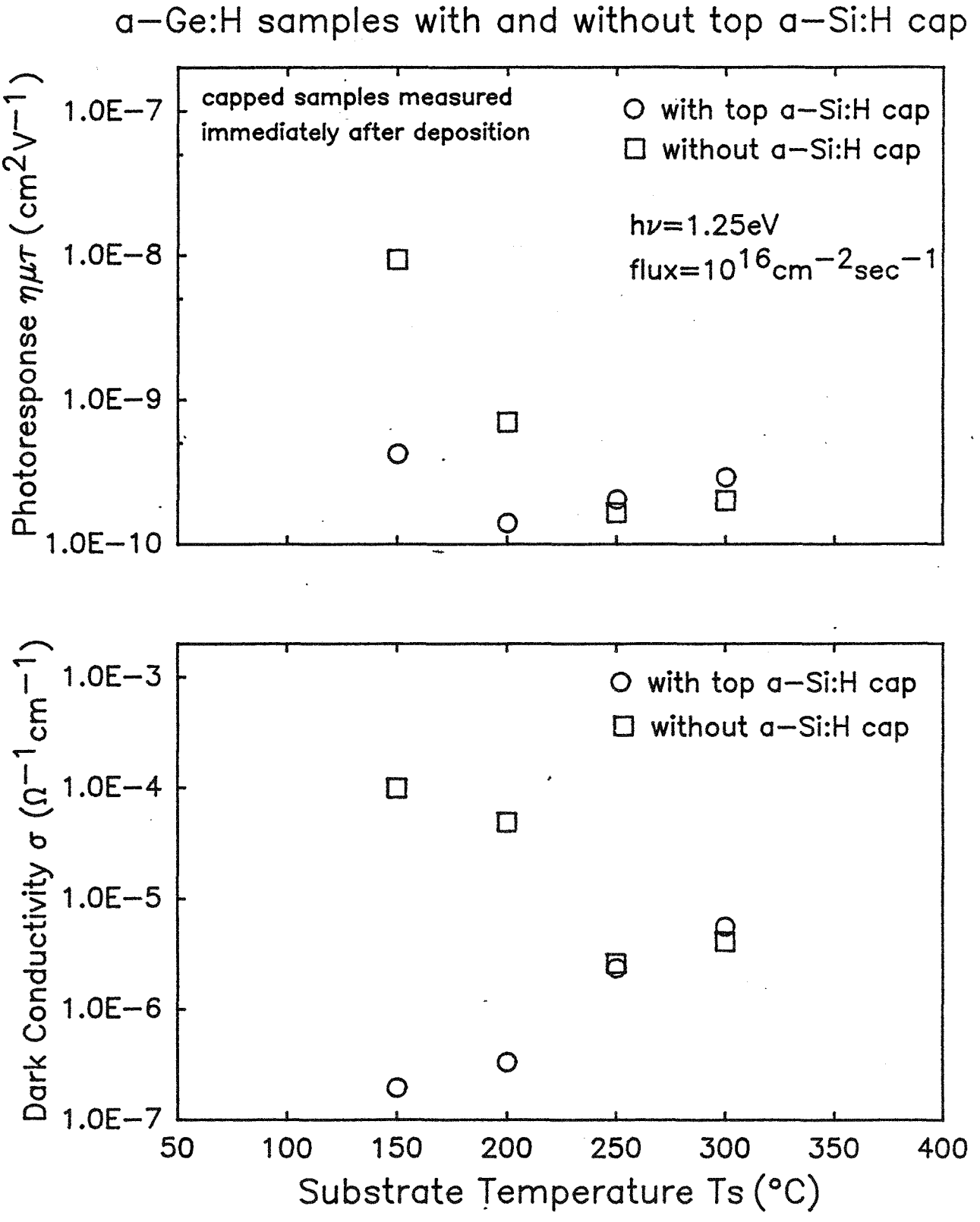

Figure 9. Dark and photoconductivity of a-Ge:H with and without a capping layer of a-Si:H.

T_s = 150°C are reduced to zero for films produced at 250°C and 300°C, while differences in $\eta\mu\tau$ of more than an order of magnitude for the lower T_s films are also reduced to negligible proportions for high T_s. It seems clear fom these measurements that the annealing of low T_s films is not sufficient to permit measurement of σ_d and $\eta\mu\tau$ for the uncontaminated Ge:H network. If low T_s films are to be used, then they need to be capped and measured soon after fabrication; otherwise, a safer procedure is to prepare all films at $T_s \geq 250^{o}C$, when capping becomes unnecessary.

Despite this encouraging rational explanation of the measured properties in terms of the degree of openness of the microstructure and the degree of gaseous contamination, it remains disappointing that the photoresponse of the films produced at the high T_s is very small. Indeed, when one examines and compares the sharpness of the optical absorption edge and the parameters of the dark transport in a-Si:H and a-Ge:H, the relative poorness of the $\eta\mu\tau$ in the latter material is very surprising. The third parameter systematically varied while holding other deposition variables constant was the H_2 dilution ratio. See Table 1. The optical and transport parameters for some of these films, after anneal, are given in Table 3 and Figures 10 and 11, where it is clear that there are no clear trends. Samples were also produced for TEM, DSC and GE studies. Representative TEM micrographs are shown in Figures 12 and 13, where dark areas inferred to be relatively high-density islands are interspersed with light areas inferred to be low-density tissue. It is found that the mean island diameter decreases monotonically from 300 ±40 A to 130 ±40 A as the dilution ratio is increased fom H_2/GeH_4 of 0 to 40/1. Thus there appear to be more island nucleation sites in the material produced from the diluted plasma. The results of the DSC and GE measurements will be dealt with in the next report, when it will be clearer whether the minor structural changes found in the TEM have any implications for the optoelectronic properties.

Table 3

Optical and transport properties for films of a-Ge:H prepared with different degrees of H_2 dilution in the GeH_4 preparation plasma. For other parameters of preparation, see Table 1.

Sample	Flow of H_2 (sccm)	E_{04} (eV)	E_{03} (eV)	$n(2\mu m)$	E_σ (eV)	σ_0 $(\Omega\ cm)^{-1}$	$\eta\mu\tau$ (cm^2/V)
561	30	1.16	1.00	4.22	0.49	1.2E3	1.2E- 9
562	20	1.15	0.99	4.22	0.52	1.6E3	1.9E- 9
563	10	1.15	0.99	4.19	0.50	5.6E2	6.7E-10
564	50	1.16	1.00	4.21	0.50	1.6E3	7.4E-10
565	5	1.14	0.96	4.10	0.49	1.4E3	9.1E-10
566	0	1.15	1.00	4.00	0.48	1.1E3	1.1E- 9
583	40	1.16	1.01	4.11	0.54	3.9E3	3.3E-11

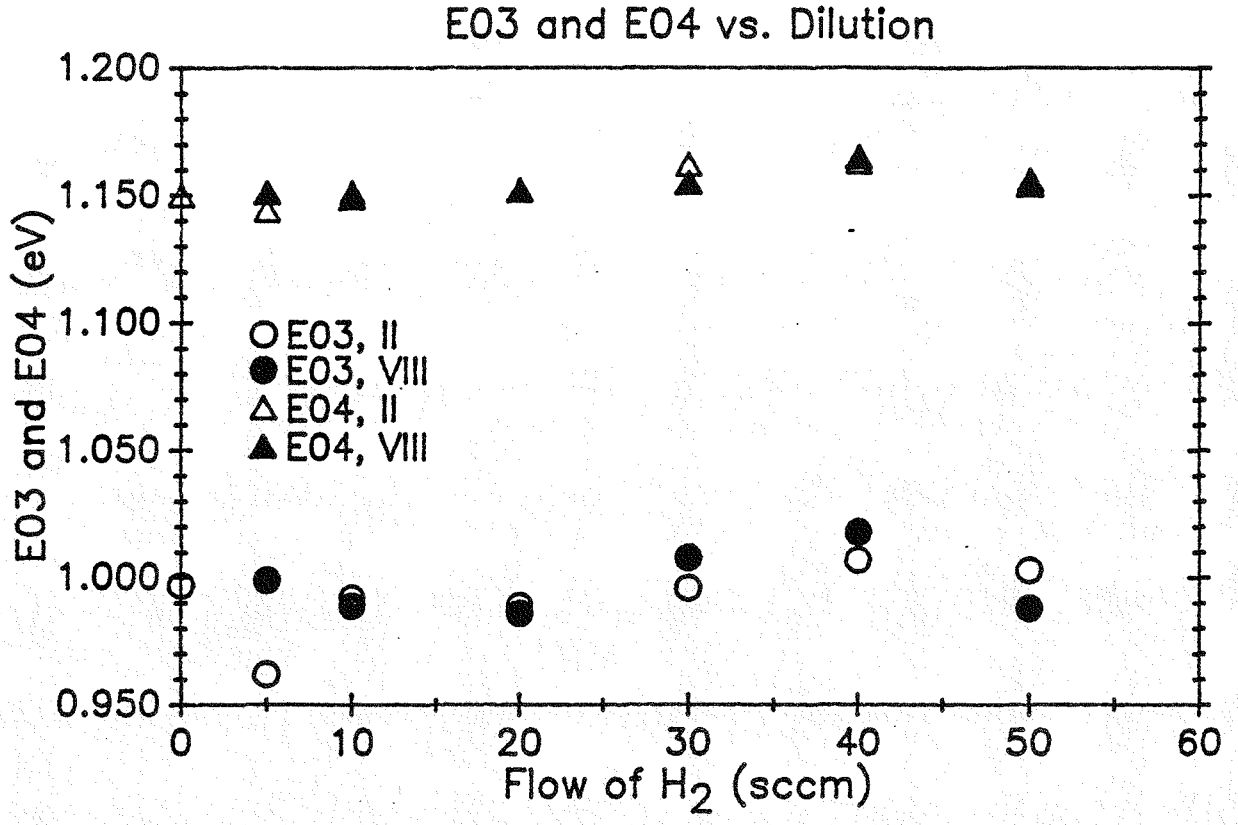

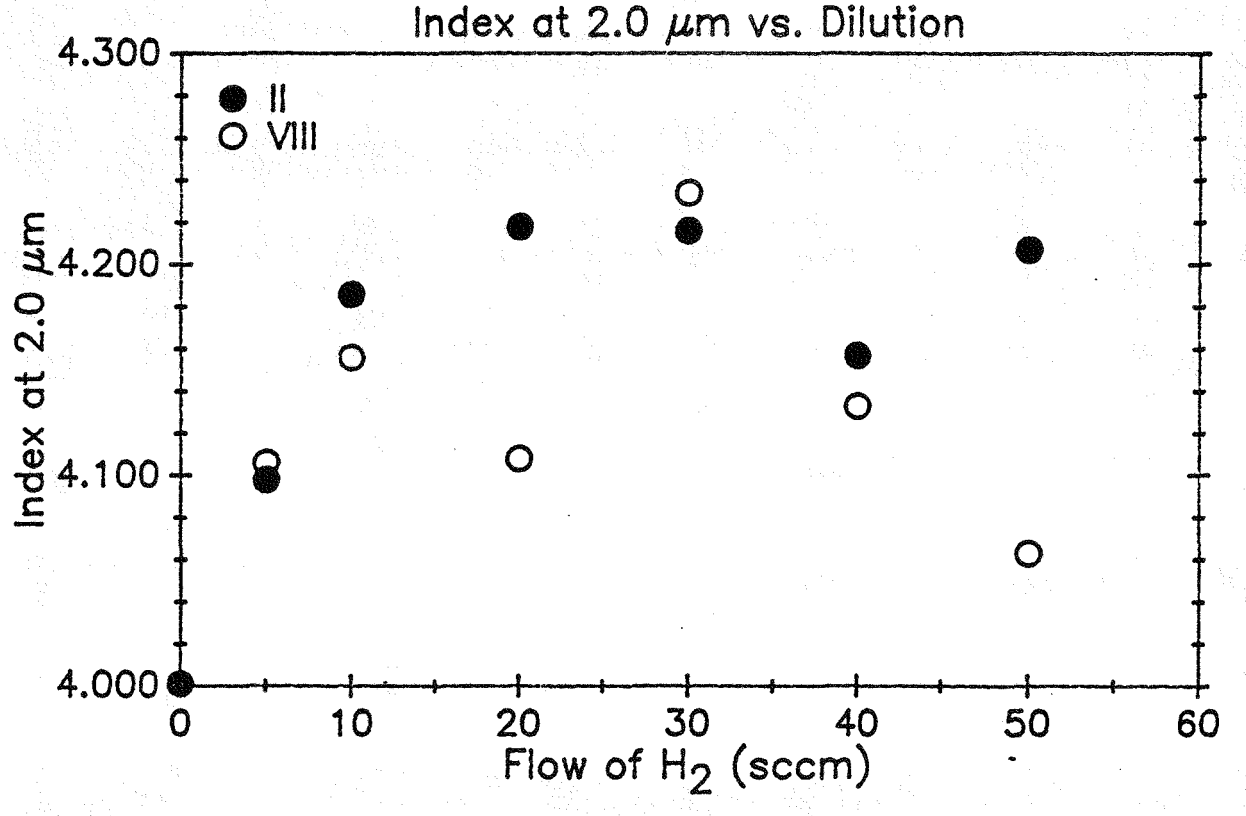

Figure 10. Changes of E_{03}, E_{04} and the refractive index of a-Ge:H prepared with different dilutions of H_2.

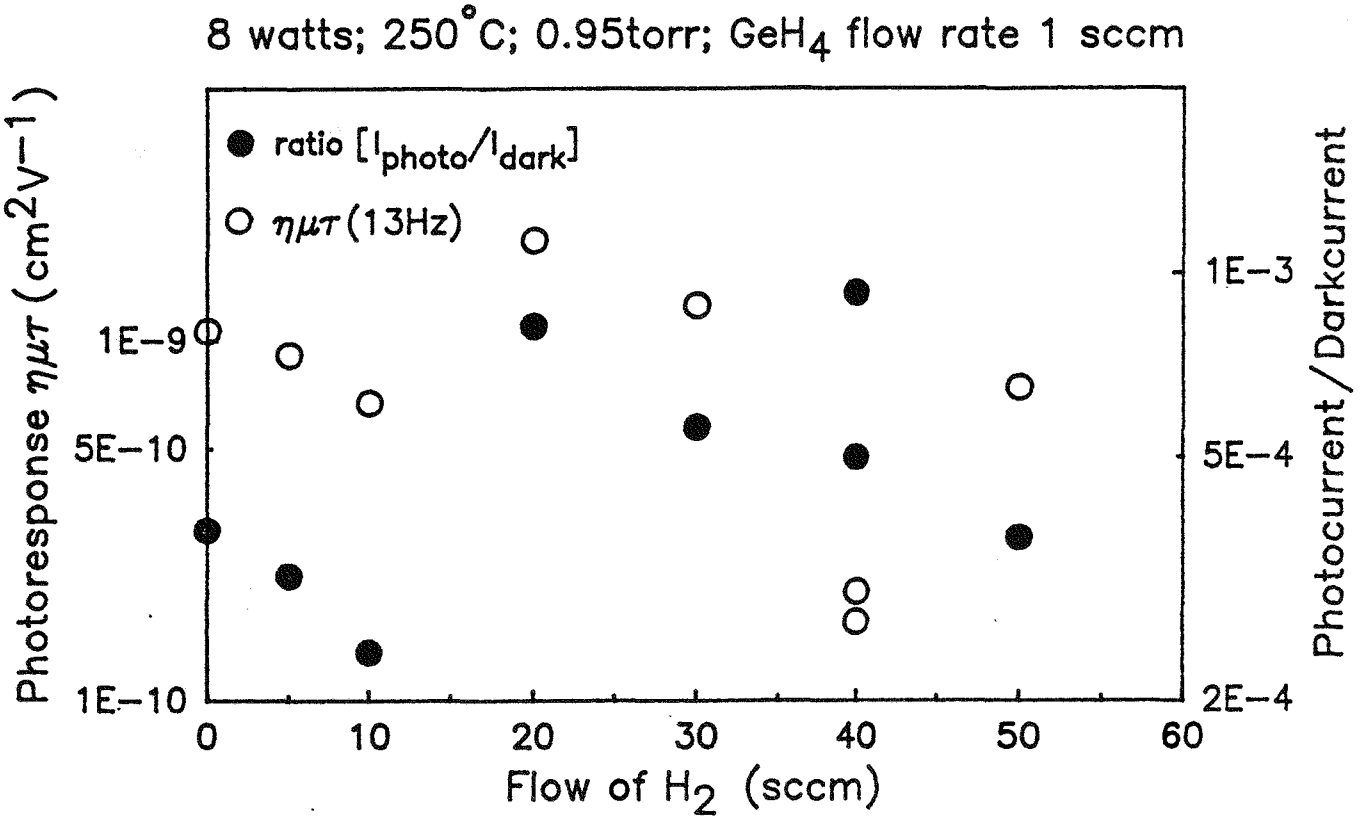

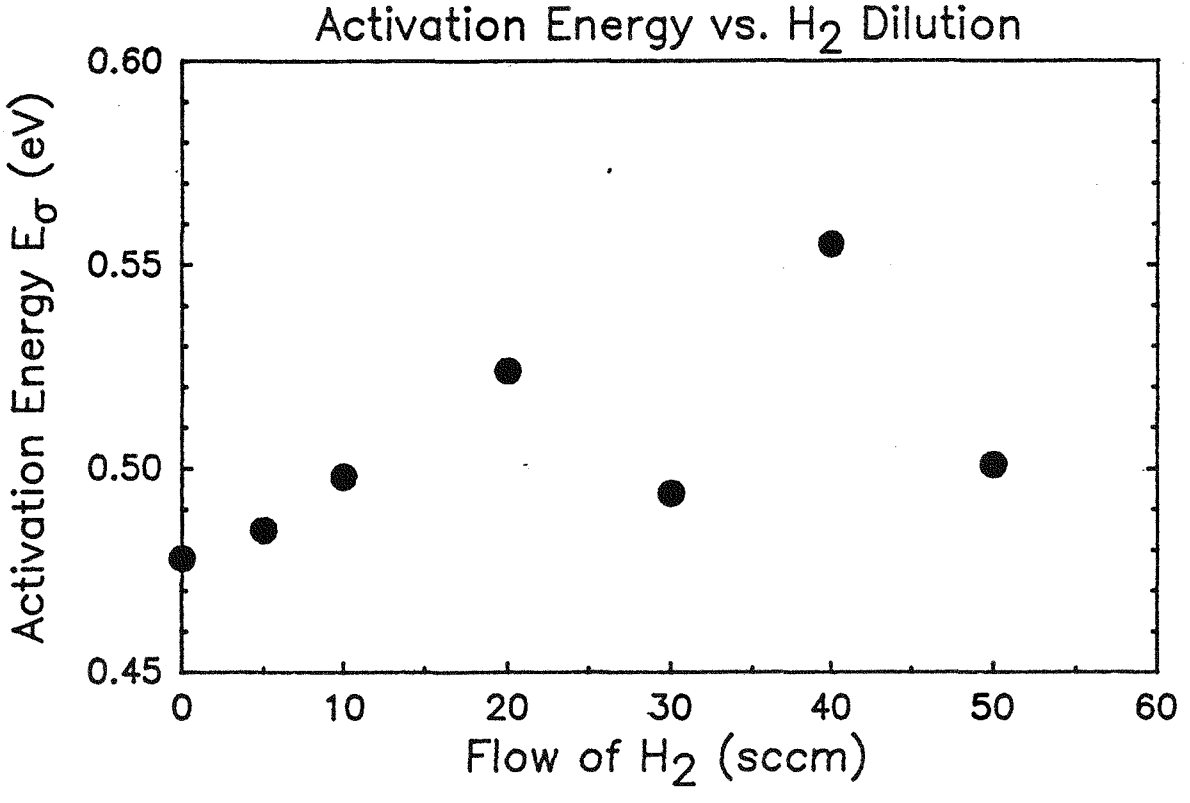

Figure 11. E_σ and $\eta\mu\tau$ of a-Ge:H as a function of H_2 dilution of GeH_4.

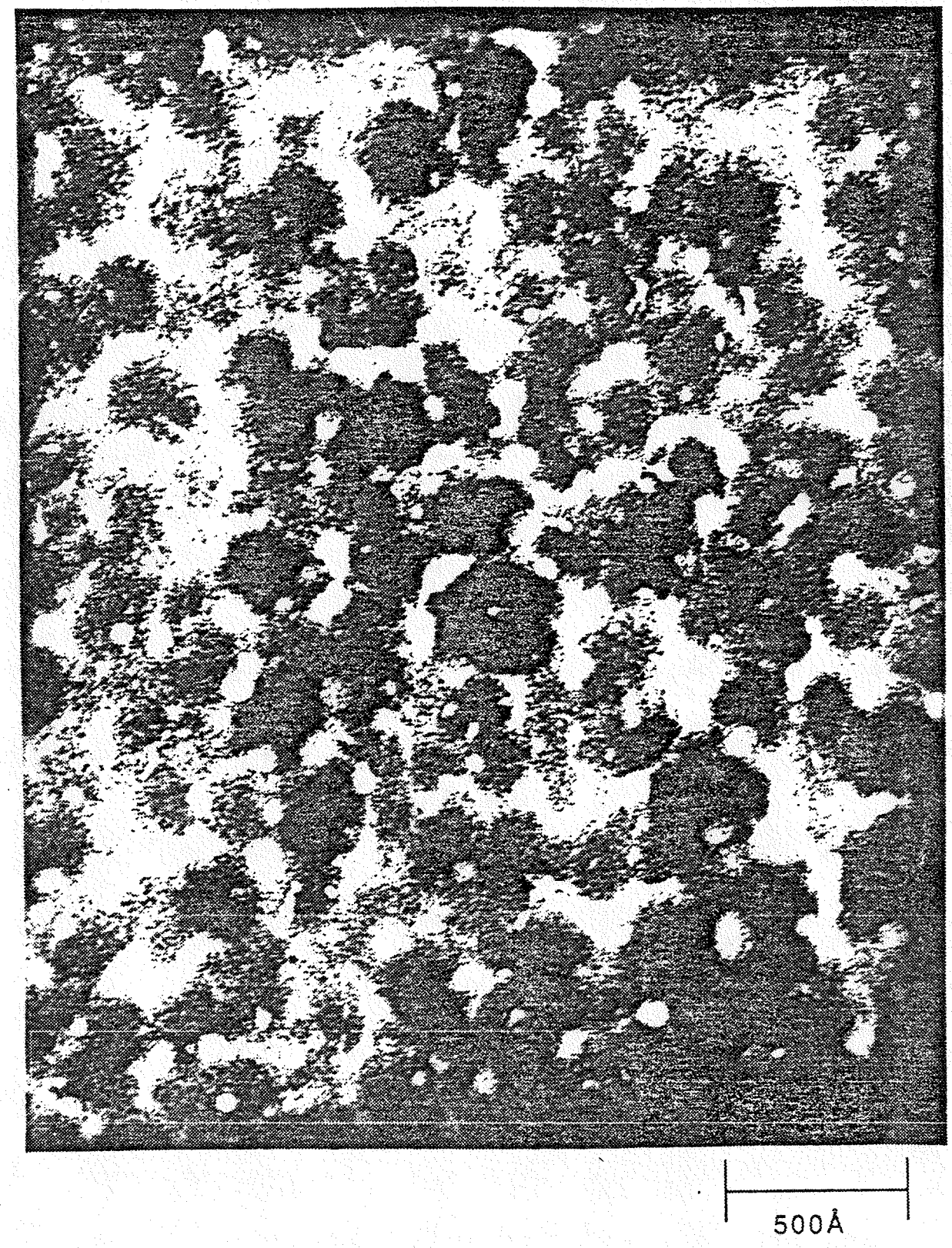

Figure 12. TEM micrograph of 500 Å of a-Ge:H prepared from GeH_4.

a-Ge:H 529 (40:1)

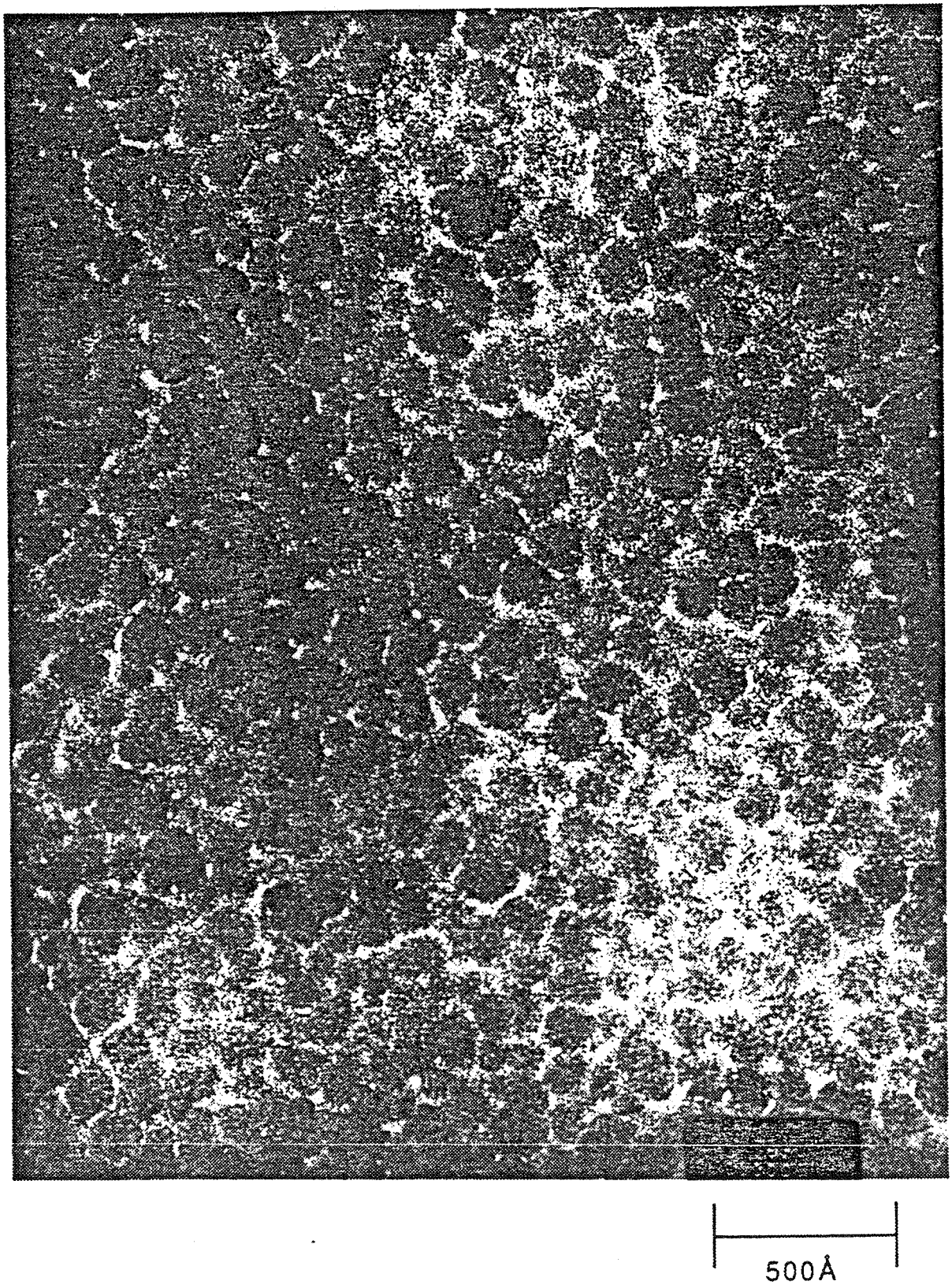

Figure 13. TEM micrograph of 500 Å of a-Ge:H prepared from $GeH_4 + H_2$.

V. *Collaborative Research*

(1) *Washington University, St. Louis, Missouri*

The continuation of our collaboration with the group of Professor Richard Norberg concerns studies of deuteron magnetic resonances in films of a-Si:H:D, a-Ge:H:D and a-$Si_{1-x}Ge_x$:H:D. Such resonances may be interpreted to give information on the structure of the films on a scale of 20-100 A by probing the local surroundings of D (and H) atoms in the inter-grain or void volumes. Here we give only a brief account of the samples prepared and their disposition, leaving the detailed reporting of DMR results to Professor Norberg[4]. The preparation details for samples prepared this year are given in Table 1, and some of our and Professor Norberg's property measurements are reported in Table 4.

(a) Samples of a-Ge:H,D 258 and 511 were measured by the DMR technique. From Table 4, we see that tightly-bound D (TBD), weakly-bound D(WBD) and molecular D_2 were identified. The component of the latter is dominant and also, the total amount of incorporated D is very low in sample 258. The data on molecular D_2 in sample 511 are interpreted to mean that the molecules inhabit very large voids with nearly zero electric field gradients.[4] These observations are generally consistent with our conclusions from our electrical and optical measurements that major deficiencies of our glow-discharge a-Ge:H are a low density microstructure and a lack of adequate compensation of Ge dangling bonds by H. The details of the resonances have been reported by Norberg[4].

(b) Two samples of a-Si:H,D, 480 and 541, were measured by the Norberg group. They are included, along with sample 479 (identical with sample 480) and sample 536 (identical with sample 541 except for the substitution of H_2 for D_2) in Table 1. Our gas evolution (GE) and differential scanning calorimetric measurements (DSC)

Table 4

Properties of samples used in deuteron magnetic resonance experiments.

Sample		DMR concentrations (%)				Evolution concentrations (%)			
		N(D)	TBD	WBD	D_2	H_2	HD	D_2	N(D)
a-Ge:H,D	510					4.7	1.4	0.2	0.9
a-Ge:H,D	511	2.3	0.9	0	1.4				
a-Si:H,D	479					3.5	4.9	3.0	5.5
a-Si:H,D	480	4.0	2.9	0.9	<0.2				
a-Si:H(H)	536					13.1			
a-Si:H,D	541	~5	~4	–	~1	3.4	4.8	2.1	4.5
a-Ge:H,D	258	0.7	0.1	0.3	0.3				
a-Si:D,F	325	3.9	2.8	0.4	0.7				
a-SiGe:D,F	357	2.4	1.5	0.8	0.1				

on sample 479 have already been reported in detail.[1] Sample 480 contained TBD, WBD, molecular D_2 and also a very small fraction of SiD_3 groups. Measurements on rotating SiD_3 groups were reported in preliminary form at the March 1988 New Orleans Meeting of the American Physical Society.[5] The abstract is included here as Appendix D.

Sample 541 yielded many new data on high quality a-Si:H,D, which will be reported in detail in Professor Norberg's Annual Report for 1988. See Tables 1 and 4 for the preparation and property measurements. We summarize here some of the conclusions.

(1) The detection of rotating silyl groups implies the presence of a microcrystalline fraction and/or columnar morphology. No such groups are observed in sample 541 or in our sample of Ge, a-Ge:H,D 511.

(2) The DMR in a-Si produced from SiD_4 or from (SiH_4 + D_2) may be different, consistent with our work (see Section II, above) on the structural and photoelectronic properties of a-Si prepared from either SiH_4 or (SiH_4 + H_4). This work concluded that the microstructures of materials produced from the two sets of plasmas can be quite different, even when most of the as-deposited electrical and optical properties are the same.

(3) The DMR in sample 541 are striking in the very long persistence of phase coherence in echo experiments, which is believed to signify the predominance of very small microvoids, perhaps with diameters of only a few A, and containing single D_2 molecules, whose translational motion is thus severely restricted. Sample 541 was prepared under conditions which we believe yield state-of-the-art a-Si:H.

(c) Samples of a-Si:F,D and a-SiGe:F,D were also measured by the Norberg laboratory.[4] As may be seen in Table 4, TBD, WBD and molecular D_2 are all identified in the DMR spectra. There is TBD in both Si-D and Ge-D configurations in the SiGe alloy but the TBD Ge-D doublet signal is much smaller than the TBD Si-D signal, despite the fact that this is close to a 50:50 alloy. It is suggested that the missing Ge-D signal may be present in an unusually large broad feature associated with D which is weakly bound. From the narrowness of the D_2 line it is inferred that there are quite large microvoids in both a-Si and a-SiGe alloy produced with SiF_4 in the preparation plasma.

Overall, the DMR experiments reveal a richness of detail concerning the D (and H) configurations and their environments in a-Si, a-Ge and their alloys. These results must be considered along with our GE, DSC and TEM data. We note, in particular, the advisability of examining the D environments in samples made from *undiluted* SiD_4 and GeD_4, and of comparing these with the results for samples prepared from (SiH_4 + D_2) and (GeH_4 + D_2).

(2) *Laboratoire d'Optique, Paris, France*

Our collaboration with the group of Dr. M.L. Theye is directed at establishing the absorption at sub-band-gap photon energies of semiconductors such as a-Si:H. Two of the principal measurements used for this purpose are photothermal deflection spectroscopy (PDS) and steady-state photoconductivity (PC). Our work prior to this report period established the importance of measuring samples in the same Staebler-Wronski state, of avoiding surface-related effects by measuring adequately thick samples when bulk absorptive properties were sought, and of recognizing the dangers of deriving absorption spectra from PC data based on the constant photocurrent method (CPM) when two processes of absorption contribute differently to PC over the spectral range studied.

Since, quite often, these spectra are uncritically analyzed to give the density of states in the band gap and to identify the energies of the principal defects, it is essential to recognize that the above-mentioned difficulties exist and that the PC and PDS spectra may emphasize different absorption processes.

Harvard is responsible for making the samples of intrinsic and doped a-Si:H required and for determining their steady-state photoconductivity spectra, while the French group studies the spectra from PDS. Our program during the current period has concentrated on two aspects (1) a comparison by PC and PDS methods of highly P-doped a-Si:H samples, and (2) a study by PDS directed at identifying the location in the sample (bulk, air-film interface, or film-substrate interface) of the measured absorption.

Figures 14-16 present a comparison of PDS and PC measurements on thick and thin films of a-Si:H:P. These are satisfactorily consistent with our earlier measurements,[1] in that they show higher absorption coefficients in PDS than in CPM below 1 eV, and a smaller difference between the thick and thin films than is the case for intrinsic samples. The higher PDS absorption coefficients at low photon energies are attributed to surface and/or interface absorption and to intraband transitions, none of which contribute significantly to PC, and the close accordance between thin and thick films to the predominance of bulk absorption over surface absorption. These results were presented by Dr. Theye at the Chelsea Amorphous Semiconductor Conference.[6] Abstracts of the presentations are included as Appendices E and F.

In connection with this collaborative study of P-doped a-Si:H, films 496, 503, 506, 514, 516 and 517 were also made, in an attempt to discover any structural differences between undoped and doped films. Film 496 showed an evolution spectrum significantly different from that for undoped a-Si:H; however, 503 and 517 gave spectra which were undifferentiable from those for undoped a-Si:H, even though 517 was prepared in 10^4 ppm of PH_3 to SiH_4. We conclude that the structure is relatively unaffected by

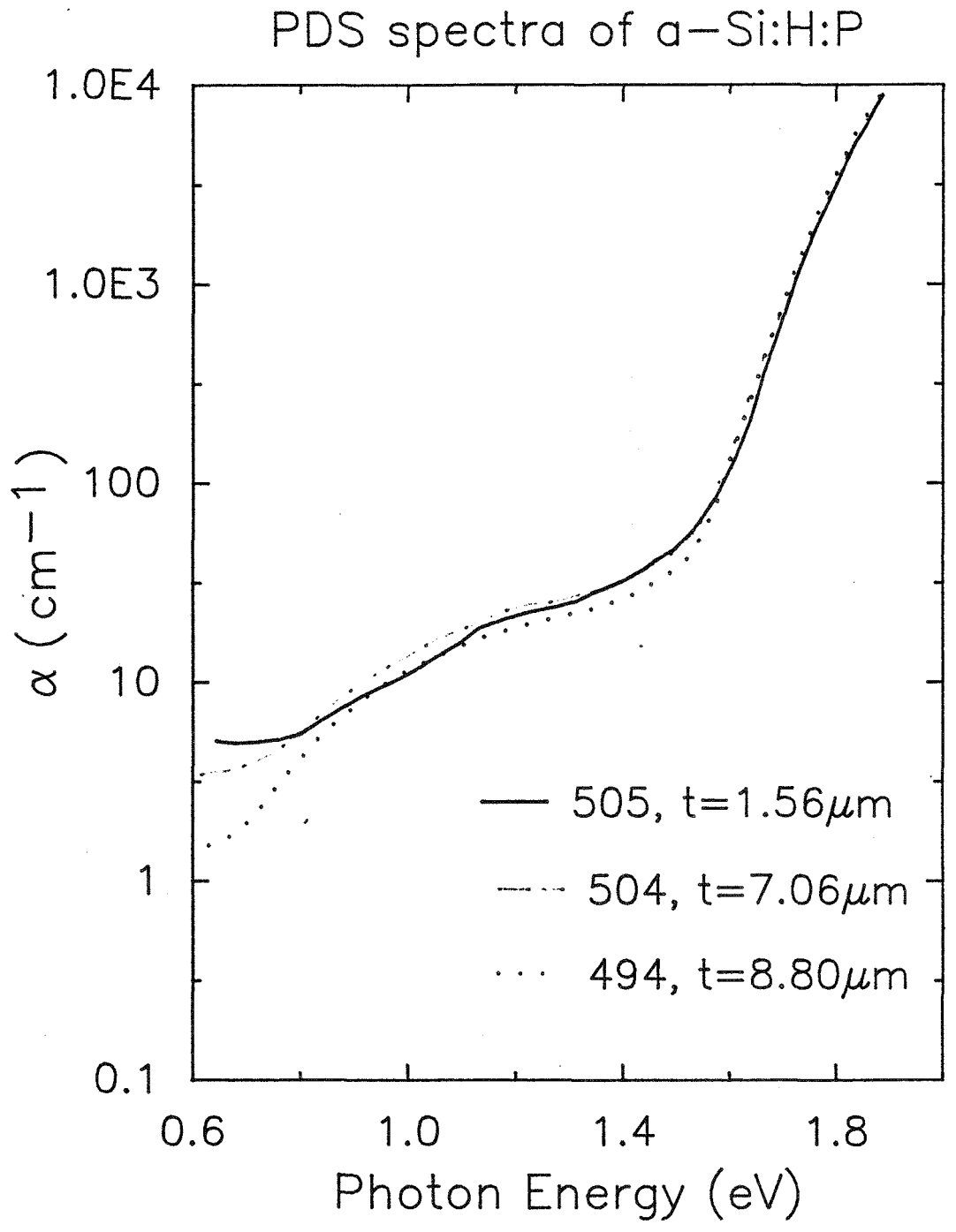

Figure 14. PDS spectra of a-Si:H:P of different thickness.

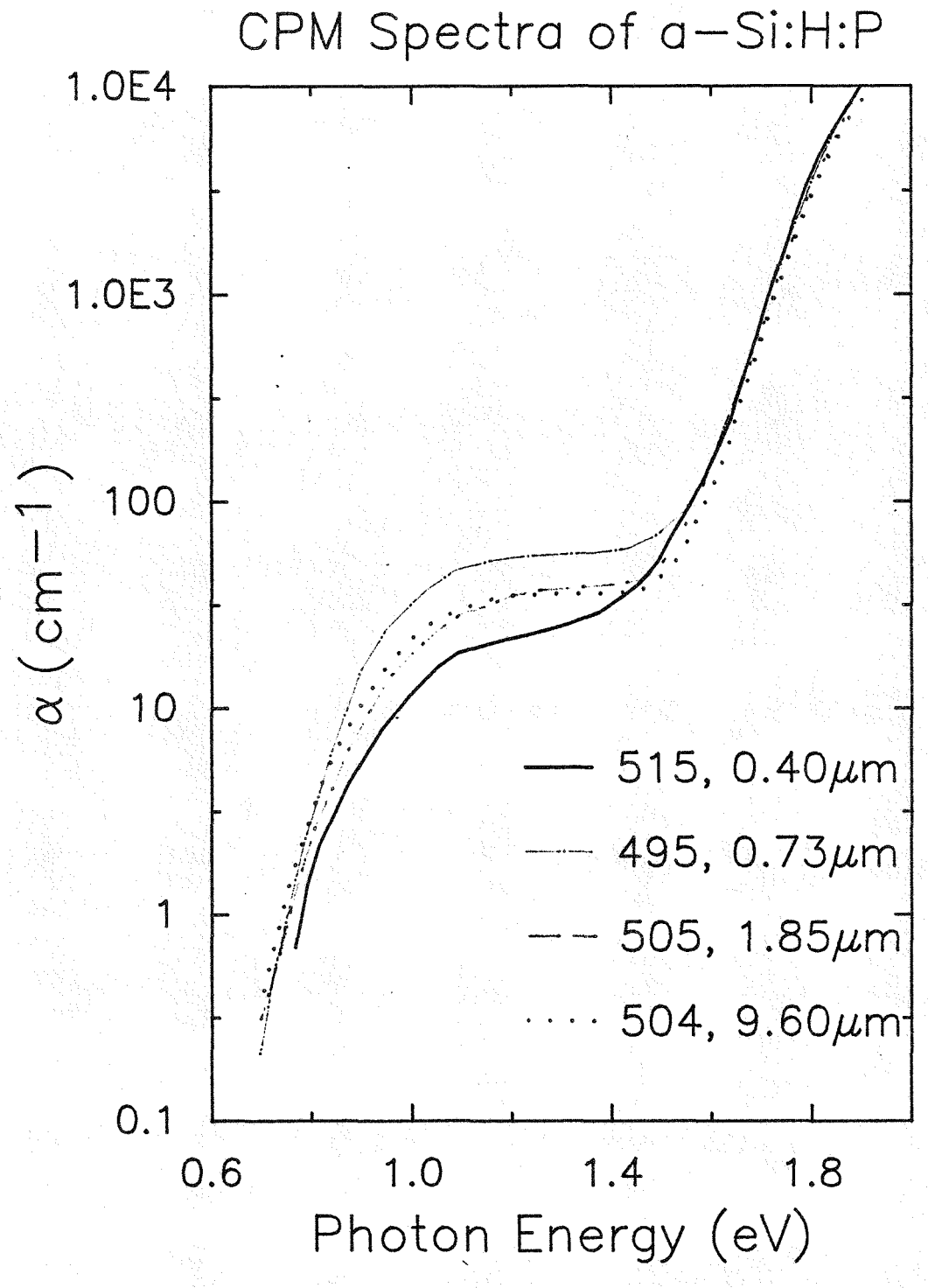

Figure 15. CPM spectra of a-Si:H:P of different thickness.

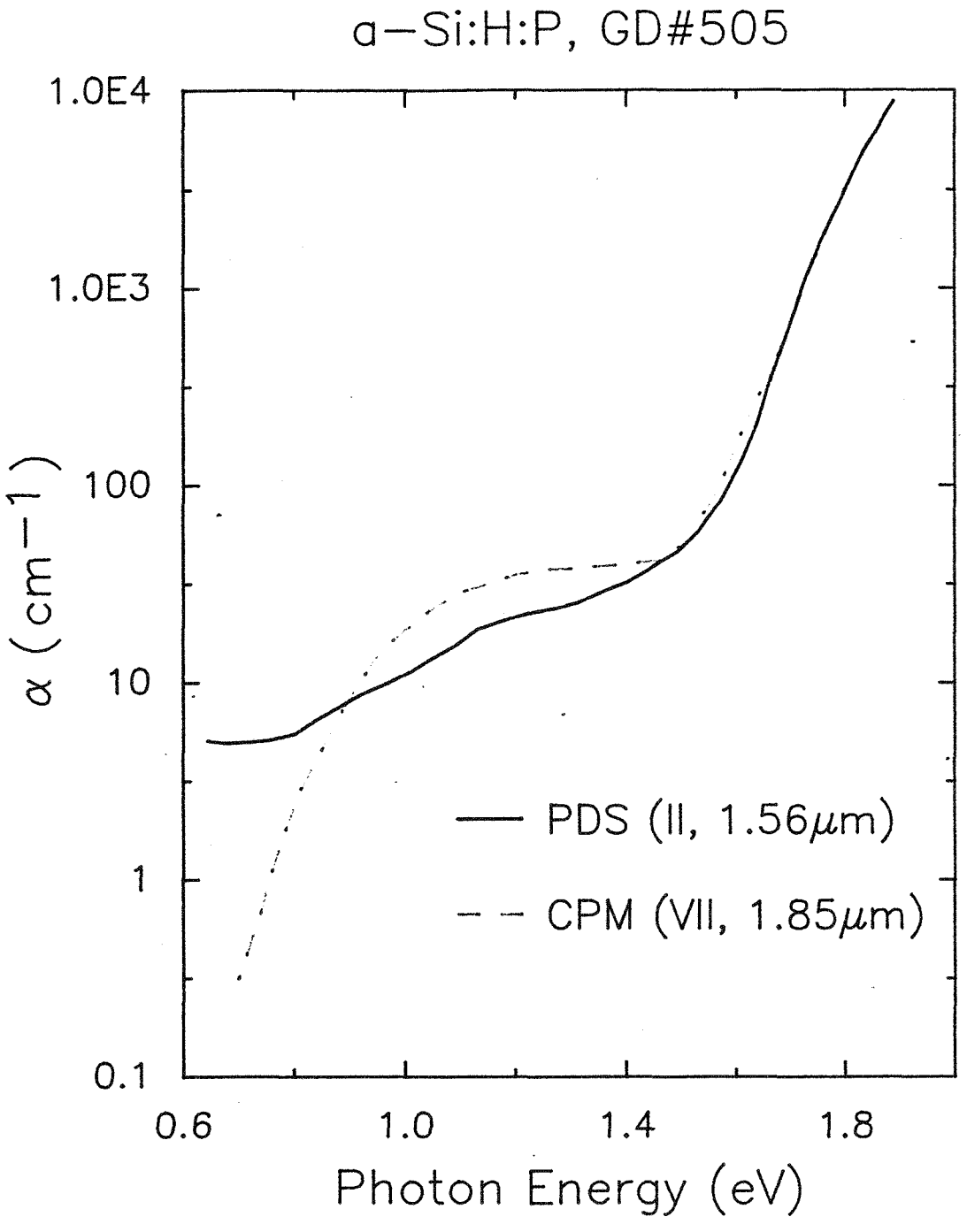

Figure 16. PDS and CPM spectra of a-Si:H:P.

P-doping, in agreement with a result reported earlier by Beyer.[7] [We note that similar gas doping by B_2H_6 has been reported to produce very large displacements of the features in a GE spectrum.[8]] Lightly doped (506) and heavily doped (516) samples were also prepared for TEM studies. The micrographs for the lightly doped sample were not differentiable from those for our optimized a-Si:H made from undiluted SiH_4. The heavily doped 516 came out partially crystallized, but the amorphous regions were not differentiable from undoped material. Thus, on the basis of both GE and TEM studies, we conclude that there are few differences in gross structure between undoped, optimized a-Si:H film and heavily P-doped material.

Sample 514 was produced at a low substrate temperature, so as to have a sub-band-gap absorption comparable to that of P-doped a-Si:H, but also to have its Fermi level near mid-gap. The P-doped films have Fermi levels close to the conduction band edge and it is supposed that transitions from band gap levels to the CB edge must dominate the absorption; by contrast, a film with a Fermi level near mid-gap will also have absorption attributable to electrons elevated from the valence band to the gap states. The PDS spectrum of 514 will be reported in the next Report.

(3) *Tata Institute, Bombay, India*

Our work with the group of Dr. K.L. Narasimhan of the Tata Institute is part of the U.S.-India collaborative effort on materials for solar energy conversion. Its purpose is to investigate barrier layers on a-$Si_{1-x}Ge_x$:H and the band structure offset in a-Si/a-$Si_{1-x}Ge_x$ heterojunctions.

During the past year we have produced more structures of a-$Si_{1-x}Ge_x$:H on c-Si substrates for this project. Measurements have been made on the forward and reverse current characteristics as a function of temperature, and on the capacitance as a function of temperature, bias and frequency, of Schottky barriers of Pd on a-$Si_{1-x}Ge_x$:H. The

barrier height has been determined and the density of states near mid-gap, as well as the origin of the forward and reverse currents. A paper on this subject accepted by the Journal of Applied Physics is included here as Appendix B.

References

1. W. Paul and K.D. Mackenzie, "Research on Amorphous Silicon-Germanium Alloys for Tandem Solar Cells", SERI/STR-211-3351, Solar Energy Research Institute, Golden, CO, 1987.

2. In the report listed under 1, Figure 4 showed the two lower temperature peaks unresolved.

3. R.J. Temkin and W. Paul, Proceedings of Int. Conf. on Amorphous Semiconductors (Garmisch, 1973) p. 1193.

4. R.E. Norberg and P.A. Fedders, "The Structures of Amorphous Silicon Alloy Films", Research performed under SERI Subcontract XB-7-06055-1, Annual Technical Report, Solar Energy Research Institute, Golden, CO, to be published.

5. P. Santos, M.P. Volz and R.E. Norberg, Bull. Am. Phys. Soc. *33*, 663 (1988).

6. Amorphous Semiconductor Conference, Chelsea, England, December, 1987.

7. W. Beyer, in *Tetrahedrally-Bonded Amorphous Semiconductors*, edited by D. Adler and H. Fritzsche (Plenum Press, N.Y. 1985), p. 129.

8. K. Chen and H. Fritzsche, Solar Energy Materials *8*, 205 (1982).

   W. Beyer, H. Wagner and H. Mell, Solid State Commun. *39*, 375 (1981).

COMPARISON OF THE STRUCTURAL, ELECTRICAL, AND OPTICAL PROPERTIES OF AMORPHOUS SILICON-GERMANIUM ALLOYS PRODUCED FROM HYDRIDES AND FLUORIDES

K.D. Mackenzie,* J.H. Burnett, J.R. Eggert,** Y.M. Li and W. Paul

Division of Applied Sciences and Department of Physics
Harvard University, Cambridge, Massachusetts 02138

Amorphous silicon-germanium alloys have been prepared in the same rf glow-discharge reactor from (SiH_4 + GeH_4) and (SiF_4 + GeF_4 + H_2) mixtures at substrate temperatures between 200°C and 400°C. The principal aim of the investigation has been to discover whether preparation of these alloys from fluorides rather than from hydrides will result in better photoelectronic properties, and if so, whether the underlying cause is the substitution of fluorine for hydrogen in the alloy, or some other structure-related alteration of the material. Thus the apparatus, preparation procedures, characterizational techniques, and property measurements follow those of an earlier publication on alloys produced from hydrides alone. The only significant difference in photoelectronic properties found has been an order-of-magnitude improvement of the photoconductivity of alloys with band-gaps near 1.5 eV. Evidence is assembled to assert that fluorine substitution for hydrogen in the alloy is not the cause of the changes in photoelectronic properties, but that these are more probably related to changes in a two-phase heterostructure, which are revealed most directly by transmission electron microscopy. A two-phase, two-transport-path model is proposed to explain the improved photoconductivity obtained with the fluoride-derived alloys.

I. INTRODUCTION

Hydrogenated amorphous silicon (a-Si:H) is presently much investigated as a material suitable for solar cell, electrophotographic, and vidicon applications.[1] For all of these structures, it would be advantageous to have a semiconductor of band-gap somewhat smaller than a-Si:H (e.g., 1.5 eV rather than 1.8 eV) but with substantially the same photoelectronic response as measured, for example, by the mobility-lifetime products for photoelectrons and holes. Alloying Ge with Si (a-$Si_{1-x}Ge_x$:H) gives a material of suitably reduced band-gap, but it is universally found, independent of the method of preparation, that the photoelectronic response is considerably poorer. In an earlier publication,[2] we reviewed the literature on this subject to September 1984, and reported on our own systematic and extensive investigation of a-$Si_{1-x}Ge_x$:H alloys prepared under a variety of conditions over the full composition range. In that paper we described the results of measurements as a function of x of dc conductivity, photoconductivity, optical and ir absorption, photoluminescence, and transmission electron microscopy, and discussed possible reasons for the changes in properties, based on a suggested band structure for the alloys and on the occurrence of increased heterostructure in the films with increasing x.

Since 1983, several research groups[3,4,5,6] have followed up on the discovery by Nozawa *et al.*[7] that preparation by glow discharge of silicon-germanium alloys from mixtures of fluorides and hydrogen ($SiF_4 + GeF_4 + H_2$) improved the photoconductivity of alloys of band-gap near 1.5 eV by about an order of magnitude. This work was based, at least in part, on the pioneering investigation by Madan *et al.*[8] of the properties of a-Si:H:F and a speculation[9] that F might be a better bond terminator *in the alloys* than in unalloyed Si. The investigation reported here concentrates primarily on the preparation of 1.4-1.5 eV band-gap a-$Si_{1-x}Ge_x$:H:F (x: 0.3-0.5) by rf glow discharge of mixtures of ($SiF_4 + GeF_4 + H_2$), in the same reactor as our earlier work on a-$Si_{1-x}Ge_x$:H,[2] and a detailed comparison of the structural, electrical, and optical properties of the two alloy preparations.[6,10-12] We have found that the differences in the electrical and optical properties, and by inference the electronic band structure, are minor (although not insignificant), with the sole exception of the photoconductivity response

which can be improved by up to an order of magnitude.[7] From examination of the properties of F in the alloys (infrared absorption spectra, Raman spectra, electron microprobe) we conclude that substitution of F for H cannot be responsible for the improved photoresponse. From a transmission electron microscope examination of alloys produced from the hydrides and the fluorides we conclude that the two-phase microstructure is different on a scale of 5-20 nm, and we infer that this probably affects phototransport more than it does optical absorption, photoluminescence, or electronic band structure. We adduce preliminary and less direct supporting evidence from studies of the infrared absorption spectra and deuteron magnetic resonance.[13] It is shown that a simple model based on two-phase microstructure is adequate to explain the difference in phototransport in the two alloy preparations.[11]

While this study focusses attention on the differences in microstructure between hydride- and fluoride-produced material as the cause of improved photoresponse in the latter, it also confirms that the changed constitution of the microstructure is responsible, at least in part, for the deterioration of the photoelectronic properties of amorphous Si-Ge alloys, howsoever prepared, from those of a-Si:H.[2] The study leaves unaffected our earlier conclusion[2] that the different density-of-states distributions in all Si-based alloys (of larger or smaller band-gap), based primarily on differences in the energy of dangling-bond states, are likely to lead to a degradation in the photoresponse. Finally, although our present study has confirmed[7] that the use of fluorides plus hydrogen can give material of improved photoresponse, we point out that other gas mixtures not involving fluorides have recently also given good photoresponses.[14] To some extent, the conclusions to be drawn from these recent studies are uncertain where the energy of the Fermi level has not been reported, but viewed overall, they suggest the necessity for more detailed examination of the structure of the alloys and its relation to the totality of conditions in the preparation plasma and at the film growth surface.

II. APPARATUS AND PROCEDURE

In our earlier paper[2] we discussed in detail our glow-discharge reactor, the method of sample deposition, and the characterization and measurement of properties of the samples. Here we shall discuss only the changes necessary in preparing a-$Si_{1-x}Ge_x$:H:F from mixtures of (SiF_4 + GeF_4 + H_2). The SiF_4 and GeF_4 were both of 99.99% purity and the H_2 of 99.999% purity.[15] The composition x depends very differently on the ratio of GeF_4 to SiF_4, and on the rf power, than it does on the ratio of GeH_4 to SiH_4, and the rf power, in the preparation of a-$Si_{1-x}Ge_x$:H. We conclude that GeF_4 molecules are much more easily dissociated than either SiF_4 or H_2. Thus low rf power results in Ge-rich films with poor photoelectronic properties. Based on such studies, the following conditions were adopted to produce alloys with $x \approx 0.5$: rf power density of 430 mW/cm^2, total pressure of 0.41 torr, and flow rates of 34.8 SCCM for SiF_4, 0.7 SCCM for GeF_4, and 6.0 to 15.0 SCCM for H_2. Minor adjustment of the GeF_4 flow rate gives alloys of different x. While the power densities used are an order of magnitude greater than in the preparation of a-$Si_{1-x}Ge_x$:H, the deposition rates are approximately the same, i.e., 1-3 A/s.

In contrast to our production of a-$Si_{1-x}Ge_x$:H from hydrides, the composition (x) of our $Si_{1-x}Ge_x$:H:F films varies across the 10 cm diameter substrate platform. This resulted very probably from the low ratio of GeF_4 to SiF_4 in the gas mixture and from the slightly asymmetric arrangement for the introduction of the reactant gases. For a typical set of deposition parameters, the Ge content, x, varies from 0.3 to 0.5 on the substrate platform and by $\pm$ 0.01 over a typical substrate dimension of about 1 cm. The Ge content variation across the platform is far greater than in our production from hydrides (there the variation is not detectable on the scale of the estimated 1% accuracy of our electron microprobe composition determination). However, in an extensive series of tests, we have found that the variation is very reproducible from run to run. Our usual procedure is to codeposit a number of samples for different property measurements. A sample for a particular property measurement is always taken from a predetermined location on the substrate platform. This, combined with our procedure of measuring composition (whenever practicable) on the actual film whose property is being measured, has permitted

us to determine systematically the changes in properties with x.

The properties measured on the alloys included electron microprobe analysis of the Si, Ge, and F contents, secondary ion mass spectroscopy (SIMS) analysis of the impurity distribution in selected films, infrared vibrational spectra from which the H and F content and configuration could be inferred, transmission electron microscopic (TEM) examination of 50 nm thick films on C-coated Ni microgrids, electrical conductivity measurements between room temperature and 475 K, optical absorption spectra in the visible and near infrared regions, photoconductivity spectra between 0.8 eV and 1.5 eV from which absorption spectra could be inferred, transient photoconductivity by the time-of-flight (TOF) method using a sandwich configuration to determine electron drift mobilities, μ, and electron drift mobility-lifetime ($\mu\tau$) products and also details on the conduction band tail, [10-12,16-17] photoluminescence spectra at 77 K, Raman spectra, space-charge-limited current measurements on $n^+ - i - n^+$ sandwich structures,[18] electron spin resonance determination[19] of neutral dangling bond densities, and measurements of deuteron magnetic resonance.[13] The details of the majority of the experimental techniques have already been given[2] and need not be repeated here.

III. CHEMICAL COMPOSITION OF FILMS PRODUCED FROM HYDRIDES AND FLUORIDES

The rf glow discharge apparatus[20] was constructed and operated so as to minimize the incorporation of unwanted species such as O. The base vacuum was 3×10^{-8} torr, the gases were the purest available and a residual gas analyzer was used periodically to monitor the gas mixture in the reactor. On selected films SIMS measurements[21] were made. Figure 1 shows the spatial distribution of the principal elements, but not their absolute concentration, as that requires calibration factors which are not reliable. It is clear that the spatial distribution is uniform over most of the film.

An electron microprobe[22] was used to determine the atomic concentration of Si, Ge, and F. The concentration of F was of the order of 1 atomic (at.)% in all of the films produced from fluorine-containing gases. The concentration of H was estimated from the area under the wagging mode of the infrared vibrational absorption spectra; as an example, it was of the order of 5 at.% for a 50:50 alloy, whether prepared from hydrides or fluorides. No attempt was made to determine the concentration of H more accurately by other techniques, as it is our observation that films of good photoelectronic properties can have a wide range of acceptable concentrations of H, so that only a very low atomic percentage (say, less than 2-3%) or a very high atomic percentage (say, larger than 15%) merits special concern. Of course, a large *variation* in the concentration of H among different films (which did not occur) implies changes in many other material properties, including the energy gap. The configuration of bonded H in the films, as revealed by the details of the stretching vibrational absorption (the occurrence of 2090 cm^{-1} Si-H and 1975 cm^{-1} Ge-H modes) and the presence of bending modes (between 800 and 900 cm^{-1}) is regarded as a more significant indicator of film quality than the absolute concentration of H.

IV. VARIATION WITH T_s OF THE PROPERTIES OF a-$Si_{0.5}Ge_{0.5}$:H AND a-$Si_{0.5}Ge_{0.5}$:H:F

In our earlier paper,[2] we discussed the variation of the optical energy gap, the photon energy of the maximum photoluminescence, the intensity of the peak in photoluminescence, the magnitude of the photoconductivity at 1.96 eV, and the hydrogen content as a function of deposition temperatures T_s between 200 and 400°C. We concluded that all of the results could be explained as a competition between two effects of increase in T_s: increased healing of defects and disorder, and decreased incorporation of H in the film. A similar but less extensive study was carried out for the fluoride-derived samples. As observed previously for hydride-derived a-$Si_{0.5}Ge_{0.5}$, the hydrogen content decreases monotonically with increasing T_s. However, the decrease is much less. For example, the hydrogen content changes from about 7 at.% at T_s of 200°C to about 4 at.% at 350°C compared to a change from about 13 at.% at T_s of 230°C to about 4 at.% at 350°C. The optical gap is essentially independent of T_s in contrast to our results for a-$Si_{0.5}Ge_{0.5}$:H that indicated a linear decrease in gap with increasing T_s. Significantly different results were obtained for the photoluminescence (PL). Figure 2 shows the variation of the energy E_{PL}, the FWHM ΔE_{PL}, and the intensity I_{PL} of the photoluminescence peak for a series of a-$Si_{0.5}Ge_{0.5}$:H:F alloys for T_s between 200 and 350°C, and compares them with those for a-$Si_{0.5}Ge_{0.5}$:H produced in the same system from (SiH_4 + GeH_4). All PL measurements were done at 77 K using 2.41 eV excitation following our standard procedure.[23] Based on the near-constancy of the PL parameters for the fluoride-derived samples near and above 300°C, and the fact that T_s = 300°C optimized the photoconductivity and photoluminescence of the hydride-derived films, we adopted a T_s of 300°C for the bulk of our measurements on the fluoride-derived alloys. We postpone further comment on the details of Figure 2 to the Discussion section.

V. VARIATION WITH x OF THE ELECTRICAL AND OPTICAL PROPERTIES OF a-$Si_{1-x}Ge_x$:H AND a-$Si_{1-x}Ge_x$:H:F

Figure 3 compares the optical absorption edges of a-$Si_{1-x}Ge_x$:H and a-$Si_{1-x}Ge_x$:H:F. Between $h\nu = 0.8$ and roughly 1.5 eV, the spectra are deduced from the spectra of photoconductivity using the constant photocurrent method.[24] The photoconductivity-derived part of the absorption spectrum is normalized to the part from direct optical transmission measurements in the range of overlap at higher photon energies near an α of $10^3 cm^{-1}$. We shall not address here legitimate questions that arise concerning the derivation of an absorption spectrum from a photoconductivity spectrum, since the significant fact for our present purpose is that the spectra for hydride- and fluoride-derived material of similar x practically coincide. From such absorption edges, we deduce three parameters:

(1) the energy gap E_g, derived from the extrapolation of the part of the edge above $10^3 cm^{-1}$ to zero absorption coefficient using the formula[25]

$$(\alpha h\nu)^{1/2} = A(h\nu - E_g);$$

(2) the energy E_{04}, the photon energy at which $\alpha = 10^4 cm^{-1}$, which is also a conventional measure of the energy gap; and

(3) the energy E_0, the so-called Urbach parameter in the exponential region of the edge, derived from the formula

$$\alpha = B \exp\left\{\frac{h\nu - E_g}{E_0}\right\} .$$

Figure 4 shows the variation with x of E_g, E_{04}, and E_0. The variations of E_g and E_{04} are identical for the two types of material. E_g follows the empirical relation $E_g = 1.76 - 0.78x$. If one excludes the points for $x = 0$ for the fluoride-derived material (where there was no attempt to optimize preparation conditions) then the Urbach parameter E_0 is the same for the two

preparations for $0.2 < x < 0.6$.

In Figure 3 the sub-band-gap absorption ($h\nu < 1.4$ eV) is the same for $x \approx 0.3$ for the two preparations of material. For other values of x, the values of α at photon energies about 0.5 eV below the absorption edge are always comparable for the two preparations; for example, for $x \approx 0.5$ the values of α at $h\nu = 0.9$ eV are 7 cm^{-1} for the hydride-derived and 14 cm^{-1} for the fluoride-derived films.

Figure 5 illustrates the dependence on x of two PL parameters for the two preparations of material.[26] The variations of I_{PL} with x are virtually identical, but those of ΔE_{PL} are quite different: there is considerable scatter in the values but the FWHM is consistently smaller in the fluoride-derived material. Examination of the spectra for these fluoride-derived samples, as well as for the hydride samples previously reported, shows no evidence for a "universal low energy tail" as reported by Gal *et al.*[27] In recent work of Street *et al.*[28] on a-$Si_{1-x}Ge_x$:H, such a tail is observed but only for a small group of the total samples investigated.

Figure 6 shows representative data of activated dark conductivity σ versus inverse temperature for samples with $x \approx 0.5$ prepared from the different gas mixtures. All specimens were heated under vacuum to about 200°C for 30 minutes before the measurements were performed, in order to ensure that any photoproduced defects were annealed out.[29] In all transport measurements, checks were made for a linear variation of current with the voltages used. The conductivity is given by the expression

$$\sigma = \sigma_{00} \exp\{(E_f - E_c)/kT\}$$

If we use the approximate (but usual) description

$$E_f - E_c = (E_f - E_c)_0 + \gamma T$$

then

$$\sigma = \sigma_{00} \exp\left[\frac{\gamma}{k}\right] \exp\left\{\frac{(E_f - E_c)_0}{kT}\right\} .$$

We then focus on the dependence on x and preparation plasma of three parameters or observables (1) the activation energy $E_\sigma = (E_c - E_f)_0$; (2) the pre-exponential $\sigma_0 = \sigma_{00}\exp(\gamma/k)$, where σ_{00} is a function of conduction band state density, temperature, and band mobility; and (3) the occurrence of a downward kink in log σ *vs.* $1/T$ at high temperatures. In Figure 6, this is seen to occur near $10^3/T = 2.3\ K^{-1}$; it must be emphasized that such a kink is a long-studied feature seen in many of the amorphous silicon and germanium films, both hydrogenated and unhydrogenated, and not an artifact of our apparatus or procedure.[30] Practically all of the alloys, whether grown with fluorine present or not, show a downward kink in log σ *vs.* $10^3/T$ for $10^3/T \leq 2.3\ K^{-1}$.

Figure 7 compares the variation of σ_0 with E_σ (a " Meyer-Neldel[31] plot") for alloys with a range of x values produced from the two different gas mixtures. While this variation is linear, inside of scatter, for a-$Si_{1-x}Ge_x$:H, that for a-$Si_{1-x}Ge_x$:H:F divides into two groups which straddle the data for a-$Si_{1-x}Ge_x$:H.

Figure 8 shows the variation of $(E_g/2 - E_\sigma)$ with x for the two types of material. For both types, the activation energies are within 100 meV of half of the gap. For the hydride-produced material, the Fermi level stays essentially at gap-center. For the fluoride-produced films, the Fermi level usually lies above the center of the gap and there is more scatter in its position.

In order to extend our knowledge of the relative gap densities-of-states in hydride- and fluoride-derived alloys we have carried out space-charge-limited-current measurements[18] for samples with $x \approx 0.5$ and have compared them with those for a-Si:H. Whereas the latter samples had a density-of-states just above the Fermi level of $10^{16}cm^{-3}eV^{-1}$, the density for a-$Si_{0.5}Ge_{0.5}$:H and a-$Si_{0.5}Ge_{0.5}$:H:F was about $10^{17}cm^{-3}eV^{-1}$. All of the samples were measured in a sandwich geometry and the results found to be repeatable on samples from different runs.

Finally, the dangling bond densities have been determined by electron spin resonance in samples with $x \approx 0.5$ produced from both hydrides and fluorides.[19] The first results for samples of a-$Si_{0.5}Ge_{0.5}$:H gave a Ge dangling bond density of $6 \times 10^{17}cm^{-3}$ and a Si dangling bond

density of 2×10^{16}cm^{-3}. For three sets of a-$Si_{1-x}Ge_x$:H:F samples, where the x-value varied from 0.20 to 0.47, a Si dangling bond density between 5×10^{16}cm^{-3} and 10^{17}cm^{-3} was found but, surprisingly, no signal at the g-value of the spin resonance from electrons on Ge dangling bonds. This intriguing result is being followed up (see Section VIII), but we note here simply that there is no evidence from the current measurements of a drastic reduction in the total dangling bond density when the alloys are made from mixtures of fluorides.

VI. VARIATION WITH x OF THE PHOTORESPONSE OF a-$Si_{1-x}Ge_x$:H AND a-$Si_{1-x}Ge_x$:H:F

Figure 9 presents the results for the (quantum-efficiency)(mobility)(lifetime) product, or $\eta\mu\tau$, deduced from our measurements of photoconductivity at room temperature on annealed (Staebler-Wronski A state)[29] samples illuminated by a flux of 10^{15} photons/cm^2-s of 1.96 eV radiation. Included are the x-dependent $\eta\mu\tau$ of our earlier study,[2] our measurements on a-$Si_{1-x}Ge_x$H:F, and data from the Shimizu group.[32] All values of $\eta\mu\tau$ are corrected to take account of the penetration depth of the light. The crucial point made in this figure is that the $\eta\mu\tau$ product is almost always larger, sometimes by an order of magnitude, in the fluoride-derived samples of roughly 50-50 composition. These results suggest that an improved photoresponse from a-Si-Ge can be achieved by preparation from fluoride-sources gases. Two important points must be made and considered. The magnitude of the $\eta\mu\tau$ product can be very sensitive to the position of the Fermi level. Recognizing this fact, we have shown in Figure 8a the variation in Fermi level, depicted as a departure of E_F from the center of the gap, for both hydride and fluoride-produced samples, and in Figure 8b the variation of $\eta\mu\tau$ for an expanded set of fluoride-produced samples as a function of their Fermi-level position. It is evident that there is no correlation between the magnitude of $\eta\mu\tau$ and the Fermi-level position for the fluoride-produced samples. The second point concerns the photoconductivity experiment itself. All the measurements in this work were performed using (Cr) contacts in a coplanar geometry and 1.96 eV radiation which penetrates only a small fraction (~ 0.1-0.2 μm) of the total thickness (2-4 μm) of the higher Ge content samples. This suggests the possibility that the 'improved' photoresponse may be associated with some surface-related phenomena, e.g., surface band bending, contact effect or surface states rather than an overall improvement in the bulk properties. (For a recent discussion of this problem related to a-Si:H and a-Ge:H, see reference 33). To test for surface-related effects, two further experiments have been conducted.[10-12] The first experiment involved the re-measurement of the steady-state photoconductivity in the coplanar electrode configuration using penetrating (1.5 eV) radiation to probe the bulk. The $\eta\mu\tau$ from steady-state photoconductivity is derived from

$$I = |e| F_0 l A(\eta\mu\tau) V/d$$

where I is the photocurrent for an applied voltage V, d is the separation of the coplanar contacts and l their length, A the absorptance (1-T), T the transmittance and F_0 the density of photons/cm^2-s entering the sample. Empirically, I varies as $(F_0\alpha)^\gamma$ where α is the absorption coefficient, which implies that $(\eta\mu\tau) \propto (F_0\alpha)^{\gamma-1}$. We have chosen arbitrarily to refer all $(\eta\mu\tau)$ determinations to $(F_0\alpha) = 10^{19}$photons/cm^3-s at a photon energy of 1.5 eV, and so put

$$(\eta\mu\tau)^{1.5}_{10^{19}} = (\eta\mu\tau)^{1.5}_{meas}\left\{\frac{(\alpha F)^{1.5}_{meas}}{10^{19}}\right\}^{1-\gamma}$$

This permits comparison of $(\eta\mu\tau)$ under the same conditions of created carrier density, thus making a first-order correction for the statistics of trapping and recombination. The explicit flux dependence of $(\eta\mu\tau)$ at any photon energy has also been experimentally confirmed. The second experiment, transient photoconductivity by the TOF method, was used as an alternative technique to determine $\mu\tau$ for electrons in the bulk, where possible on samples co-deposited with the steady-state photoconductivity specimens. For the TOF experiments,[16] 2-5 μm thick sandwich structures were produced consisting of 100 nm of Cr on Corning 7059 glass, the alloy, and a 10-20 nm, 3 mm diameter, semitransparent top Cr Schottky contact. In this experiment, a weak 8 ns pulse of 3.68 eV radiation from a nitrogen laser creates an electron-hole density of approximately 10^{15}cm^{-3} to a depth of about 100 nm in the samples beneath the semi-transparent electrode. A reverse bias electric field pulse (– 7 ms), E, is applied to the top contact about 20 to 200 μs before the laser pulse, i.e., in a time interval much less than the samples' dielectric relaxation time. This field extracts the electrons through the sample to the opposite (collecting) contact and the resulting phototransient, $I(t)$, is recorded with a digitizer interfaced to a computer. The repetition rate of the laser is about 1 Hz. The integrated collected charge Q (= $\int I(t)dt$) is determined as a function of the applied field, E. The electron $\mu\tau$ product may be found by fitting the Q *vs.* E plot to the Hecht[34] relation when all the electrons are collected, i.e., for low Ge contents, $x \leq 0.26$. For larger Ge contents, severe carrier loss prevents complete charge collection

even at large E, and only the initial (low E) part is used. Decrease in the dielectric relaxation time with increasing conductivity and x-value necessarily limits our $\mu\tau$ determination to x-values of 0.4 or smaller. As for the steady-state experiments, the TOF measurements were taken in the Staebler-Wronski A state.[29]

Figure 10 summarizes the results from the two experiments. The x-dependence of $\eta\mu\tau$ for the fluoride- and hydride-derived material is similar to that shown in Figure 9, with the fluoride-derived material still possessing a superior photoresponse in the region $x \approx 0.5$. Thus surface-related effects in this x-range are negligible. Independent confirmation of this result is suggested from analysis of TOF data[16] which indicate that while the depletion layer widths are about 1 μm for $x \approx 0$, they decrease rapidly down to about 0.1 μm at $x \approx 0.4$, with surface band-bending of a few hundredth's of an eV. The $\mu\tau$ products from TOF are about two orders of magnitude lower than the $(\eta\mu\tau)$'s deduced from steady-state photoconductivity, in the range of overlap $0.25 < x < 0.35$. This apparent discrepancy will be taken up in Section VIII. For a-$Si_{1-x}Ge_x$:H, the $\mu\tau$ products from TOF show a similar monotonic decrease with increasing x to that reported recently by Karg *et al.*[35] and Street *et al.*[28] Also, the behavior of $\mu\tau$ with x parallels that of $\eta\mu\tau$. The admittedly sparse data for $\mu\tau$ by TOF for a-$Si_{1-x}Ge_x$:H:F are comparable in magnitude to those for a-$Si_{1-x}Ge_x$:H.

VII. VARIATION WITH x OF THE STRUCTURAL PROPERTIES OF a-$Si_{1-x}Ge_x$:H AND a-$Si_{1-x}Ge_x$:H:F

In this section, we report an extension of our earlier studies of infrared vibrational absorption and transmission electron microscopy[36] in a-$Si_{1-x}Ge_x$:H to similar studies on a-$Si_{1-x}Ge_x$:H:F. Figure 11, drawn from our earlier paper,[2] shows the principal H-related features of the spectrum: stretch modes of Si-H at 2090 cm^{-1} and 2000 cm^{-1}, and of Ge-H at 1975 cm^{-1} and 1875 cm^{-1}; bending modes in the region of 800-900 cm^{-1}; and a broad wagging vibration of Si-H and Ge-H centered on 630 cm^{-1}. With increasing T_s, the 2000 cm^{-1} Si-H mode and the 1875 cm^{-1} Ge-H mode dominate the stretch-mode spectrum and the bending modes disappear. In all of the spectra the Si-H modes dominate those of Ge-H in a ratio of approximately 8:1. A fuller description of these absorptions and their interpretation has already been given and will be discussed in Section VIII.

Figure 12 shows for comparison the infrared spectra of a-$Si_{0.5}Ge_{0.5}$:H:F and a-$Si_{0.5}Ge_{0.5}$:D:F prepared at $T_s = 300^{\circ}C$. The displacement of the H-related features at 2000 cm^{-1}, 1875 cm^{-1}, and 630 cm^{-1} to approximately $1/\sqrt{2}$ of these frequencies on replacing H with D is evident. It is clear that there are no *major* absorption frequencies to be associated with F, but that *minor* features near 1240 cm^{-1} and 1100 cm^{-1} may be so connected. Figure 13 shows an FTIR transmission spectrum of an a-$Si_{0.5}Ge_{0.5}$:D:F sample between 400 and 1400 cm^{-1}. The peaks in absorption are superimposed on a spectrum showing interference fringes. The dip at 1350 cm^{-1} is assignable to Ge-D, that at 630 cm^{-1} to a bending mode of Si-D_2, and that near 1240 cm^{-1} is easily shown to be caused by an absorption in the Si substrate which is not quite balanced in a reference substrate. The dip at 1085 cm^{-1} is mysterious, but the frequency does not match any of the stretch modes suggested for SiF_n in the literature, the highest of which are 1010-1015 cm^{-1} (SiF_4, SiF_3, $(SiF_2)_n$).[37] The small dip near 824 cm^{-1} is not identified, but lands in the range suggested for SiF_2 bending modes. We conclude that the latter mode may be F-connected, but that any absorption produced by F is inconsequential compared to those associated with H or D. This conclusion fits, of course, with the result of our elec-

tron microprobe examination that the concentration of F in our films is of the order of, or less than, 1 at.%. Analysis of the spectra of Figure 12 shows that the preference ratio for attachment of H to Si rather than to Ge in a 50:50 alloy remains the same in the fluoride-derived films as it was in those made from a mixture of hydrides.

In our earlier work, we reported that a-$Si_{0.5}Ge_{0.5}$:H prepared at low temperature (230°C), where the 2090 cm^{-1} stretch mode dominated that at 2000 cm^{-1}, showed clear evidence of an uptake of O as a function of time (1 at.% after 10 days). Samples of a-$Si_{0.5}Ge_{0.5}$:H prepared at 300°C also showed clear evidence of O pick-up with time, although much less than for those prepared at 230°C, while no O contamination and no O uptake with time was found for samples of a-$Si_{0.5}Ge_{0.5}$:H:F prepared at substrate temperatures between 200°C and 350°C.

Figure 14 compares the Raman spectra[38] of a-$Si_{0.5}Ge_{0.5}$:H and a-$Si_{0.5}Ge_{0.5}$:H:F. These spectra were taken, with a resolution of 3.9 cm^{-1}, on films approximately 50 nm thick codeposited with the samples used for the transmission electron microscopy studies. The increase in counts below ~ 150 cm^{-1} is caused by stray light, and is greater for the fluoride-produced sample because it has a slightly rougher surface. The three peaks near 270 cm^{-1}, 370 cm^{-1}, and 470 cm^{-1} are assigned respectively to Ge-Ge, Ge-Si, and Si-Si optical mode vibrations.[39]. There is some indication of a small peak near 200 cm^{-1} which we assign to a Si-Si acoustic mode. The peaks have the same positions and widths in the two preparations of sample, indicating that there are no major differences in the short-range order. Moreover, the areas under the three peaks have about the same ratios, indicating that the relative numbers of Ge-Ge, Ge-Si and Si-Si bonds are the same. Finally, there is no evidence of a mode attributable to F_2 near 890 cm^{-1}. Figure 15 shows the Raman spectrum of an a-SiGe:H:F film grown under conditions of low power such that the composition was over 99 atomic percent of Ge. The figure shows a clear crystalline Ge peak at 300 cm^{-1}.[40] This indicates the sensitivity of the Raman spectrum to small volumes of crystallinity and verifies that spectra such as those of Figure 14 correspond to fully amorphous material.

Figure 16 shows TEM micrographs of approximately 50 nm thick a-Si:H,

a-Ge:H, and a-$Si_{0.5}Ge_{0.5}$:H films all prepared near 230°C. The micrograph of a-Si:H shows weakly discernible microstructure; bulk films made under similar preparation conditions exhibit good photoelectronic properties. In contrast, a-Ge:H shows distinct two-phase microstructure consisting of non-coalescing island regions (10-20 nm) of high electron density (dark regions) surrounded by lower density tissue material. The a-$Si_{0.5}Ge_{0.5}$:H possesses a similar form of island/tissue structure. The bulk forms of both these materials show clear evidence of O uptake *and* poorer photoelectronic properties than unalloyed a-Si:H. As discussed in a previous publication,[2] structural inhomogeneity increases and the photoresponse deteriorates when the substrate temperature is decreased below the optimum value of 300°C. In this paper we focus attention on Figure 17, which compares TEM micrographs of a-$Si_{0.5}Ge_{0.5}$:H and a-$Si_{0.5}Ge_{0.5}$:H:F films, codeposited with films whose (identical) Raman spectra were shown in Figure 14 and which were prepared at a T_s of 300°C to have identical thicknesses of about 50 nm. It is evident that the microstructures are very different. Both show a two-phase structure on a similar scale. However, the fluoride-derived material shows much stronger contrast between the two phases and the boundaries are very different (more angular) in shape suggesting a quite different growth mechanism. Amorphicity of these specimens along with all other TEM specimens was confirmed by electron diffraction measurements. An attempt was made to probe the chemical composition on the 100 A scale using X-ray microanalysis in a scanning transmission microscope. Problems associated with beam broadening through the films made this impossible.

VIII. DISCUSSION

Our discussion will be directed at two problems: first, the reason for the deterioration of the photoelectronic properties of amorphous silicon-germanium alloys compared to unalloyed silicon and second, the reason for the improved photoconductivity of alloys produced from fluorides compared to those produced from hydrides.

Four solutions have been proposed for the first of these problems[2] *viz.*

(1) preferential attachment of H to Si dangling bonds, leaving many Ge-related defects and gap states in the alloys;

(2) valence and conduction band tails of states which are at least as broad as in a-Si:H, which implies a larger density-of-states near the middle of the energy gap in the narrower gap material;

(3) different gap density-of-states distribution in the alloys, involving both Si and Ge dangling bond states at different energies so that, for most positions of the Fermi level, there are charged defects which easily trap carriers; and

(4) increased heterostructure in the alloys, i.e., increased differences in island/tissue composition and properties, which affect phototransport.

In discussing these proposed solutions, we shall at first set aside the discrepancy in the $\mu\tau$ products estimated from photoconductivity and time-of-flight measurements displayed in Figure 10, since the deterioration in $\mu\tau$ on adding Ge to the Si is present for both experiments.

The first solution has already been argued[41] to be inadequate since the magnitudes of the photoconductivity and photoluminescence are actually larger than would be expected if the Ge dangling bonds were as little "hydrogenated" as the infrared vibrational absorption would suggest. Dual magnetron sputtering[42] has been applied to equalize the H-attachment to Si and Ge, but this does not appear to be the panacea for radical improvement of the properties. Our finding that the ratio of H-attachments is the same in hydride- and fluoride-derived material, while the photoconductivity is much improved in the latter, also argues against the preferential attachment

of H to Si as the root cause of problems with the alloys.

In order to consider the second and third possible reasons for deteriorated properties in the alloys, we show in Figure 18 our proposed band structure[2] for a-$Si_{0.5}Ge_{0.5}$:H which is based on the following data and assumptions: (a) the decrease in *N(E)* above the valence band edge is given by the slope of the Urbach tail, i.e., by the magnitude of the E_0 of Figure 3; (b) the decrease in *N(E)* below the conduction band edge is deduced from the time-dispersive transport of electrons in a-Si:H;[43] (c) the dangling bond bands D^0 and D^- have the same FWHM, 0.2 eV, the maximum of the Ge D^0 band is at midgap in a-Ge:H,[44] the maximum of the Si D^0 band at roughly 1.0 eV below the conduction band in a-Si:H,[45] and the Ge and Si dangling bond correlation energies are 0.1[44] and 0.35 eV,[46] respectively; (d) there may be, and probably are, so far unidentified defect states with energies below mid-gap. Models differing in some of the details have also been published, particularly in the relative ordering of the Ge and Si dangling bond levels.[47]

It is evident from Figure 4 that the decrease in N(E) above the *valence* band edge is slower in the alloys than in a-Si:H. Our TOF measurements[16] and those so far published imply that the *conduction* band tail of a-$Si_{1-x}Ge_x$:H broadens slightly with increasing Ge content. Unfortunately, information on the conduction band tail is limited to alloys of low x ($x < 0.35$) due to severe carrier loss and problems associated with dielectric relaxation at higher x. The evidence from our experiments for the broadening of the tail comes from the observation of a reduction in the electron drift mobility and an increase in the mobility thermal activation energy, E_μ with increasing x; thus, for $x = 0$, $\mu \sim 1$ $cm^2s^{-1}V^{-1}$ and $E_\mu = 0.11$ eV while for $x = 0.18$, $\mu \sim 0.3$ $cm^2s^{-1}V^{-1}$, and $E_\mu = 0.17$ eV (both mobilities measured with the same applied field of $10^4 Vcm^{-1}$). Similar results have been reported elsewhere.[28,35] The actual slope of the (exponential) tail has also been determined from TOF data. For instance, Weller *et al.*[14] find that the slope changes from 35 meV in a-Si:H to 60 meV in 1.45 eV band gap alloy. Vanderhaghen and Longeaud[48] deduced a slope of 41 meV for an alloy of x-value of 0.18. Karg *et al.*[35] obtain slopes of 22, 26 and 30 meV for x-values of 0, 0.15 and 0.25, respectively. Con-

sideration of these new data and details of bandstructure in Figure 18 suggest that broadening of the conduction band tail (and of the valence band tail), howsoever caused, will contribute to the deterioration of the photoresponse. However, it is clear from Figure 18 that the density- of-states near mid-gap is unlikely to be determined predominantly by the tail states. It therefore seems unlikely that altered tail state distributions are the sole cause of the deterioration in the alloy photoelectronic properties.

The third proposed reason for deterioration of the photoresponse of the alloys has two aspects to it: first, the probability that the total of defects may increase on alloying and second, the probability that even for a fixed total of dangling bond and other defects, their wider distribution in energy will lead to the existence of charged traps. Both of these aspects seem to eventuate. The dangling bond density from ESR,[49,50] the sub-band-gap absorption from photoconductivity spectra, the density-of-states below the conduction band edge as inferred from the drift mobility and dispersion parameters for electrons by TOF (see above), and the defect density to which the PL intensity is inversely proportional,[51] all increase with x. For $x \approx 0.5$, the gap density-of-states (GDOS) appears to be about an order of magnitude larger in the alloys, explaining the deterioration in their properties, without, of course, providing the basic reason for the state density increase.

The fourth proposed solution would appear to provide adequate reason for the larger GDOS.[65] The new results on the fluoride-derived materials support this model. Thus, contributions (2), (3) and (4) provide adequate reasons why the photoresponse in the alloys is poorer than in unalloyed a-Si:H. We now return to discuss the problem of the very different $\mu\tau$'s estimated, even for $x = 0$, from the photoconductivity and TOF measurements shown in Figure 10. This difference has been found before, but is seldom discussed.[52] In fact, a difference is not unexpected. First, the measuring conditions, particularly the photon flux and sample configuration in the two experiments, are very different. In the TOF technique, the total density of photo-excited electrons in one experiment is given by the product of the density in one optical pulse ($\sim 10^{15} cm^{-3}$ over a depth of about 100 nm) multiplied by the number of pulses (about 100).

This averages to about $2.5 \times 10^{15} cm^{-3}$ for a 4 μm thick sample. By contrast, in the photoconductivity experiment, we illuminate with a steady-state photon flux of $10^{15} cm^{-2} s^{-1}$, and other experimenters use densities (AM1) about a factor of 300 higher. Thus the photocarrier densities involved, the resultant carrier distribution in gap states, and the trapping lifetimes, are likely to be very different. Indeed, as we discussed in Section VI, the $\eta\mu\tau$ product is explicitly dependent on the photon flux or more specifically on the carrier generation rate. Another important difference is in the configuration of the experiment: the TOF experiment is carried out in a sandwich configuration, while the photoconductivity experiment involves transport between two coplanar electrodes. Thus the latter experiment is much more susceptible to surface states and surface band bending.[33] However, from Figure 10 (normalized $\eta\mu\tau$ measured using penetrating radiation) and depletion layer width, surface-band bending calculations from TOF data, we see that surface effects are negligible, at least for the Ge contents investigated ($x > 0.25$). Even if the TOF and steady-state photoconductivity experiments were performed with the same photocreated carrier densities, a difference in $\mu\tau$ would *still* be observed; the important factor is time-scale. If the mobility μ is taken to be the mobility in the extended states of the conduction band, then the τ in the TOF experiment is the integrated time in the band before the first deep trapping event. Since the TOF measurement lasts of the order of 10 μs, release from a deep trap (as distinct from release from a shallow band tail trap) does not occur on the time-scale of the experiment. In the steady-state experiment, on the other hand, trapping is followed by release until the carrier ultimately recombines with a hole. It is well known that this can be a lengthy process and many experiments have been done to demonstrate the release of such trapped carriers.[53]

It may be concluded from the above that both the TOF and steady-state photoconductivity experiments confirm a deterioration in $\mu\tau$ with alloying and that the apparent discrepancy in the magnitude of the $\mu\tau$ reflects the (very) different trapping statistics involved in the two experiments.

We now direct our attention to the second problem, that of the reason for the improved photoresponse of fluoride-derived alloys. Our experimental results demonstrate that any changes in

gap density-of-states structure between the hydride- and fluoride-derived materials are subtle.

First, as already noted, the sub-band-gap absorption and PL intensity, which are presumably measures of the relative gap density-of-states,[54] do not change significantly or consistently in the hydride and fluoride materials. In fact, we usually find an increased sub-band-gap absorption in our fluoride-derived material, whereas Guha[3] reports the opposite; in any event, the magnitude of the change is insufficient to account for the change in $\eta\mu\tau$.

We consider next our SCLC results, which must be presented with carefully described caveats. Our preliminary SCLC measurements[18] on $n^+ - i - n^+$ structures of a-$Si_{0.5}Ge_{0.5}$:H and a-$Si_{0.5}Ge_{0.5}$:H:F indicate densities-of-states just above the Fermi level which are both about an order of magnitude larger than in a-Si:H. However, the activation energies for transport across these sandwich structures are different, and suggest a Fermi level about 0.2 eV closer to the conduction band edge in the material produced from fluorides. Thus, there remains the possibility that the densities-of-states at the same energetic position in the band gap are different in the two preparations. We expect that the conductivity activation energies, 0.6 eV for the a-$Si_{0.5}Ge_{0.5}$:H sandwiches and 0.4 eV for the a-$Si_{0.5}Ge_{0.5}$:H:F ones, are reduced from the values we usually find (0.72 ± 0.01 eV and 0.63 ± 0.06 eV, respectively) for intrinsic layers of this composition, by P doping after the n^+ deposition in our single-chamber system. If so, it is interesting that the Fermi level displacement is consistently different between the three unfluorinated and two fluorinated samples examined. A greater incorporation of P in the fluorinated sample, or a smaller gap DOS to be compensated in the fluorinated sample, or a change in the ratio of P incorporated in 4-fold (doping) or 3-fold (nondoping but potentially defect-creating) configurations are all possible explanations for the observations. In addition to these uncertainties, it must be remembered that a consistently higher Fermi level will lead to improved electron photoconductivity, which will be discussed below. One relief from these difficulties would be to make the $n^+ - i - n^+$ structures in a multiple-chamber system. Another is to study SCLC in a coplanar configuration. We have attempted such measurements, but have encountered two difficulties. The first is that the current-voltage relationship did not follow the

expected scaling law when the distance between the contacts was varied, and the second was an unacceptable irreproducibility in the measured current-voltage characteristic. One possible reason for these problems is the occurrence of surface conductivity. In any event, more study needs to be done before these data can be interpreted with confidence. In summary, although the SCLC results appear to show about the same density-of-states in the two preparations of alloy, there do remain problems of interpretation connected with Fermi levels displaced by different amounts from the intrinsic material. Similar densities-of-states from SCLC measurements to those reported here have been obtained by Guha *et al.*[55]

The neutral dangling bond density in our a-$Si_{0.5}Ge_{0.5}$:H films is similar to values reported elsewhere[49,50] for this Ge concentration and is about at least two orders of magnitude greater than the density found in high quality undoped a-Si:H films.[56] However, no signal corresponding to the known g-value for Ge dangling bonds was found by the NRL group[19] in the fluoride-derived set of alloys of four different x-values. Interestingly, the Shimizu group[57] found a low spin density putting an upper limit of $7 \times 10^{15}cm^{-3}$ for their a-$Si_{1-x}Ge_x$:H:F material which had an x-value of 0.3. Also, preliminary results by Aljishi *et al.*[5] indicate neutral Ge dangling bond densities in their fluoride-derived alloys which are at least an order of magnitude lower ($\sim 10^{16}cm^{-3}$ cf $\sim 10^{17}cm^{-3}$) than found for hydride-derived alloys. There are several possible explanations for a low or apparently absent ESR signal for Ge. The obvious one is that the density of dangling bonds is at or below the detection limit for the apparatus and the sample volume used, but this seems implausible, at least for our material, since the signal from Si dangling bonds ($5 \times 10^{16} - 10^{17}cm^{-3}$) is easily seen. A second possibility is that any Ge dangling bonds are either empty or doubly occupied. The latter circumstance is consistent with a displaced Fermi level which is highly probable since the results shown in Figure 8 indicate that the Fermi level for the fluoride-derived material is usually slightly above midgap. A similar conclusion was reached by Aljishi *et al.*[5] Interpretation of the significance of the results for a-$Si_{1-x}Ge_x$:H:F in terms of density-of-states is therefore limited. More study is required.

The fourth route to a determination of the gap state densities is through $\mu\tau$ measurements

by the TOF method. The assembly of measurements on hydride-derived material displayed in Figure 10 is consistent with a monotonic decrease in electron $\mu\tau$. The variation in $\mu\tau$ product with x for the fluoride-derived material is less surely established, but it does appear that the $\mu\tau$'s for electrons are little different from those for hydride-produced samples. In order to separate out the changes in μ and τ, we have analyzed our current versus time photoconductivity transients to obtain the drift mobilities μ in the two types of preparation. The results indicate no significant differences in the drift mobilities for the same x and therefore, also, no differences in the deep trapping times. This fits the observations of parallel monotonic increases in trap state densities in both types of material.

In partial summary, our analysis of our measurements of sub-band-gap absorption, photoluminescence, space-charge-limited-currents, electron spin resonance and time-of-flight transport suggests that there are few significant differences in the gap densities-of-states in hydride- and fluoride-derived alloys. The explanation for the order-of-magnitude higher photoconductivity in the latter preparation must be sought elsewhere. Before doing so, we wish to mention and reject two other reasons for improvement in fluoride-derived alloys. The first of these is the possibility that a Fermi level consistently closer to the conduction band edge in the bulk of the fluoride-derived material might explain the improved photoresponse. As was stated in Section VI we found no correlation between the magnitude of $\eta\mu\tau$ and the Fermi level position for the fluoride-derived samples of band gap near 1.5 eV.

The second possible reason for improvement in the fluoride-derived material is the presence of F *in the alloy*. Our microprobe measurements suggest a concentration of F of the order of 1 at.%, and our infrared and Raman results confirm this small percentage. For comparison, Tsuda *et al.*[4] report less than 0.6%, S. Oda *et al.*[57] less than 1%, and the ECD group less than 1%.[58] The Princeton group[59] reports F concentrations of about 1 at.%. We conclude that the presence of F *in the film* must be rejected as a major contributory factor to the improved photoresponse, in contradiction to the position advocated by Ovshinsky and Adler.[60] This was, indeed, anticipated by Weil *et al.*[61] who reported from studies on a-Si:F (no H present) that,

while both H and F passivated dangling bonds, the H led to a relief of strain in the network while F did not. Weil *et al.* found that a-Si:F had rather poor photoelectronic properties.

Changes in the heterostructure have been consistently advocated by our group as a contributory reason for the deterioration in photoelectronic properties. The present results confirm that increased nonuniformity of the alloy films, on a scale of 10-50 nm, compared to unalloyed a-Si:H as evidenced by the TEM micrographs,[2] the changes in infrared absorption spectra,[2] the low temperature evolution of hydrogen in gas evolution studies[62] - occurs coincidentally with the observation of poorer photoelectronic properties. The present data also provide significant evidence for differences in the heterostructure of hydride- and fluoride-derived alloys, which we hypothesize is the fundamental reason for the differences in photoresponse of alloys with $x \approx 0.5$. We list next, in approximate order of significance, the evidence concerning these differences:

(1) TEM micrographs,

(2) Deuteron quadrupole magnetic resonance measurements,

(3) Uptake of O as a function of time, and

(4) Photoluminescence peak linewidth.

The TEM micrographs indicate that there are major differences in the island/tissue in the two preparations of material. However, we have been unable to this point to determine with our microscope any local differences in chemical composition on a scale of 5-10 nm.

Deuteron quadrupole magnetic resonance measurements[13] have recently been carried out by the group of Professor R. Norberg at Washington University on samples prepared at Xerox Palo Alto and at Harvard. We briefly summarize their findings here. DMR line shapes and relaxation times have distinguished five different localized hydrogen (deuterium) configurations *viz.*, (a) tightly bound D, (b) weakly bound D, (c) molecular D_2 "absorbed" on rough microvoid surfaces, (d) bulk molecular D_2 located well removed from microvoid surfaces, and (e) isolated molecular D_2 in poor "contact" with other D or D_2. The results depend on the deposition conditions, but, specifically, they show clear differences in void morphology between silicon-

germanium alloys produced from hydrides and fluorides, as if the D_2 in the hydride material were isolated, while the D_2 in the fluoride were interacting, as in bulk D_2. Obviously this powerful technique needs to be developed further in order to make precise the inferences from it, but the conclusion of the existence of structural differences revealed by it should remain unaffected.

Our third item of evidence is the observation that films of a-$Si_{1-x}Ge_x$:H:F do not take up O as a function of time, as had been very clearly demonstrated for a-$Si_{1-x}Ge_x$:H.

Our information concerning the FWHM of the *PL*, although statistically significant, is hard to interpret in a very definite fashion. The narrower line widths for the a-$Si_{0.5}Ge_{0.5}$:H:F films would normally be interpreted as implying a less disordered structure. However, the slopes of the Urbach tails in the absorption spectra are the same, and the gap-state densities also. It is possible, though unlikely based on the TOF results, that the conduction band tail is sharper in the fluoride-derived material. Aljishi *et al.* report that the tail is much broader in the fluoride-derived alloy than in a-Si:H.[63] This would rule out any influence of the microstructure on the FWHM.

It is possible to construct a simple model to explain the improved photoresponse achieved with the fluoride-derived alloys, based on the above evidence for a different two-phase microstructure and on the specific details of dark transport for the two alloy preparations. We recall from Figure 7, which shows the pre-exponential factor σ_0 *versus* the thermal activation energy, E_σ, for dark conductivity, that the data for a-$Si_{1-x}Ge_x$:H were bunched together in one group sandwiched between the a-$Si_{1-x}Ge_x$:H:F data. From this, we may postulate a structural model, illustrated in Figure 19, which permits two transport paths at different energies. Transport in the dark may proceed by either of the paths, which are not too different in conductance. Phototransport, which is not subject to equilibrium carrier statistics, is postulated to occur via the islands - the path of higher σ_0 and presumably higher μ. Consistent with this, *all* of the a-$Si_{1-x}Ge_x$:H:F samples of Figure 9, with either low or high σ_0, give $\eta\mu\tau$ products in the same range. These $\eta\mu\tau$'s are as much as an order of magnitude larger than those for a-$Si_{1-x}Ge_x$:H, which show

values lying between the high and low extremes for a-$Si_{1-x}Ge_x$:H:F. On the basis of this model, one might expect the $\mu\tau$ products from the TOF experiment, which essentially measures transport in the dark, to follow the σ_0 values. However, the data for the fluoride-derived samples are too sparse to test this prediction.

An alternative model for the improved photoresponse achieved with the a-$Si_{1-x}Ge_x$:H:F alloy is simply that the recombination lifetime (but not necessarily the first deep trapping time) is larger. One might expect some evidence of this to show in one of the measurements to probe the gap DOS - which is not clear. An improved recombination lifetime may be linked speculatively to the different microstructure.

We note, in passing, that Slobodin *et al.*[64] have studied the properties of films prepared either from plasmas of (SiH_4 + GeF_4) or (SiF_4 + GeF_4 + H_2). Although the ir spectra, sub-band-gap absorption spectra, dark conduction activation energies, carrier drift mobilities, and deep trapping lifetimes of the two preparations of alloy were very similar, the films made from the latter gas combination had an order-of-magnitude greater photoconductivity. These workers concluded that they agreed with our earlier deduction,[6] based on preliminary data, that altered microstructure was the cause, and speculated that the plasma of (SiF_4 + GeF_4 + H_2) might have fewer polymerization reactions and thus yield films with a closer microstructure.

IX. CONCLUSIONS

This work reinforces the conclusions of our earlier study[2] that both band-structure changes and an increased nonuniformity of microstructure are responsible for the deterioration in photoelectronic properties of Ge-rich alloys of a-$Si_{1-x}Ge_x$:H. It establishes also that there are significant differences in *microstructure* when the Si-Ge alloys are made from a mixture of SiF_4 and GeF_4 with H_2, rather than from a mixture of SiH_4 and GeH_4. This conclusion is based on the following facts, here summarized from the main text: (1) differences in TEM micrographs for films which have identical Raman spectra and for which similarly produced films have very different properties, (2) differences in deuteron nuclear quadrupole resonance, interpreted in terms of a different void structure, and (3) differences in post-deposition pick-up of O revealed by infrared absorption spectra, which imply differences in accessible paths into the film. These differences in microstructure are hypothesized to cause, or could be correlated with, differences in structure near the surface of the film, which result in very different photoconductivities. Facts suggesting that the structure and the related band structure in the *bulk of the film* are *not* responsible for the differences in photoresponse, on the other hand, include: (4) the Raman spectra are identical, (5) the absorption spectra from 0.8 to 2.0 eV are essentially the same, (6) the PL spectra are principally different only in the FWHM, and (7) the gap densities-of-states, measured by SCLC or ESR, are the same. Finally, local passivation of dangling bonds by F rather than H is not regarded as an important cause, since (8) only 1% of F is incorporated in any of the films. Finally, we note again[14] that silicon-germanium alloys with photoelectronic properties possibly as good as, or even superior to, those of the alloys made from fluorine-containing gases reported here, but which contain only hydrogen as bond compensator, have been reported from several laboratories. Unfortunately, in most instances the position of the Fermi level has not been reported and there is no discussion of microstructure.

ACKNOWLEDGEMENTS

The authors wish to thank B.F. Bateman, Y.F. Chen, J. Hanna, C. Hayzelden, Y.L. He, S.J. Jones, P.B. Kirby, S.M. Lee, F. Moraes, W.A. Turner, and Z.L. Sun for their collaboration in our experimental program. We also acknowledge collaborations with S. Asher of the Solar Energy Research Institute (Golden, CO), W.E. Carlos and U. Strom of the Naval Research Laboratory (Washington, DC), and R.E. Norberg and co-workers at Washington University (St. Louis, MO) and discussions with E.A. Schiff of Syracuse University (Syracuse, NY). This work was funded in part by Contract XB-7-06071 with the Solar Energy Research Institute, in part by Grant DMR-86-14003 with the NSF and in part by the Division of Applied Sciences of Harvard University.

* Present address: Amoco Research Center, Naperville, IL 60566 USA

** Present address: MIT Lincoln Laboratory, Lexingon, MA 02173 USA

REFERENCES

1. See, for instance, articles in "Semiconductors and Semimetals", Vol. *21D*, edited by R.K. Willardson and A.C. Beer (Academic Press, Orlando, 1984).

2. K.D. Mackenzie, J.R. Eggert, D.J. Leopold, Y.M. Li, S. Lin and W. Paul, Phys. Rev. *B31*, 2198 (1985).

3. S. Guha, J. Non-Cryst. Solids *77 & 78*, 1451 (1985).

4. S. Tsuda, H. Tarui, H. Haku, Y. Nakashima, Y. Hishikawa, S. Nakano and Y. Kuwano, J. Non-Cryst. Solids *77 & 78*, 845 (1985).

5. S. Aljishi, Z.E. Smith, D. Slobodin, J. Kolodzey, V. Chu, R. Schwarz and S. Wagner, in "Materials Research Society Symposia Proceedings", Vol. *70*, edited by D. Adler, Y. Hamakawa and A. Madan (Materials Research Society, Pittsburgh, 1986), p. 269.

6. K.D. Mackenzie, J. Hanna, J.R. Eggert, Y.M. Li, Z.L. Sun and W. Paul, J. Non-Cryst. Solids *77 & 78*, 881 (1985).

7. K. Nozawa, Y. Yamaguchi, J. Hanna and I. Shimizu, J. Non-Cryst. Solids *59 & 60*, 533 (1983).

8. A. Madan, S.R. Ovshinsky and E. Benn, Philos. Mag. *40*, 259 (1978).

9. W. Paul, in "Fundamental Physics of Amorphous Semiconductors", Vol. *25* of "Springer Series in Solid State Sciences", edited by F. Yonezawa (Springer, Heidelberg, 1981), p. 72.

10. K.D. Mackenzie and W. Paul, in "Materials Research Society Symposia Proceedings", Vol. *95*, edited by D. Adler, Y. Hamakawa, A. Madan and M. Thompson (Materials Research Society, Pittsburgh, 1987), p. 281.

11. K.D. Mackenzie, J.H. Burnett, J.R. Eggert, Y.M. Li and W. Paul in "Proceedings of 12th

International Conference on Amorphous and Liquid Semiconductors", J. Non-Cryst. Solids *97* and *98*, 1019 (1987).

12. K.D. Mackenzie and W. Paul, in "Proceedings of 12th International Conference on Amorphous and Liquid Semiconductors", J. Non-Cryst. Solids *97* and *98*, 1055 (1987).

13. V.P. Bork, P.A. Fedders, R.E. Norberg, D.J. Leopold, K.D. Mackenzie and W. Paul, J. Non-Cryst. Solids *77* & *78*, 715 (1985); V.P. Bork, P.A. Fedders, R.E. Norberg, D.J. Leopold, K.D. Mackenzie and W. Paul, in "Hydrogen in Disordered and Amorphous Solids", edited by G. Bambakidis and R.C. Bowman, Jr. (Plenum, New York, 1986), p. 111; and V.P. Bork, P.A. Fedders, R.E. Norberg, D.J. Leopold, K.D. Mackenzie and W. Paul, in "Materials Research Society Symposia Proceedings", Vol. *70*, edited by D. Adler, Y. Hamakawa and A. Madan (Materials Research Society, Pittsburgh, 1986), p. 307.

14. By conventional (diode) rf glow discharge, triode rf glow discharge and photochemical vapor deposition techniques, higher quality a-$Si_{1-x}Ge_x$:H alloys have been produced. See, for instance, Ref. 4; H. Itozaki, N. Fujita and H. Hitotsuyanagi, in "Materials Research Society Symposia Proceedings", Vol. *49*, edited by D. Adler, A. Madan and M.J. Thompson (Materials Research Society, Pittsburgh, 1985), p. 161; B. von Roedern, A.H. Mahan, T.F. McMahon and A. Madan, *ibid.*, p. 167; M. Konagai, H. Takei, T. Tanaka, W.K. Kim, A. Yamada, J. Kenne, S. Nishida, H. Tasaki, P. Sichanugrist, C. Katagiri, J. Takada and K. Takahashi, in "Amorphous Si Subcontractors Annual Review Meeting", SERI/CP2112654 (1985), p. 17C; A. Matsuda, M. Koyama, N. Ikuchi, Y. Imanishi and K. Tanaka, Jpn J. Appl. Phys. *25*, L54 (1986); S. Tsuda, H. Haku, H. Tarui, T. Matsuyama, K. Sayama, Y. Nakashima, S. Nakano, M. Ohnishi and Y. Kuwano, in "Materials Research Society Symposia Proceedings", Vol. *95*, edited by D. Adler, Y. Hamakawa, A. Madan, M. Thompson (Materials Research Society, Pittsburgh, 1987), p. 311; T. Watanabe, M. Tanaka, K. Azuma, M. Nakatani, T. Sonobe and T. Shimada, Jpn. J. Appl. Phys. *26*, L288 (1987); H.C. Weller, S.M. Paasche, C.E. Nebel and G.H. Bauer, in "Proceedings of 12th International Conference on Amorphous and Liquid Semiconductors" J. Non-Cryst. Solids *97* and *98*,

1071 (1987).

15. The SiF_4 and H_2 gases were supplied by Matheson and the GeF_4 gas supplied by Cerac.

16. K.D. Mackenzie and W. Paul, to be published.

17. A description of the TOF apparatus is given in P.B. Kirby and W. Paul, Phys. Rev. *B29*, 826 (1984).

18. Space-charge-limited current measurements performed by Y.F. Chen and W.A. Turner. See R.L. Weisfield, J. Appl. Phys. *54*, 6401, (1983) for details on the analysis.

19. Measurements carried out by Drs. W.E. Carlos and U. Strom of the Naval Research Laboratory, Washington, D.C.

20. A technical description of the apparatus may be found in the SERI Technical Reports of February 1983 and October 1983 under SERI Subcontract No. XB-2-02144-1 and also in Ref. 2.

21. SIMS analysis carried out by Dr. S. Asher of the Solar Energy Research Institute, Golden, CO.

22. Cameca MBX unit with Tracor Northern automation operated by David Lange of Harvard University.

23. R.W. Collins, Ph.D. thesis, Harvard University (1982); J.R. Eggert, Ph.D. thesis, Harvard University (1986).

24. H.G. Grimmeiss and L.A. Ledebo, J. Appl. Phys. *46*, 2155 (1975); M. Vanecek, J. Kocka, J. Stuchlik, Z. Kozisek, O. Sticka and A. Triska, Sol. Energy Mater. *8*, 411 (1983); J. Kocka, J. Vanecek, A. Kozisek, O. Sticka and J. Beichler, J. Non-Cryst. Solids *59 & 60*, 293 (1983).

25. J. Tauc, R. Grigorovici and A. Vancu, Phys. status solidi *15*, 627 (1966).

26. As noted earlier, variations in x across the substrate platform in depositions from fluorides rendered an estimate of x for the PL samples more difficult than for the hydride-derived ones. Consequently, we used the value of E_{PL} *versus* x for the hydride-derived samples to

estimate x for the fluoride materials. To check the validity of this procedure, we determined the actual Ge content of some of the fluoride-derived samples by electron microprobe analysis.

27. M. Gal, J.M. Viner, P.C. Taylor and R.D. Wieting, Phys. Rev. *B31*, 4060 (1985); R. Ranganathan, M. Gal, J.M. Viner and P.C. Taylor, to be published.

28. R.A. Street, C.C. Tsai, M. Stutzmann and J. Kakalios, Philos. Mag. *B56*, 289 (1987).

29. D.L. Staebler and C.R. Wronski, Appl. Phys. Lett. *31*, 292 (1977).

30. See, D.A. Anderson and W. Paul, Philos. Mag. *B44*, 187 (1981) or W. Paul and D.A. Anderson, Sol. Energy Mater. *5*, 229 (1981) for illustration and earlier references.

31. W. Meyer and H. Neldel, Z. Tech. Phys. *18*, 588 (1937).

32. K. Nozawa, Master's thesis, Tokyo Inst. of Tech. (1984).

33. M. Tanelian, Philos. Mag. *B45*, 435 (1982); R.A. Street, M.J. Thompson and N.M. Johnson, Philos. Mag. *B51*, 1 (1985); P.B. Kirby, D.W. MacLeod and W. Paul, Philos. Mag. *B51*, 389 (1985); G.N. Parsons, C. Kusano and G. Lucovsky, J. Vac. Sci. Technol. *A5* (4), 1655 (1987).

34. K. Hecht, Z. Phys. *77*, 235 (1932).

35. F. Karg, W. Kruhler, M. Moller and K. von Klitzing, J. Appl. Phys. *60*, 2016 (1986).

36. Investigation done in collaboration with Professor Clive Hayzelden of Harvard University on a Philips EM420T electron microscope.

37. See, for example, B.K. Agrawal, Phys. Rev. Lett. *46*, 774 (1981).

38. The Raman spectra were taken with a SPEX double monochromator using a photomultiplier tube in the photon counting mode. The excitation source was the Ar^+ 5145 A line, focused with a cylindrical lens. Collection was done in the near backscattering geometry.

39. J.S. Lannin, in "Semiconductors and Semimetals", Vol. *21B*, edited by R.K. Willardson and A.C. Beer (Academic Press, Orlando, 1984), p. 159.

40. D.S. Shen, J. Kolodzey, D. Slobodin, J.P. Conde, C. Lane, I.H. Campbell, P.M. Fauchet and S. Wagner in, "Materials Research Society Symposia Proceedings", Vol. *70*, edited by D. Adler, Y. Hamakawa and A. Madan (Materials Research Society, Pittsburgh, 1986), p. 301.

41. B. von Roedern, D.K. Paul, J. Blake, R.W. Collins, G. Moddel and W. Paul, Phys. Rev. *B25*, 7678 (1982).

42. R.A. Rudder, J.W. Cook, Jr. and G. Lucovsky, Appl. Phys. Lett. *45*, 887 (1984); R.A. Rudder, G.N. Parsons, J.W. Cook, Jr. and G. Lucovsky, J. Non-Cryst. Solids *77* & *78*, 885 (1985).

43. T. Tiedje, J.M. Cebulka, D.L. Morel and B. Abeles, Phys. Rev. Lett. *46*, 1425 (1981).

44. M. Stutzmann, J. Stuke and H. Dersch, Phys. status solidi *B115*, 141 (1983).

45. See discussion in Ref. 2 and also P.G. LeComber and W.E. Spear, Philos. Mag. *B53*, L1 (1986).

46. See, for instance, H. Dersch, J. Stuke and J. Beichler, Phys. status solidi *B105*, 265 (1981); W.B. Jackson, Solid State Commun. *44*, 477 (1982).

47. M. Stutzmann, R.J. Nemanich and J. Stuke, Phys. Rev. *B30*, 3595 (1984); A. Skumanich, A. Frova and N.M. Amer, Solid State Comm. *54*, 597 (1985); C.Y. Huang, S. Guha and S.J. Hudgens, J. Non-Cryst. Solids *66*, 187 (1984); G. Lucovsky, J.W. Cook Jr., R.A. Rudder and G.N. Parsons, in "Amorphous Si Subcontractors Annual Review Meeting", SERI/CP2112654 (1985), p. 97, and also Ref. 5.

48. R. Vanderhaghen and C. Longeaud, in "Proceedings of 12th International Conference on Amorphous and Liquid Semiconductors", J. Non-Cryst. Solids *97* and *98*, 1059 (1987).

49. M. Stutzmann, W.B. Jackson and C.C. Tsai, J. Non-Cryst. Solids *77* & *78*, 363 (1985).

50. T. Shimizu, M. Kumeda, A. Morimoto, Y. Tsujimura and I. Kobayashi, in "Materials Research Society Symposia Proceedings", Vol. *70*, edited by D. Adler, Y. Hamakawa and A. Madan (Materials Research Society, Pittsburgh, 1986), p. 313.

51. See paper in Ref. 18.

52. E.A. Schiff, Philos. Mag. Lett. *55*, 87 (1987).

53. See, for instance, R. Carius and W. Fuhs, in "Optical Effects in Amorphous Semiconductors", edited by P.C. Taylor and S.G. Bishop, AIP Conf. Proc. *120*, p. 125 (1984); F. Boulitrop, *ibid.*, p. 178.

54. See, for instance, G. Moddel, Ph.D. thesis, Harvard University (1981), and paper in Ref. 18.

55. S. Guha, J.S. Payson, S.C. Agarwal and S.R. Ovshinsky, in "Proceedings of 12th International Conference on Amorphous and Liquid Semiconductors", J. Non-Cryst. Solids *97* and *98*, 1455 (1987).

56. R.A. Street, J.C. Knights and D.K. Biegelsen, Phys. Rev. *B18*, 1880 (1978).

57. S. Oda, Y. Yamaguchi, J. Hanna, S. Ishihara, R. Fujiwara, S. Kawate and I. Shimizu, in "Technical Digest of the International PVSEC-1" (Kobe, 1984), p. 429.

58. S. Guha, private communication.

59. S. Wagner, private communication.

60. S.R. Ovshinsky and D. Adler, in "Materials Research Society Symposia Proceedings", Vol. *49*, edited by D. Adler, A. Madan and M.J. Thompson (Materials Research Society, Pittsburgh, 1985), p. 251.

61. R. Weil, I. Abdulhalim, R. Beserman, M. Janai and B. Pratt, J. Non-Cryst. Solids *77 & 78*, 261 (1985).

62. Hydrogen evolution measurements carried out at Harvard by F. Moraes and S.J. Jones. See also work on hydride-derived alloys by D.K. Paul, B. von Roedern, S. Oguz, J. Blake and W. Paul, J. Phys. Soc. Jpn (Supp. A) *49*, 1261 (1980) and W. Beyer, H. Wagner and F. Finger, J. Non-Cryst. Solids *77* and *78*, 857 (1985).

63. S. Aljishi, D.S. Shen, V. Chu, Z.E. Smith, J.P. Conde, J. Kolodzey, D. Slobodin and S. Wagner, in "Materials Research Society Symposia", Vol.*95*, edited by D. Adler, Y. Hamakawa, A. Madan and M. Thompson (Materials Research Society, Pittsburgh, 1987), p.

323.

64. D. Slobodin, S. Aljishi, Y. Okada, D.S. Shen, V. Chu and S. Wagner, in "Materials Research Society Symposia Proceedings", Vol. *70*, edited by D. Adler, Y. Hamakawa and A. Madan (Materials Research Society, Pittsburgh, 1986), p. 275.

65. Speculations concerning the increase in GDOS, applicable to homogeneous material, have been discussed by G. Muller, Appl. Phys. A *45*, 103 (1988) in a paper published after the first submission of our article.

LIST OF FIGURE CAPTIONS

Figure 1. SIMS depth profile of an a-$Si_{1-x}Ge_x$:H:F alloy. The Ge and F contents as determined from electron microprobe are 41 at.% and ~ 1 at.%, respectively.

Figure 2. E_{PL}, ΔE_{PL}, and I_{PL} *versus* T_s for a-$Si_{0.5}Ge_{0.5}$ samples prepared from hydrides and fluorides.

Figure 3. Optical absorption spectra for a-$Si_{1-x}Ge_x$ alloys produced from hydrides and fluorides.

Figure 4. Variation of E_{04}, E_g, and E_0 with x.

Figure 5. Variation of (a) I_{PL} and (b) ΔE_{PL} with x.

Figure 6. Dark conductivity σ *versus* inverse temperature for a-$Si_{0.5}Ge_{0.5}$ produced from hydrides and fluorides.

Figure 7. Pre-exponential factor σ_0 for electrical conduction *versus* thermal activation energy E_σ.

Figure 8(a). Variation of $(E_g/2 - E_\sigma)$ with x. Open symbols refer to hydrides. Closed symbols refer to fluorides.

Figure 8(b). Variation of $\eta\mu\tau$ with dark conductivity activation energy E_σ for a series of a-$Si_{1-x}Ge_x$:H:F alloys with band gap near 1.4 eV.

Figure 9. Photoconductivity $\eta\mu\tau$ products *versus* x for hydride- and fluoride-derived alloys, measured at a photon energy of 1.92 eV.

Figure 10. Variation of normalized $\eta\mu\tau$ product fom photoconductivity and $\mu\tau$ product from time-of-flight with x. The photoconductivity measurements were made with pho-

tons of energy 1.5 eV.

Figure 11. Infrared absorption spectra of a-$Si_{0.5}Ge_{0.5}$:H prepared at T_s = (a) 230°C, (b) 275°C, and (c) 312°C. The main features are labeled in (a). The numbers in parentheses identify the samples. (After Ref. 2.)

Figure 12. Infrared absorption spectra of a-$Si_{0.5}Ge_{0.5}$:H:F and a-$Si_{0.5}Ge_{0.5}$:D:F alloys.

Figure 13. FTIR transmission spectrum of a-$Si_{0.5}Ge_{0.5}$:D:F.

Figure 14. Raman spectra of (a) a-$Si_{0.5}Ge_{0.5}$:H and (b) a-$Si_{0.5}Ge_{0.5}$:H:F.

Figure 15. Raman spectrum of a microcrystalline sample produced from fluorides.

Figure 16. Bright field TEM images of (a) a-Si:H, (b) a-Ge:H and (c) a-$Si_{0.5}Ge_{0.5}$:H. The specimens were prepared at substrate temperatures near 230°C and are about 50 nm thick.

Figure 17. Comparison of bright field TEM images of (a) a-$Si_{0.5}Ge_{0.5}$:H, and (b) a-$Si_{0.5}Ge_{0.5}$:H:F. The specimens were prepared at 300°C and are about 50 nm thick.

Figure 18. Schematic band structure for a-$Si_{0.5}Ge_{0.5}$:H showing the energy of Si and Ge D^0 and D^- dangling bonds with respect to the conduction and valence bands, *CB* and *VB*. (After Ref. 2.)

Figure 19. Model for phototransport in fluoride-derived alloys.

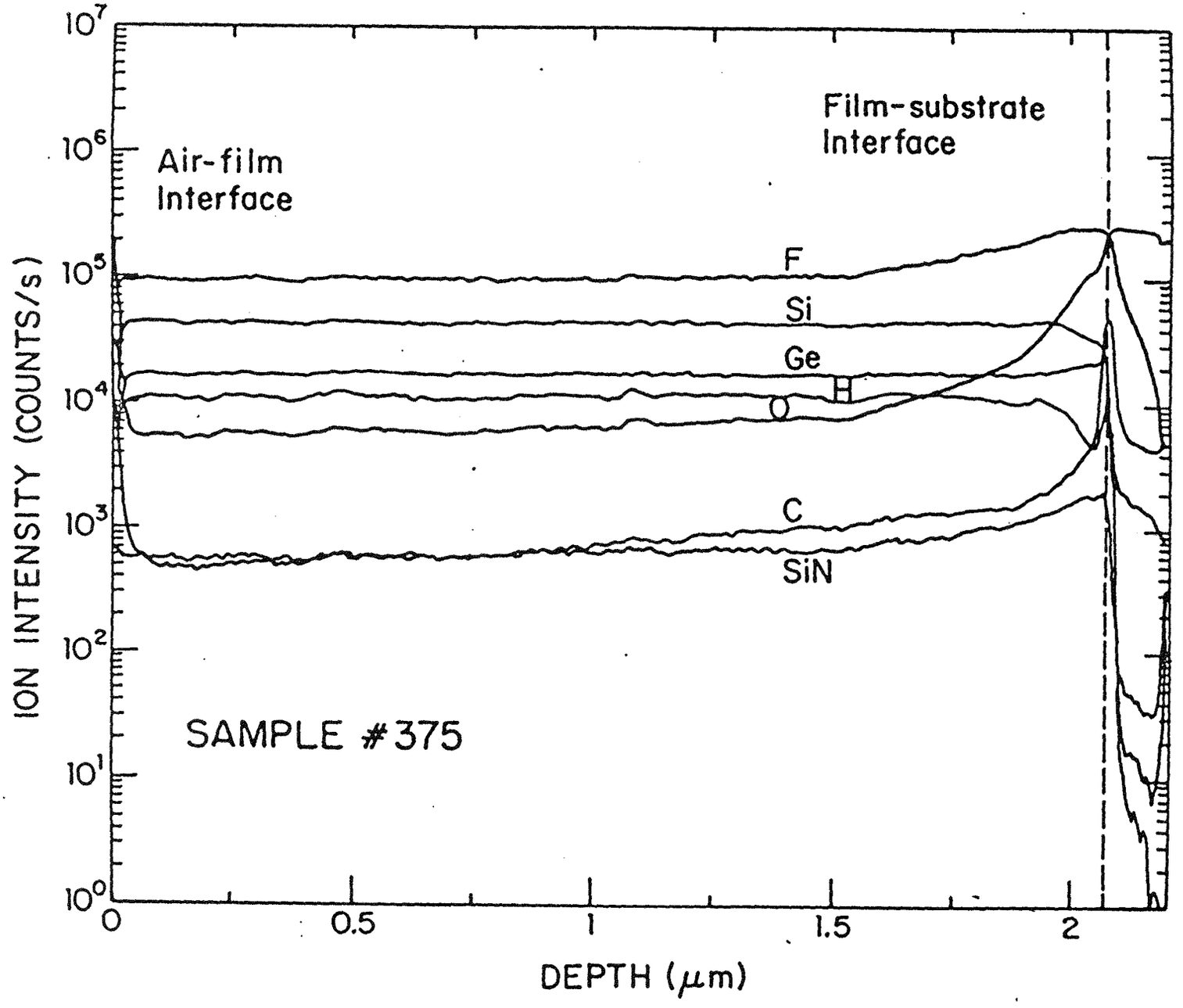
Air-film
Interface
Film-substrate
Interface
F
Si
Ge
H
O
C
SiN
SAMPLE #375
ION INTENSITY (COUNTS/s)
DEPTH (μm)
10^7
10^6
10^5
10^4
10^3
10^2
10^1
10^0
0
0.5
1
1.5
2

Figure 2

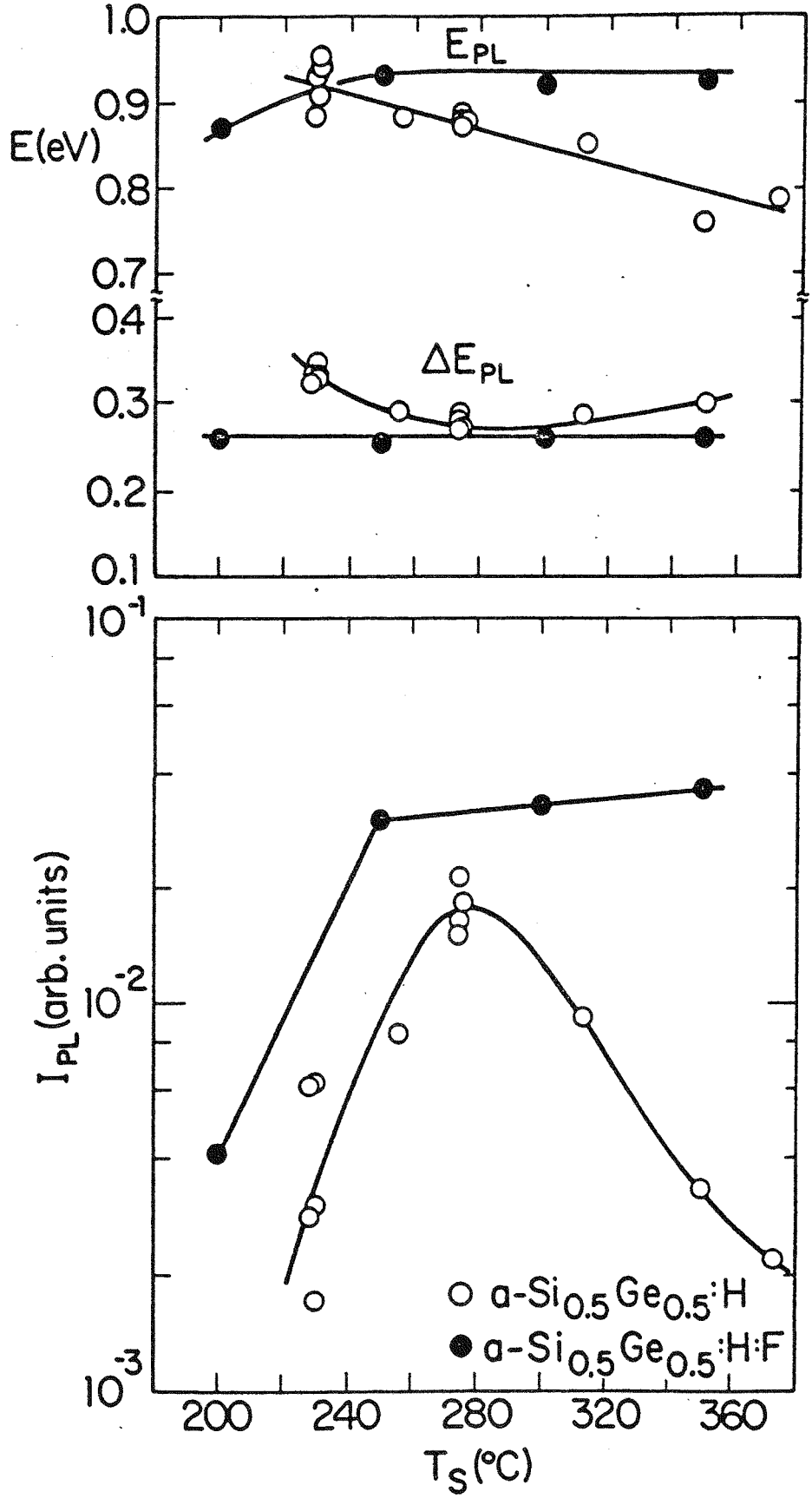
1.0
0.9
0.8
0.7
E(eV)
E_{PL}
0.4
0.3
0.2
0.1
ΔE_{PL}
10^{-1}
10^{-2}
10^{-3}
I_{PL}(arb. units)
○ a-$Si_{0.5}Ge_{0.5}$:H
● a-$Si_{0.5}Ge_{0.5}$:H:F
200
240
280
320
360
T_S(°C)

Figure 1

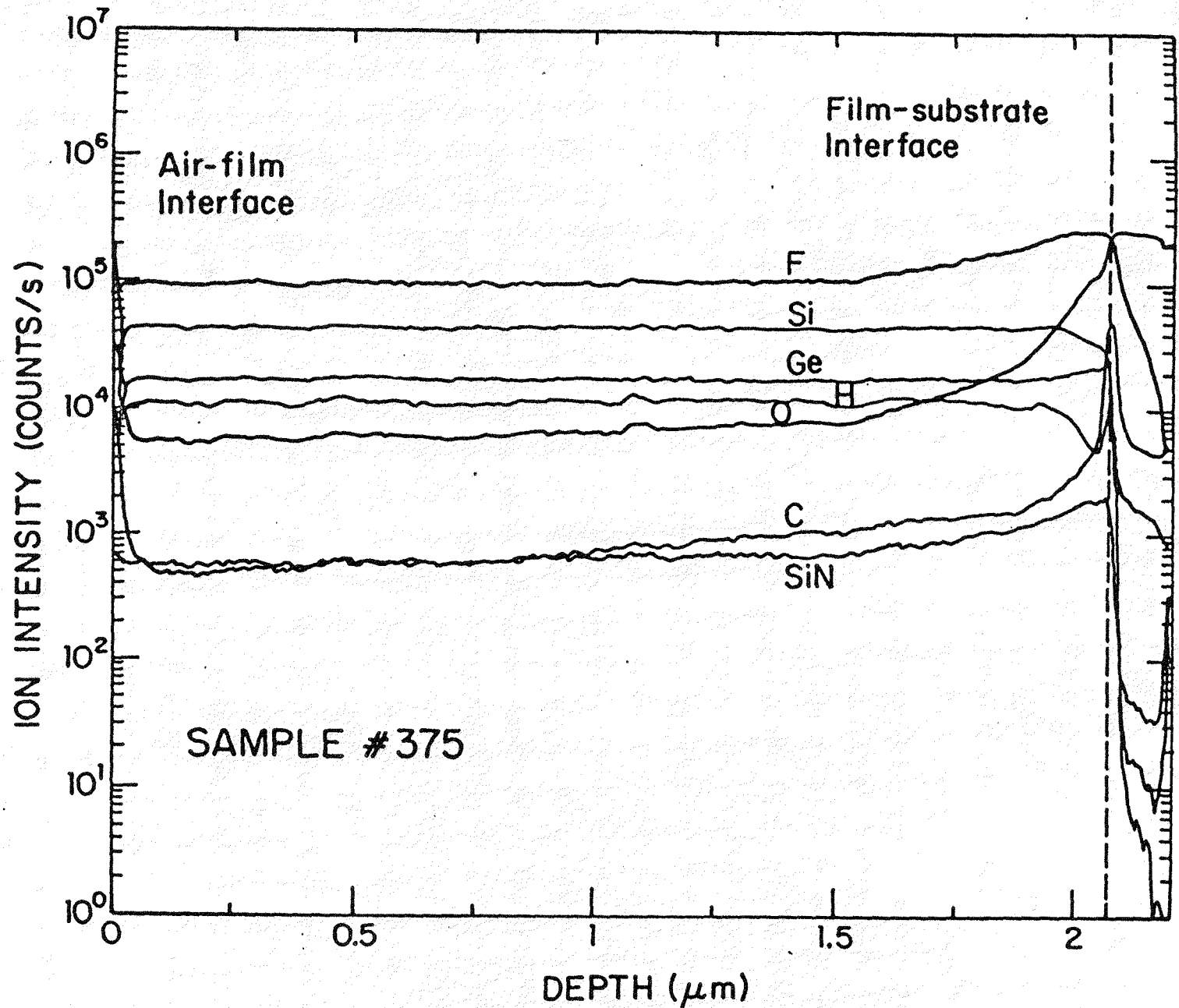

Figure 3

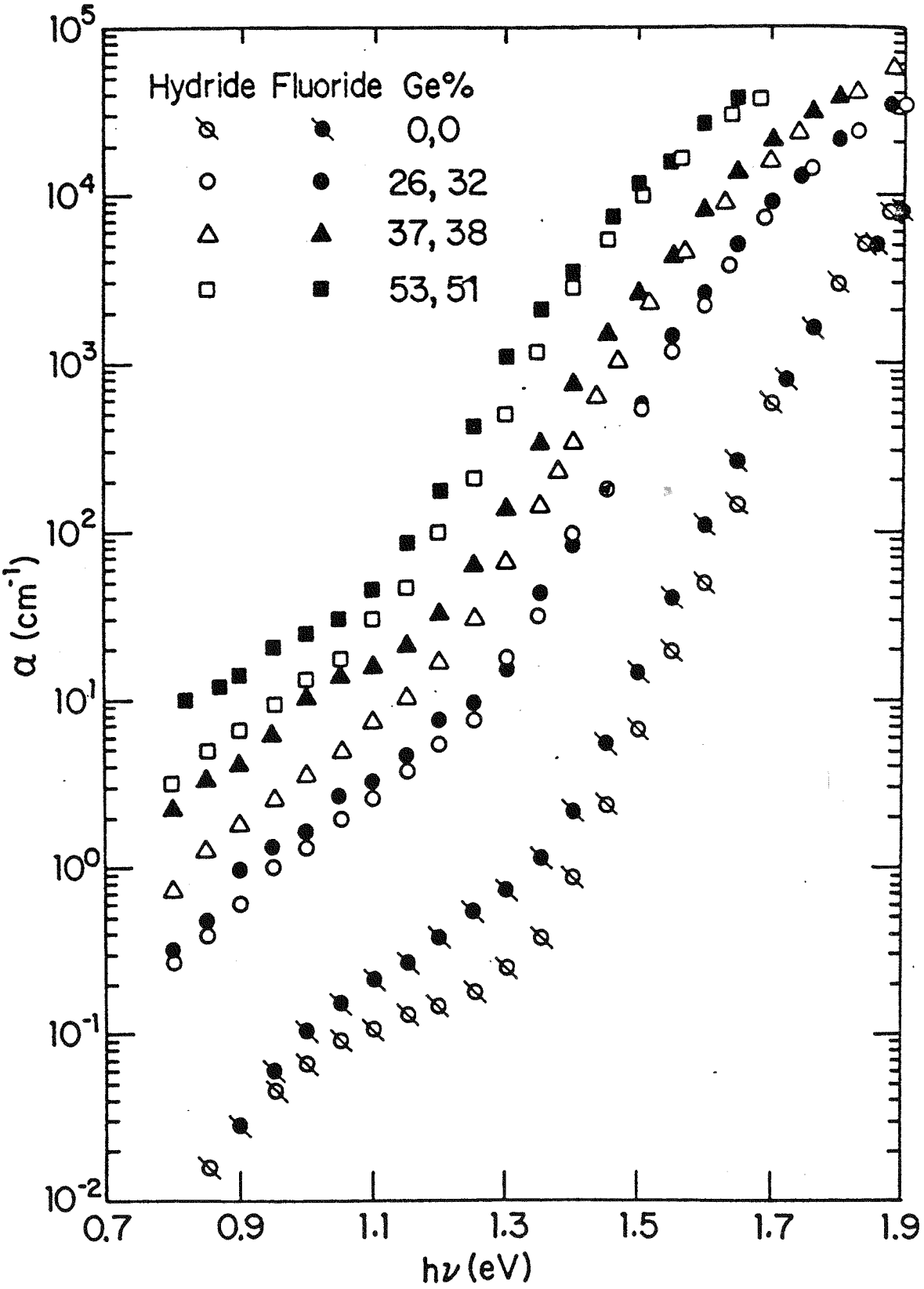
Hydride Fluoride Ge%
0,0
26, 32
37, 38
53, 51
α (cm⁻¹)
hν (eV)
10⁵
10⁴
10³
10²
10¹
10⁰
10⁻¹
10⁻²
0.7
0.9
1.1
1.3
1.5
1.7
1.9

THCL
Figure 4

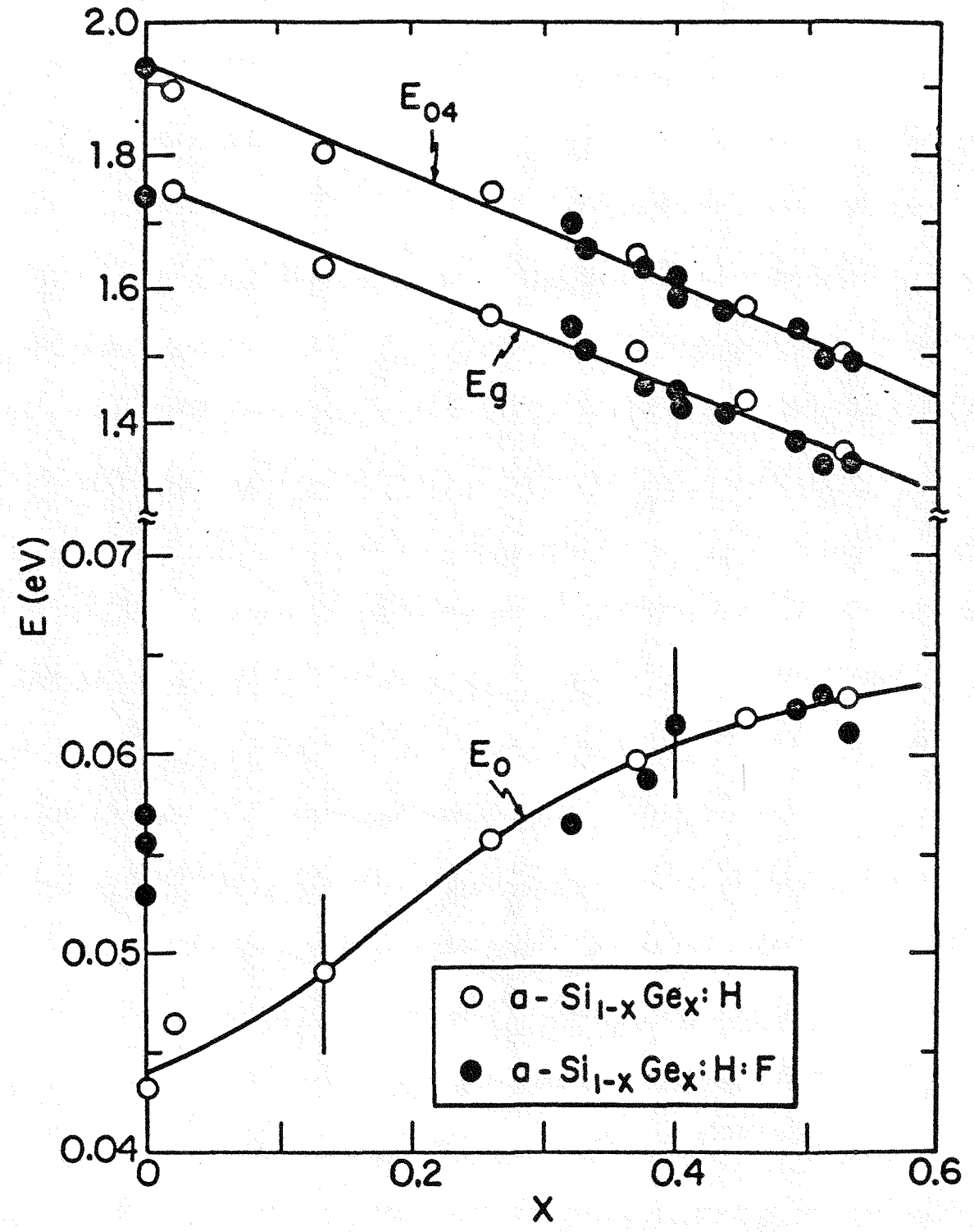

Figura 5a

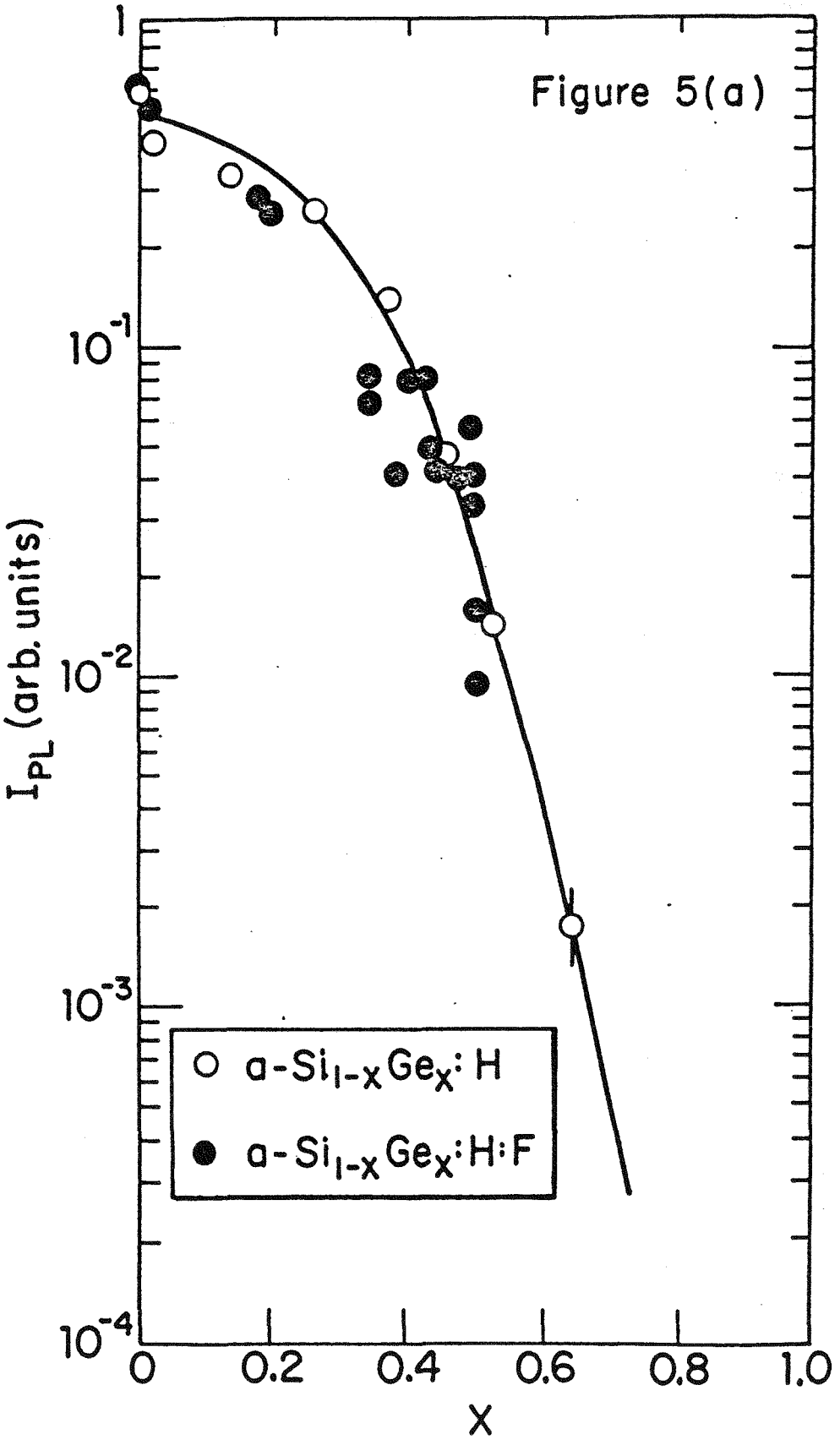
Figure 5(a)
1
10^{-1}
10^{-2}
10^{-3}
10^{-4}
I_{PL} (arb. units)
0
0.2
0.4
0.6
0.8
1.0
X
○ a-$Si_{1-x}Ge_x$: H
● a-$Si_{1-x}Ge_x$: H:F

Figure 5b

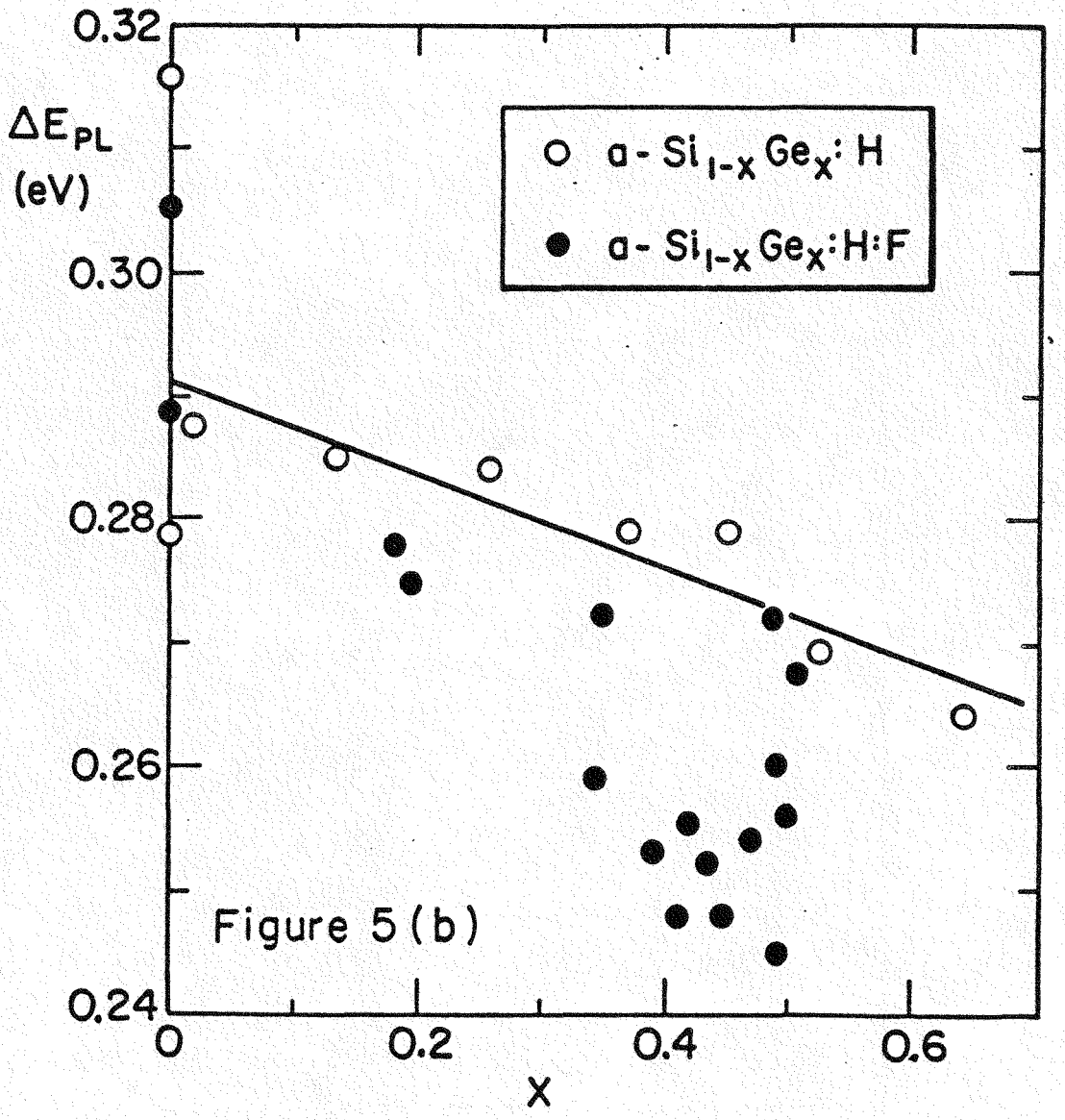

Figure 5 (b)

Figure 6

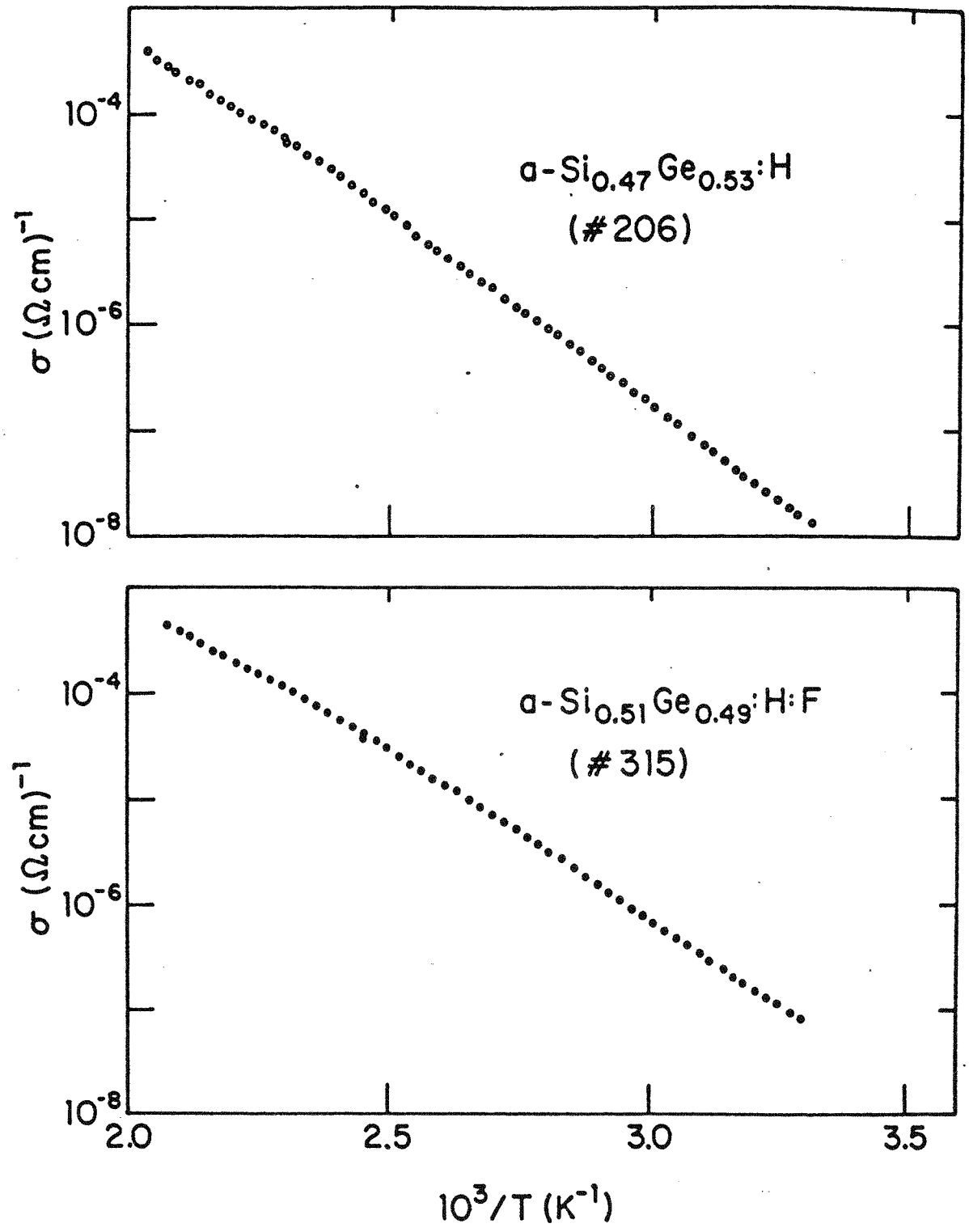
a-Si0.47Ge0.53:H
(#206)
a-Si0.51Ge0.49:H:F
(#315)
σ (Ωcm)-1
10-4
10-6
10-8
2.0
2.5
3.0
3.5
10³/T (K-1)

Figure 7

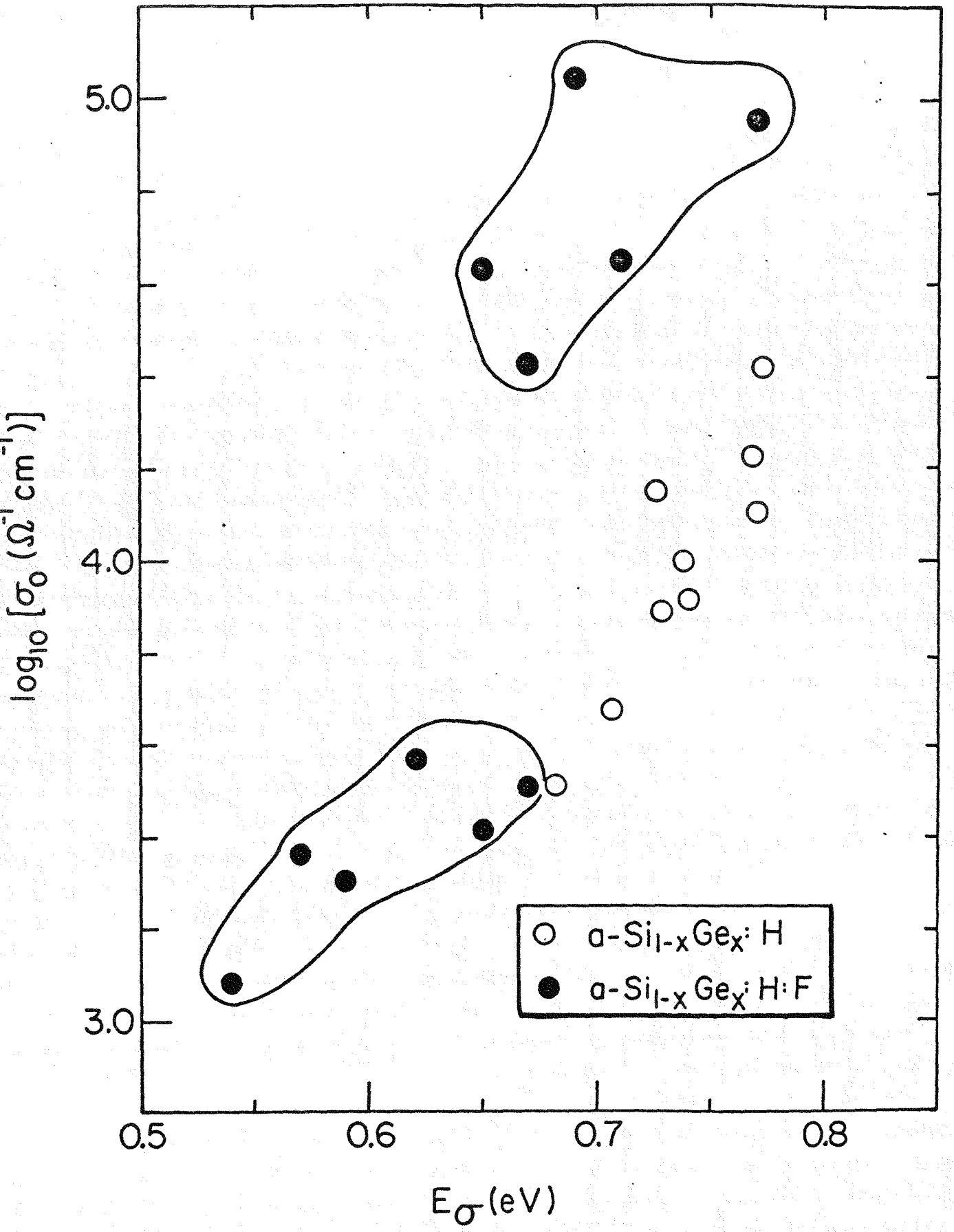
5.0
4.0
3.0
0.5
0.6
0.7
0.8
$\log_{10}[\sigma_o\ (\Omega^{-1}\,cm^{-1})]$
E_σ (eV)
a-$Si_{1-x}Ge_x$: H
a-$Si_{1-x}Ge_x$: H:F

Figure 8a

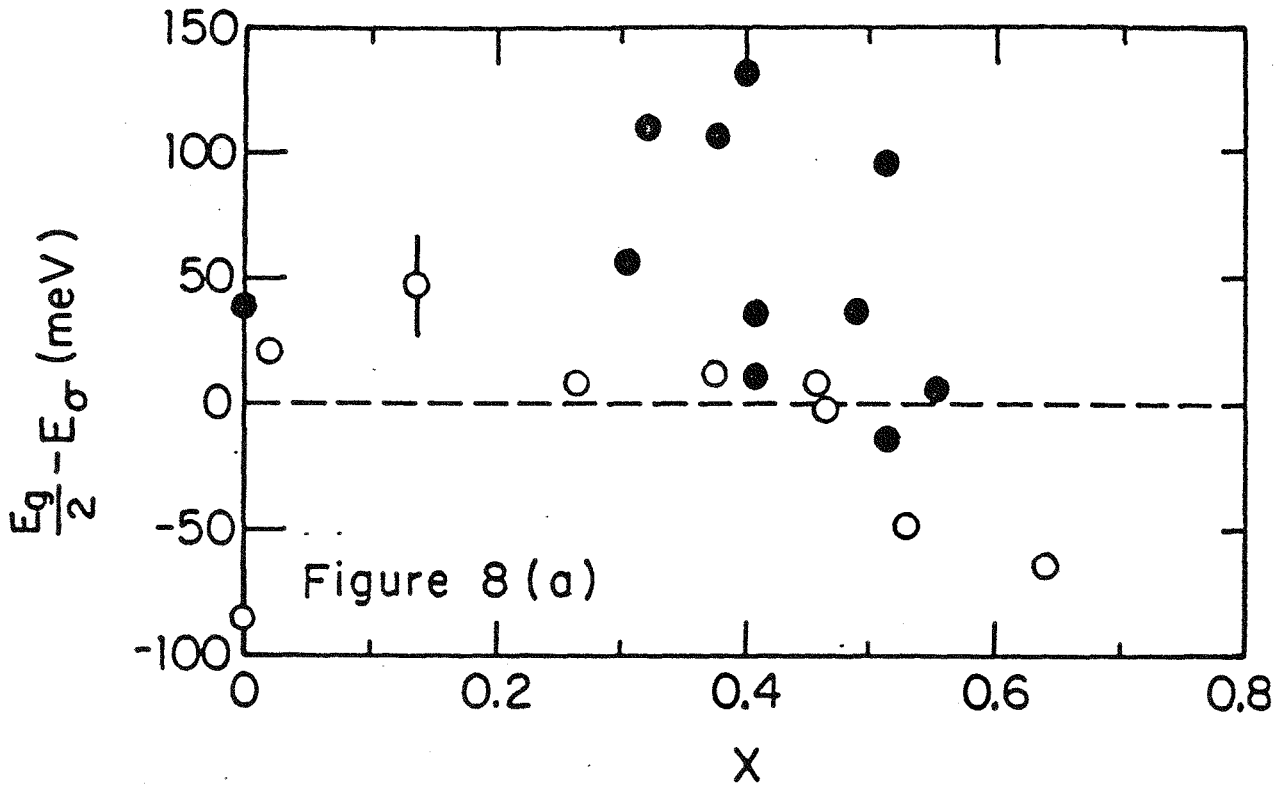

Figure 8 b

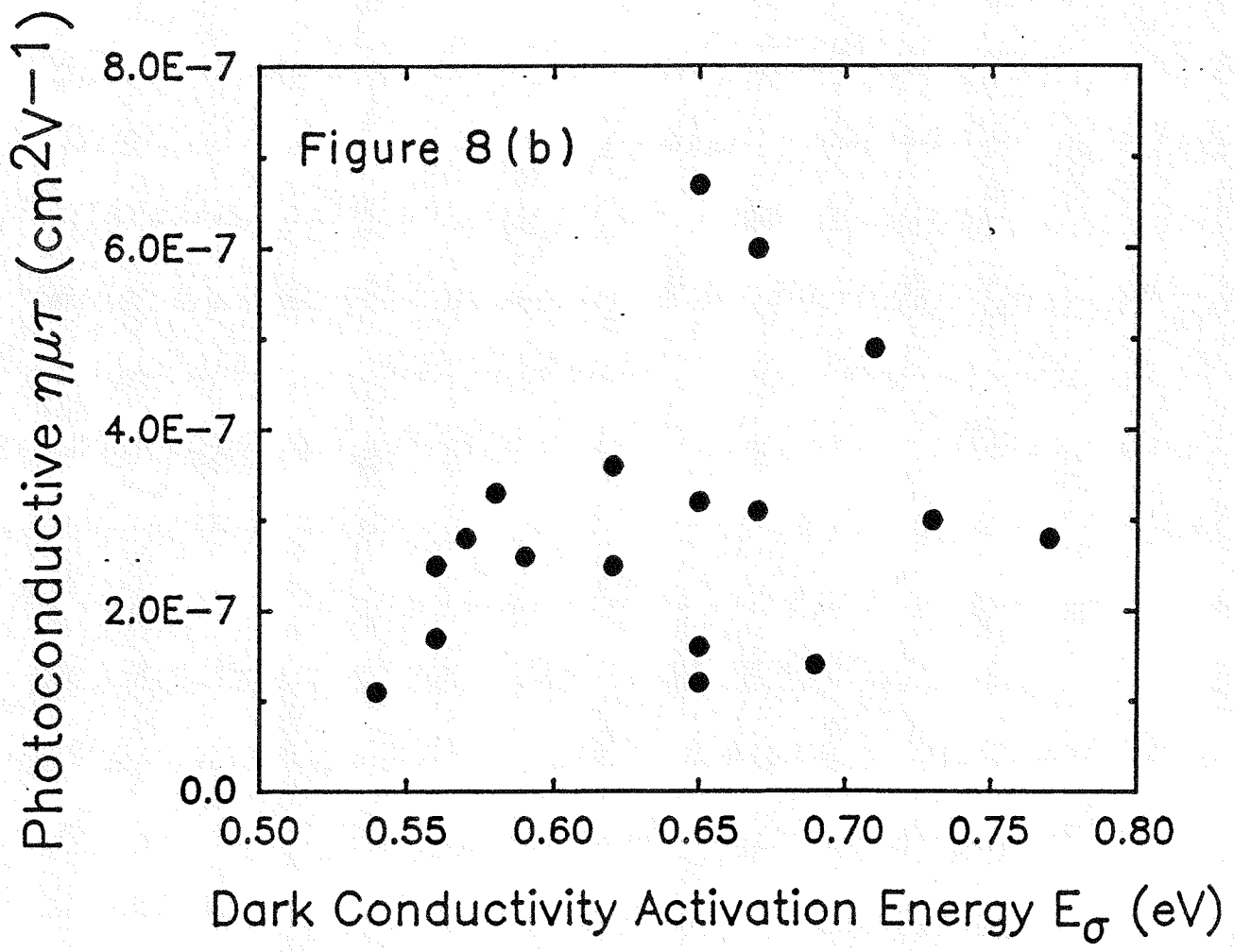
Figure 8 (b)
Photoconductive $\eta\mu\tau$ (cm2V−1)
8.0E−7
6.0E−7
4.0E−7
2.0E−7
0.0
0.50
0.55
0.60
0.65
0.70
0.75
0.80
Dark Conductivity Activation Energy E_σ (eV)

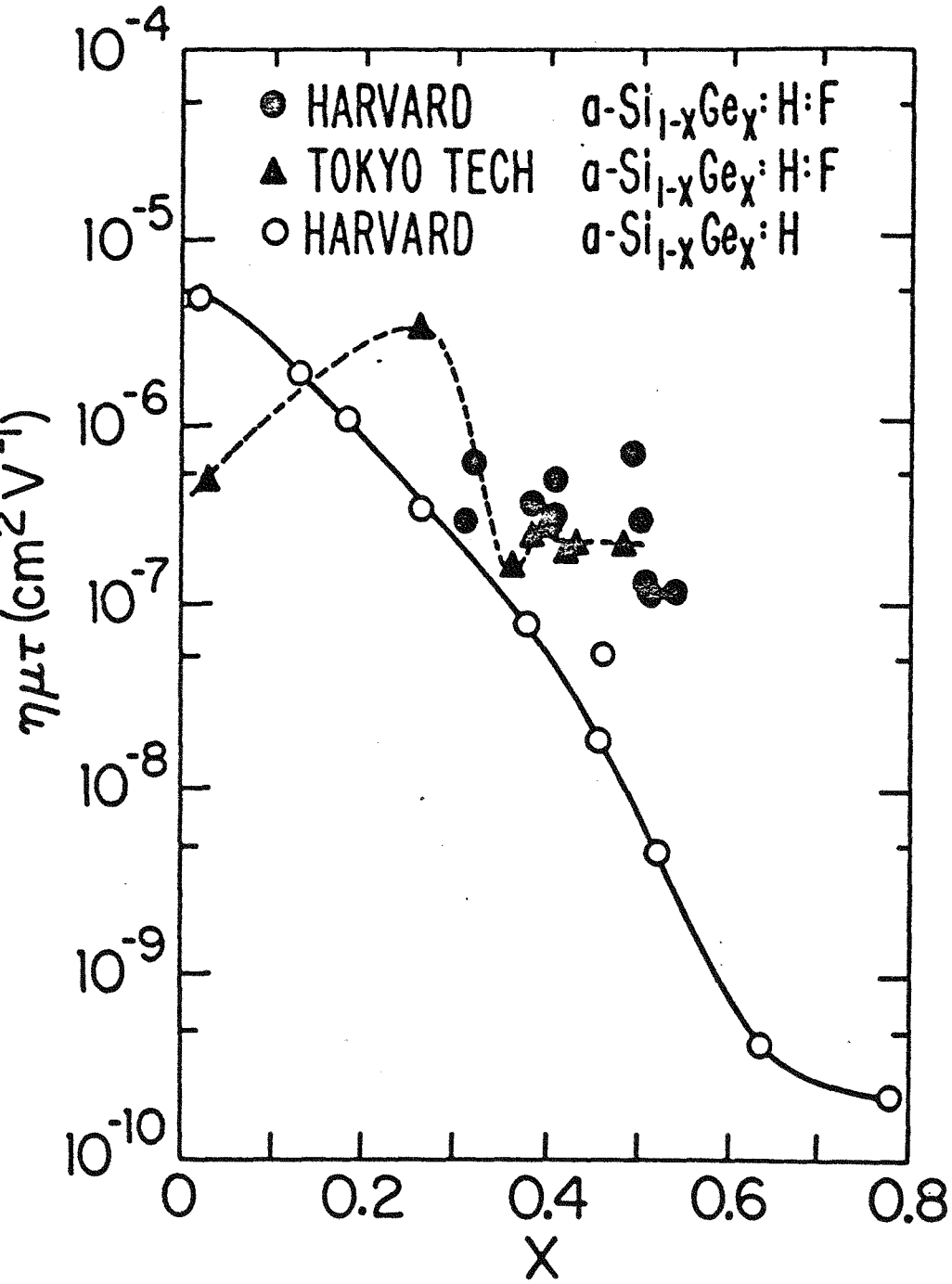
HARVARD a-Si1-xGex:H:F
TOKYO TECH a-Si1-xGex:H:F
HARVARD a-Si1-xGex:H
ημτ (cm2V-1)
10-4
10-5
10-6
10-7
10-8
10-9
10-10
0
0.2
0.4
0.6
0.8
X

Figure 10

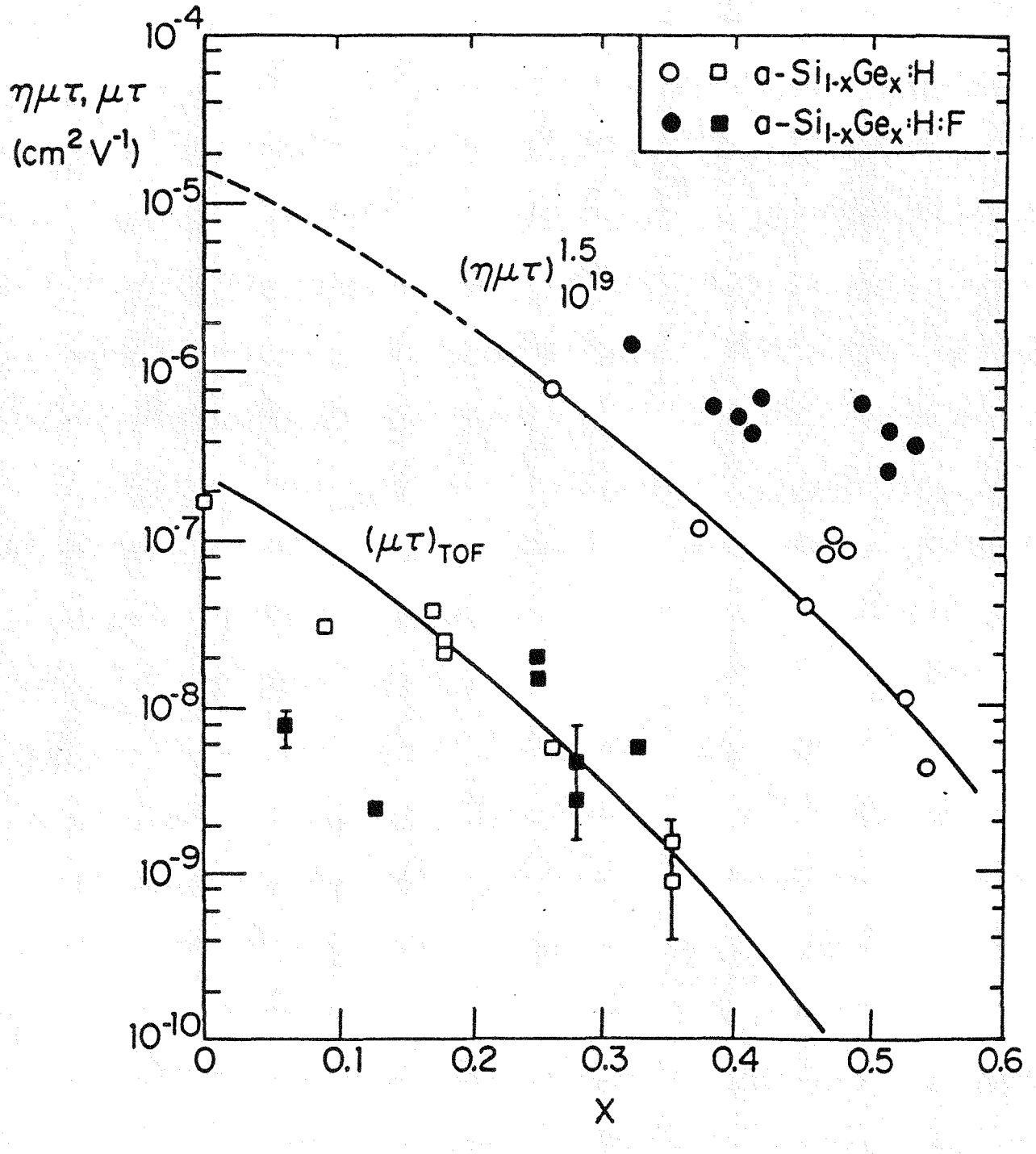
$\eta\mu\tau, \mu\tau$
$(cm^2 V^{-1})$
10^{-4}
10^{-5}
10^{-6}
10^{-7}
10^{-8}
10^{-9}
10^{-10}
0
0.1
0.2
0.3
0.4
0.5
0.6
X
a-$Si_{1-x}Ge_x$:H
a-$Si_{1-x}Ge_x$:H:F
$(\eta\mu\tau)\frac{1.5}{10^{19}}$
$(\mu\tau)_{TOF}$

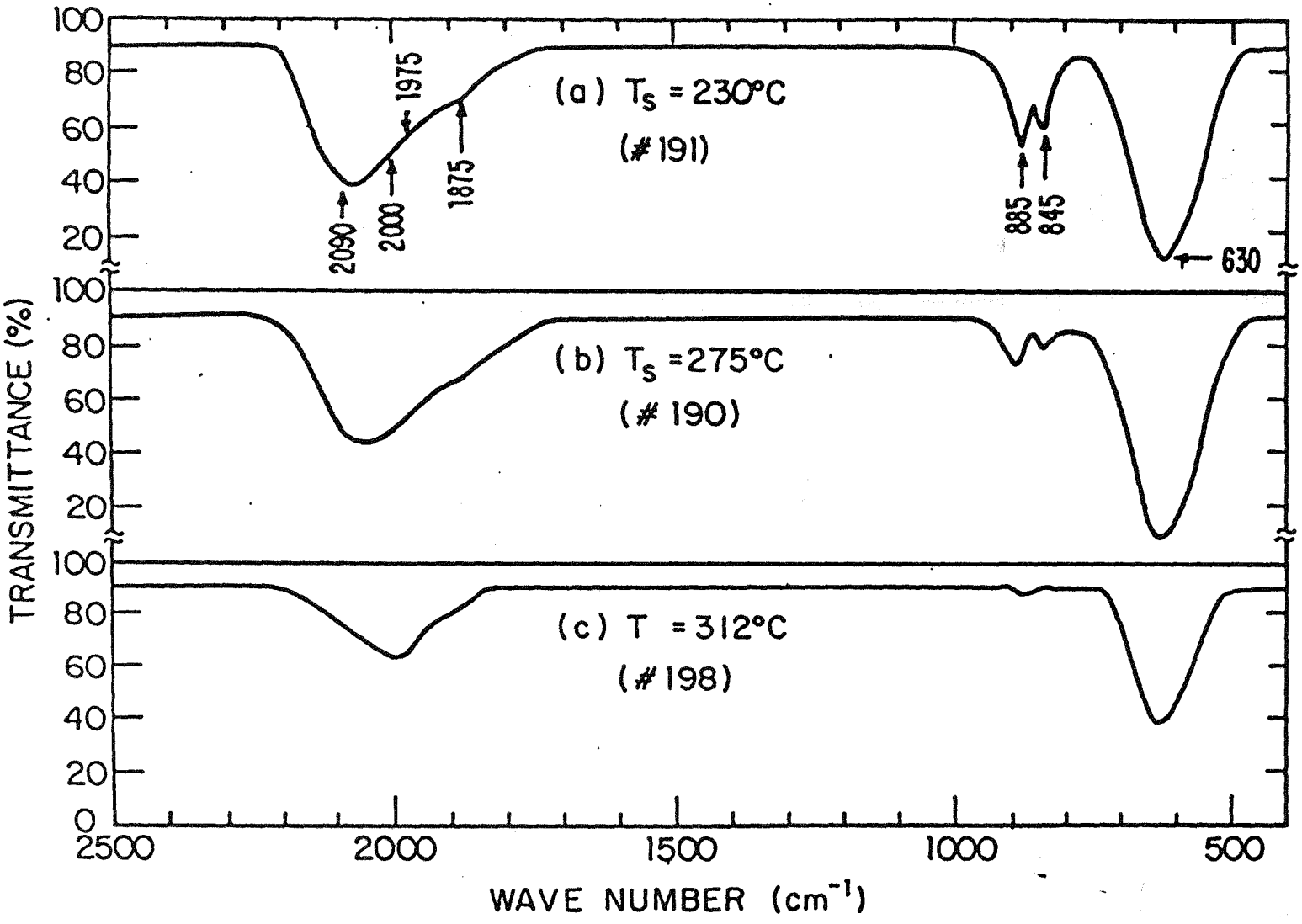
(a) T_s = 230°C
(#191)
(b) T_s = 275°C
(#190)
(c) T = 312°C
(#198)
2090
2000
1975
1875
885
845
630
TRANSMITTANCE (%)
WAVE NUMBER (cm^{-1})
2500
2000
1500
1000
500
0
20
40
60
80
100

Figure 12

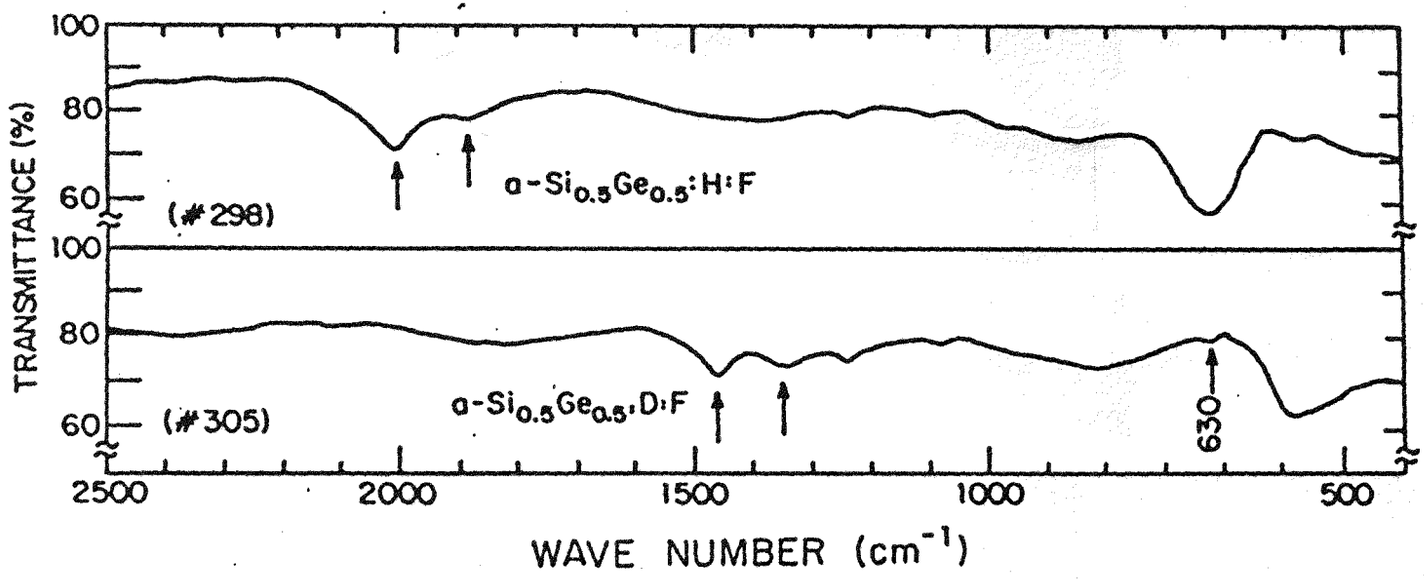
100
80
60
TRANSMITTANCE (%)
(#298)
a-Si0.5Ge0.5:H:F
100
80
60
(#305)
a-Si0.5Ge0.5:D:F
630
2500
2000
1500
1000
500
WAVE NUMBER (cm-1)

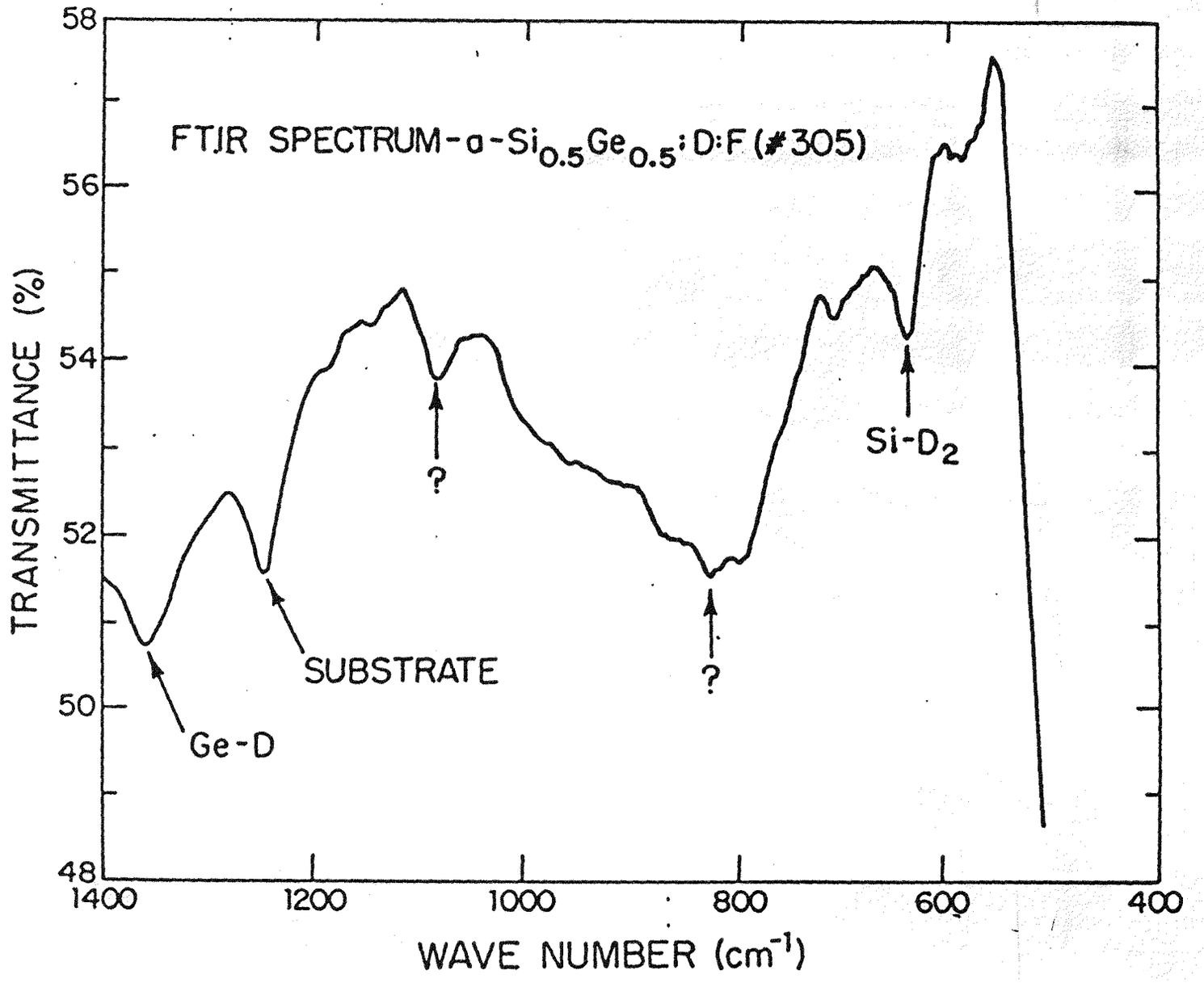
FTJR SPECTRUM - a-$Si_{0.5}Ge_{0.5}$:D:F (#305)
TRANSMITTANCE (%)
58
56
54
52
50
48
1400
1200
1000
800
600
400
WAVE NUMBER (cm^{-1})
Ge-D
SUBSTRATE
?
?
$Si-D_2$

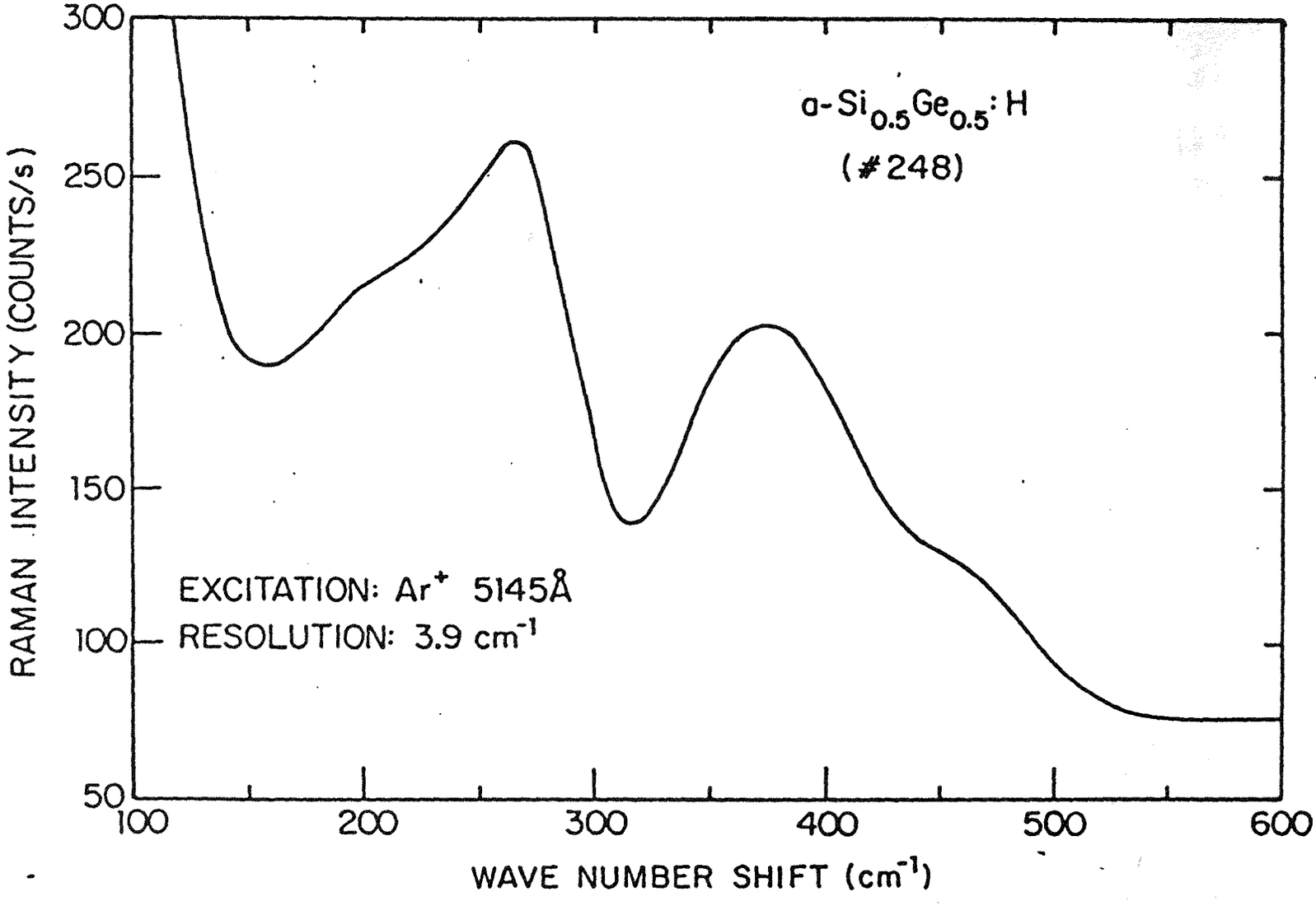
a-Si0.5Ge0.5:H
(#248)
EXCITATION: Ar+ 5145Å
RESOLUTION: 3.9 cm-1
RAMAN INTENSITY (COUNTS/s)
WAVE NUMBER SHIFT (cm-1)
300
250
200
150
100
50
100
200
300
400
500
600

Figure 14b

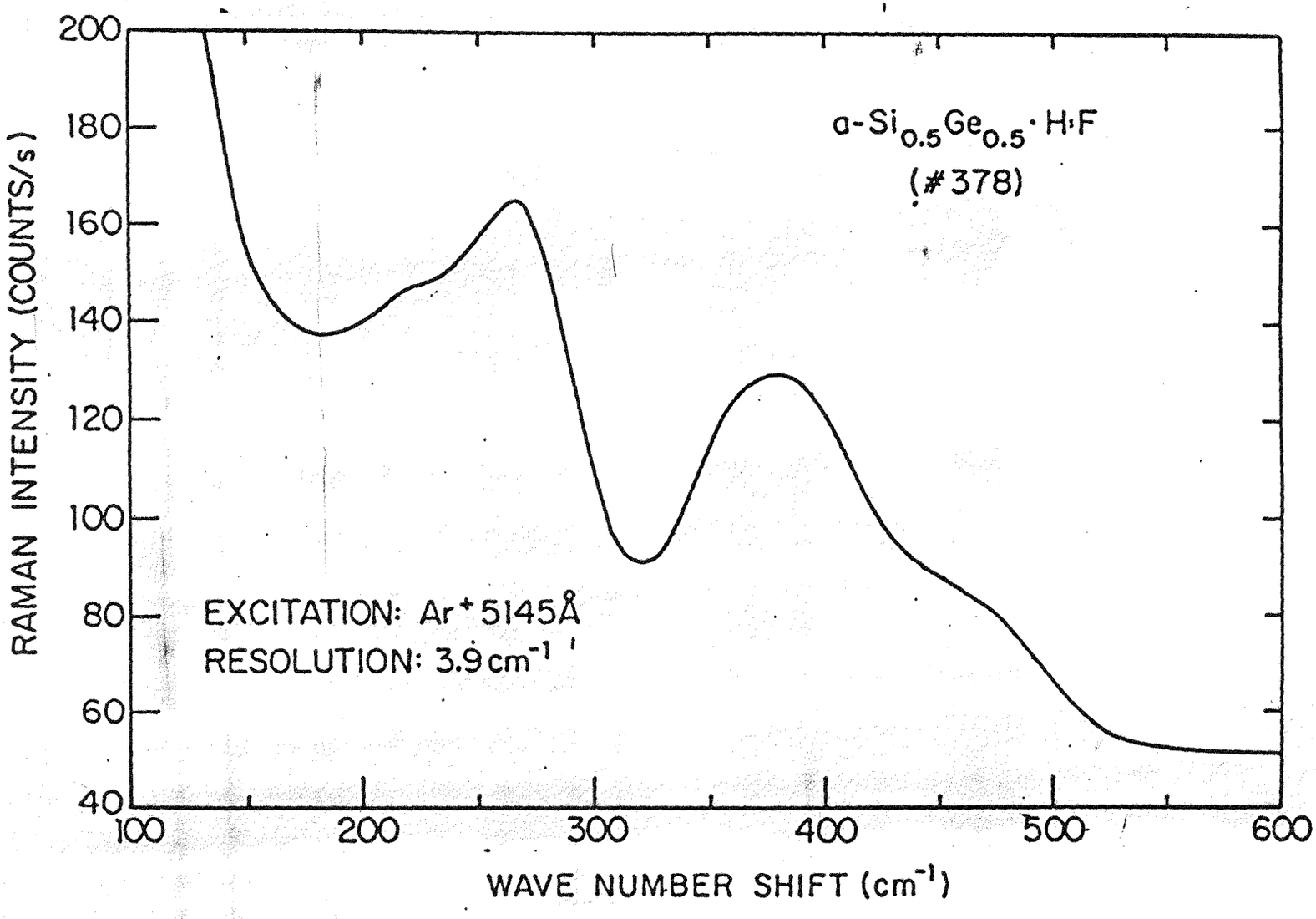
a-Si0.5Ge0.5 · H·F
(#378)
EXCITATION: Ar+ 5145Å
RESOLUTION: 3.9 cm-1
RAMAN INTENSITY (COUNTS/s)
WAVE NUMBER SHIFT (cm-1)
200
180
160
140
120
100
80
60
40
100
200
300
400
500
600

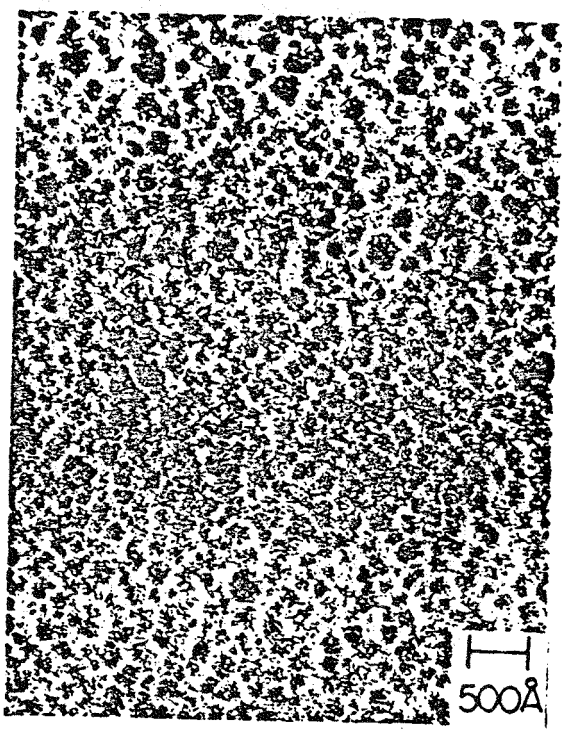

Figure 17a

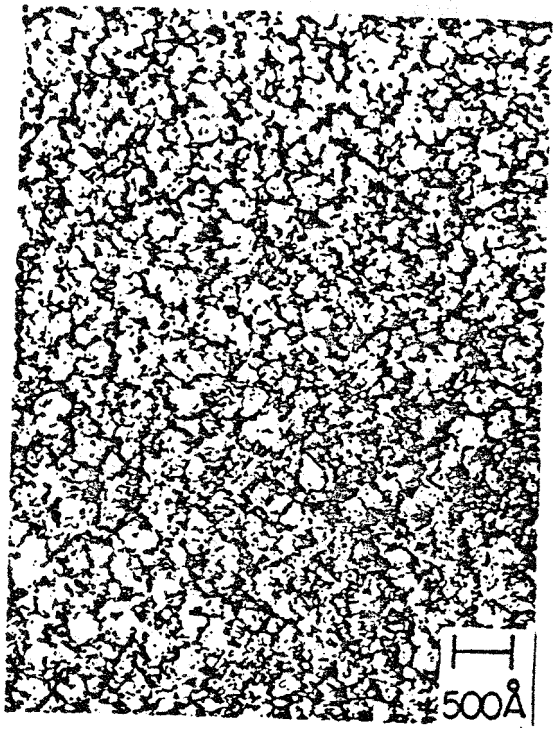

Figure 17b

MACKENZIE

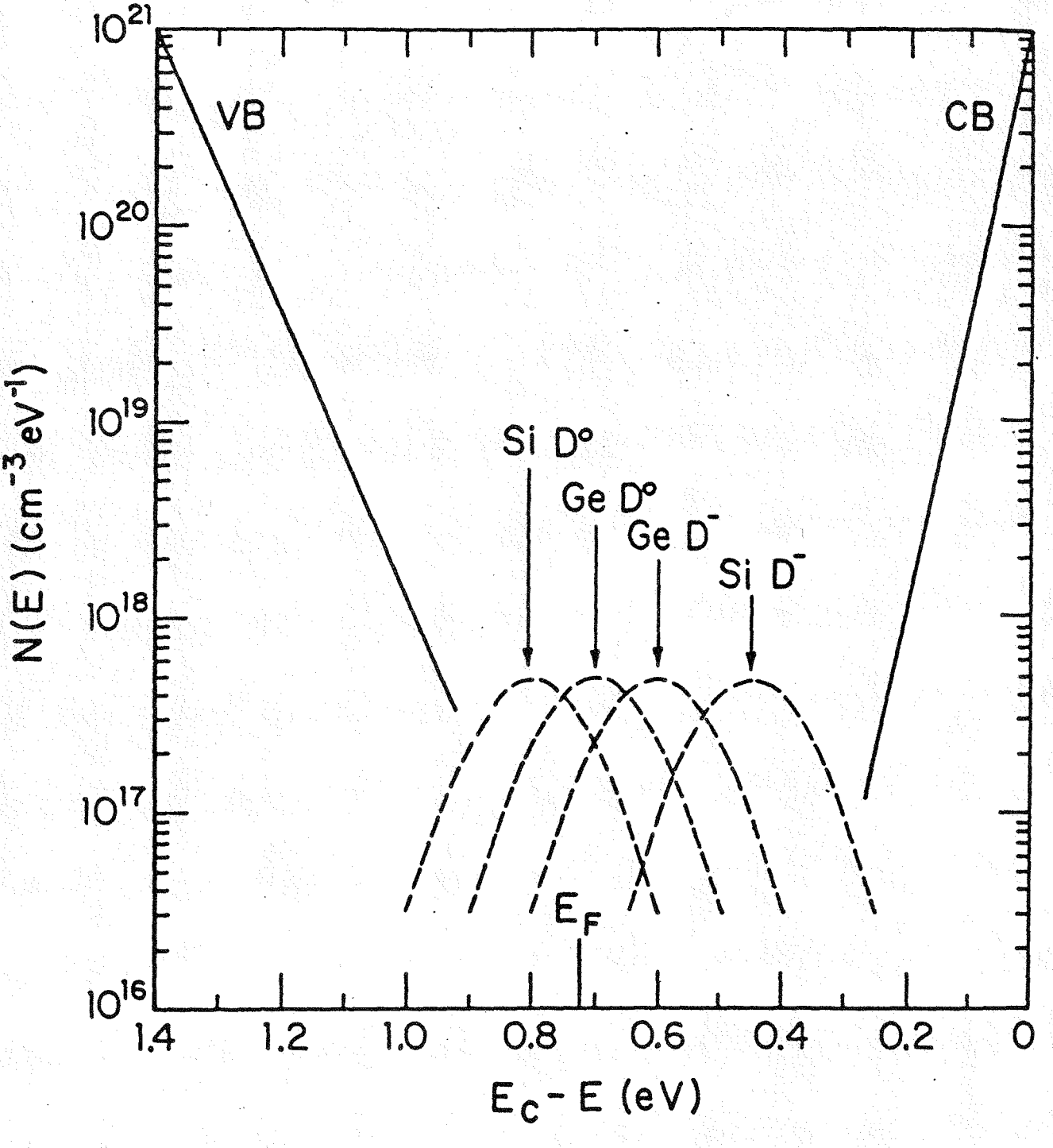
10^{21}
10^{20}
10^{19}
10^{18}
10^{17}
10^{16}
N(E) ($cm^{-3} eV^{-1}$)
VB
CB
Si D°
Ge D°
Ge D⁻
Si D⁻
E_F
1.4
1.2
1.0
0.8
0.6
0.4
0.2
0
$E_c - E$ (eV)

PAUL Figure 17

(VALENZIE)

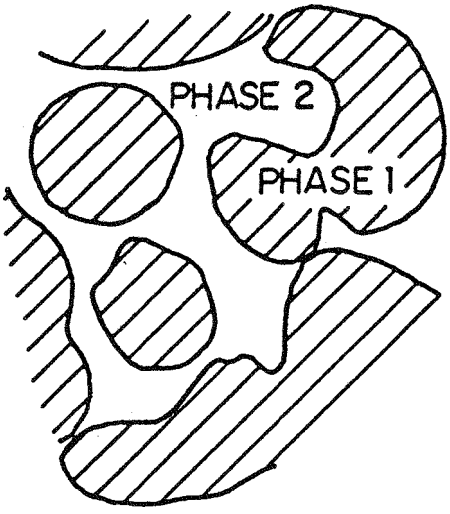

ISLAND/TISSUE

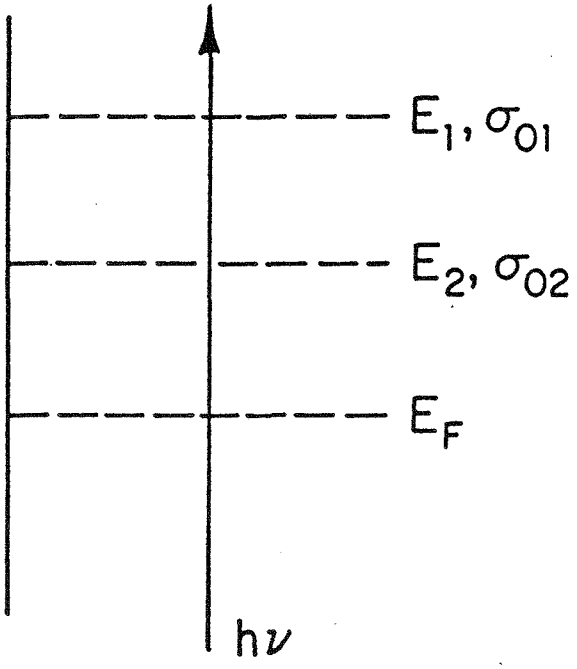

$\sigma_0 \propto \mu$

Current Transport in a-Si:Ge Alloy Schottky Barriers

D. K. Sharma, K. L. Narasimhan, Shailendra Kumar, and B. M. Arora

Tata Institute of Fundamental Research, Bombay, 400005, India

W. Paul and W. Turner

Division of Applied Sciences, Harvard University, Cambridge, Massachusetts, 02138, U.S.A.

Abstract. In this paper, we have investigated the temperature dependence of forward and reverse currents of a-Si:Ge:H-Pd barriers. In contrast to a-Si:H, we find that the diode quality factor is 2 and is independent of temperature. We have confirmed quantitatively that the forward current is recombination limited and the reverse current generation limited. The barrier height $\Phi_B = 0.7$ eV which is half the measured optical gap. The frequency, bias and temperature dependence of capacitance has also been investigated. From the capacitance measurements, we infer that the density of states near midgap is approximately 2×10^{17} cm^{-3}eV^{-1}.

Introduction

Amorphous Si_xGe_{1-x}:H alloys play an important role in high efficiency solar cells.[1] It is, therefore, of great interest to obtain reliable estimates of the density of gap states in these materials and to understand the nature of transport across the barrier region in these materials. In this paper we study the d.c. transport in a-$Si_{0.5}Ge_{0.5}$:H-Pd Schottky barriers. We have also investigated the temperature, bias and frequency dependence of capacitance and obtained an estimate for the density of states in these materials.

Sample Preparation and Characterization

The a-$Si_{0.5}Ge_{0.5}$:H samples used in this study were prepared in a manner previously described in the literature.[2] The structures were made on Corning 7059 glass substrates under the following conditions. First, an n-type layer of a-Si:H:P of 0.1 μm thickness was deposited at 300°C out of a plasma of (SiH_4+PH_3) at a chamber pressure of 0.2 torr and total gas flow of 20 sccm. The system was then flushed with H_2 gas for 5 hours and 1μm of a-$Si_{0.5}Ge_{0.5}$:H deposited, again at 300°C, out of a plasma of (SiH_4+GeH_4), chamber pressure of 0.25 torr, power density of 60 mW/cm^2, and gas flows of 12 sccm of SiH_4 and 2.15 sccm of GeH_4. Finally, approximately 10 nm thick Pd contacts were evaporated for Schottky barrier contacts.

The SiGe alloy was characterized electrically and optically using standard procedures. The optical gap, deduced from the formula

$$\alpha(h\nu) = A(h\nu - Eg)^2$$

was found to be 1.35 eV. The values of E_{03} and E_{04}, the photon energies at which the absorption coefficients were 10^3 cm^{-1} and 10^4 cm^{-1} respectively, were 1.36 eV and

1.54 eV. The parameters E_σ and σ_0 in the formula for the conductivity

$$\sigma = \sigma_0 \exp(-E_\sigma/kT)$$

were 0.38 eV and 2.7×10^2 (ohm-cm)$^{-1}$ respectively. This value for E_σ is significantly below that expected for an alloy of this composition and is an indication of residual doping contamination from the n-type layer deposited prior to the alloy layer.

Current-Voltage Measurements

The current voltage $(J-V)$ relationship of an ideal Schottky barrier can be written as[3]

$$J = J_0(\exp qV/kT - 1)$$

where

$$J_0 = J_{00} \exp(-\Phi_B/kT)$$

and

Φ_B is the barrier height.

Real diodes are found to actually satisfy an equation of the form[4]

$$J/(1 - \exp(-qV/kT)) = J_{FO} \exp qV/nkT \qquad (1)$$

where n is the diode quality factor, which can be obtained from a plot of $\ln J/(1 - \exp(-qV/kT))$ *vs.* V. Figure 1 shows one such plot for an a-Si:Ge:H alloy. At room temperature we find that $n = 2$ and that n is independent of temperature. This suggests

that the forward current in this barrier is recombination limited.[3] In such a case we can write for J_{FO} in eqn. (1)[5]

$$J_{FO} = qW\sigma v N_t n_i/2 \tag{2}$$

where W is the depletion width, N_t the number of states at midgap and σ their capture cross-section, v the carrier thermal velocity and n_i the intrinsic carrier concentration.[6] It is easy to see from eqn. (2) that a plot of $\ln J_{FO}$ *vs.* $1/T$ will have a slope of $-E_g/2k$.

Figure 2 is a plot of $\ln J_{FO}$ *vs.* $1/T$. We see that the value of $E_g/2$ is ~ 0.67 eV suggesting that the energy gap is close to 1.4 eV. This is consistent with the measured optical gap.

Since the forward current is dominated by recombination current, it is natural to expect the reverse current to be dominated by generation current. In such a case, the reverse current J_R should be given by

$$J_R = qn_i W(1 - \exp(-qV/2kT))/2\tau \tag{3}$$

where τ is the effective lifetime.[5] In this case, we see that a plot of $\ln(J_R/(1-\exp(-qV/2kT)))$ at any given voltage V as a function of $1/T$ should be thermally activated with an activation energy $\Delta E = E_g/2$. Figure 3 is a plot of $\ln(J_R/(1-\exp(-qV/2kT)))$ at different values of V *vs.* $1/T$. We see that all these curves have the same slope and have $\Delta E = 0.7$ eV in agreement with the value of E_g obtained from the forward characteristics. This confirms the fact that generation is responsible for the reverse characteristics.

Capacitance Measurements

In crystalline semiconductors, capacitance measurements play an important role in defect spectroscopy. In a-Si:H, the interpretation of capacitance is complicated as deep

levels dominate the capacitance. Only those levels that cross E_F in the space charge region and can change their charge state in a time $1/w$ (where w is the angular frequency of measurement) contribute to the capacitance.[7-14] This gives rise to a dispersion of capacitance with frequency. The situation is further complicated by the fact that we are dealing with high resistivity materials. This results in a large value of series resistance which can also give rise to a frequency dependence. The inset in Fig. 4 shows an equivalent circuit of the sample. R_1 is the bulk series resistance and C_1 its associated capacitance. R_2 and C_2 are the resistance and capacitance respectively of the Schottky barrier and R_m and C_m the equivalent (measured) parallel resistance and capacitance. If $R_2 >> R_1$, then R_m and C_m approximate closely to R_2 and C_2. A simple equivalent circuit analysis shows that

$$R_2 = (X^2 + w^2Y^2)/X$$

and

$$C_2 = Y/(X^2 + w^2Y^2)$$

where

$$X = (R_m/(1 + w^2C_m^2R_m^2)) - (R_1/(1 + w^2C_1^2R_1^2))$$

and

$$Y = (C_mR_m^2/(1 + w^2C_m^2R_m^2)) - C_1R_1^2/(1 + w^2C_1^2R_1^2)\ .$$

Unlike a-Si:H, we have already seen that in the a-Si:Ge:H alloys, the reverse currents are dominated by the generation current and R_2 is not large compared to R_1 even at low

frequencies. The measured R_m and C_m are hence not truly representative of R_2 and C_2 and need to be corrected as detailed above. The effects of this correction can be quite dramatic as will be seen below.

Figure 4 shows the measured C_m as a function of frequency at room temperature. The dotted line shows the true Schottky capacitance C_2 after correcting for R_1 and C_1. R_1 was obtained at the frequency of measurement by measuring the current in phase with the applied a.c. voltage when the diode is biased into far forward bias. For C_1, we have taken the geometrical capacitance as measured at high frequency. We see that the true capacitance has a smaller dispersion with frequency when compared with C_m. The effect of the series resistance can be seen more dramatically when we look at the bias dependence of capacitance.

It is expected that the application of a reverse bias will result in a lowering of the capacitance. We see instead in Fig. 5, that for small reverse bias, C_m initially increases and then decreases with further increase in reverse bias. This "anomalous" behaviour of capacitance becomes "normal" if we correct for the series resistance as shown in Fig. 5. The "anomalous" effect arises because, not unexpectedly, R_2 is also a function of bias.

Having obtained the true capacitance, we can now estimate the density of deep levels. We first note that the cutoff energy $E_c - E_t$ below which states will not contribute to the capacitance at a frequency w and temperature T is given by

$$E_c - E_t = kT \ln(\nu_0/w)$$

where ν_0 is assumed to be of the order of 10^{13}/sec. At $f = 4$ Hz and at $f = 90$ Hz with $T = 300°$K, $E_c - E_t = 0.67$ eV and 0.6 eV, respectively. Thus the capacitance measurements in the 4 to 90 Hz frequency range effectively probe the region between 0.6 eV and 0.7 eV below E_c.

If we assume that E_F is flat in the space charge region (valid exactly at zero bias) and E_t (the deepest level that responds at a frequency w) intersects E_F at a distance x_e from the junction, then the region between the junction ($x = 0$) and x_e is essentially an insulator and only states between E_F and E_t (for $x > x_e$) contribute to the capacitance[7-14] (Fig. 6). The junction capacitance is then given by

$$C_2 = \epsilon\rho_e/(x_e\rho_e + \epsilon F_e)$$

where F_e is the field and ρ_e is the charge density at $x = x_e$.

On application of a reverse bias, C decreases as x_e moves further into the bulk of the semiconductor keeping $\rho_e/F_e = C_{sc}$ constant.[7] Thus, the variation of C^{-1} with V is really a measure of the variation of x_e with V.

Since we expect nearly all the states up to midgap to respond at 4 Hz, at zero bias x_e can be very small. This is easily justified when we note that the band bending at zero bias $V_d = \Phi_B - E = 0.1$ eV is also very small. ΔE was obtained from the temperature dependence of the series resistance. If we assume $g(E) = g_0$, a constant between E_{FO} and the statistical midgap level E_i, then $C_{sc} = A\sqrt{qg_0\epsilon}$ and for $C_{sc} = 6.5$ nF we get $g_0 \sim 2 \times 10^{17}/\text{cm}^3\text{-eV}$. It should be recognized that this is a lower limit for $g(e)$.

The density of states can also be estimated independently from $C - V$ data under suitable conditions. The quasi-Fermi level (under reverse bias conditions) is flat in the depletion region only for small reverse bias voltages. Once E_F equals E_i in the depletion region, it stays pinned to E_i.[7] In such a case, it is easy to see that the space charge density is constant independent of position, and the normal Schottky barrier analysis is valid if the capacitance of this "insulator-like" region dominates the total capacitance (which is true at large reverse bias). If $g(E,x)$ is independent of x, then $1/C^2$ *vs.* V is a straight

line and the slope is given by $-1/\epsilon A^2 g_0 \rho$ where ρ is

$$\rho = \int_{E_i}^{E_{FO}} g(E)\, dE \ .$$

We really would expect this behaviour to be valid at large reverse bias. In the a-Si:Ge:H alloys reported here, since $E_{FO} - E_i = 0.1$ eV, this can occur at fairly small voltages.

Figure 7 shows $1/C^2$ *vs.* V measured at 8 Hz at room temperature. We find g_0 to be about 3×10^{17}/eV-cm^3 which is similar to our estimate of g_0 from the low frequency capacitance. This is in satisfactory agreement with a value of 10^{17}/eV-cm^3 estimated from SCLC measurements.[15]

The temperature dependence of capacitance provides us with an independent check on the assumption that the "insulator-like" region dominates the total capacitance. The width of the region where $E_F = E_i$ is not a very sensitive function of temperature. Consequently, if this capacitance dominates the total capacitance, C will be reasonably independent of temperature. Figure 8 shows C as a function of temperature for $1V$ reverse bias and zero bias, further confirming our hypothesis.

It should also be possible in principle to obtain an estimate for $g(E)$ from a plot of $C^2(dC/dT)^{-1}$ *vs.* T. It can be shown[7] that $C^2(dC/dT)^{-1} = A(\epsilon q g_0)^{1/2}\,[(T - T_0) + \cdots]$ where $g_0 = g(E_{FO})$ for $T > T_0$. T_0, the "freeze-out" temperature of the a.c. response, is close to $-10°$C for our samples. However, we find that this plot is only pseudo-linear in T. If we use an average slope to determine g_0, we estimate it to be 8×10^{18}/cm^3-eV. Such a large value for g_0 is unreasonable as it would preclude the formation of Schottky barriers with any significant rectification.

The estimate is probably erroneous because the above expression for $g(E)$ is valid only if $g(E)$ is not a function of depth in the material. At zero bias, in view of the small

barrier height, this may not be valid because of the proximity of x_e to the surface where material properties are expected to vary.

In summary, we have measured the temperature dependence of the dark forward and reverse d.c. currents in a-Si:Ge:H-Pd Schottky barriers. We find that, unlike a-Si:H, the currents are governed by the midgap states suggesting that the density of defects in these alloys is larger than in a-Si:H alloys. We have measured the temperature, frequency and bias dependence of capacitance in these alloys. We find that since these alloys are leaky, the measured parallel equivalent capacitance (conductance) is not that of the Schottky barrier but needs to be corrected or else the interpretation of the data can be very misleading. We have estimated the density of states from both the bias and the frequency dependence of capacitance and estimate $g(E_F)$ to be $2 \times 10^{17}/\text{cm}^3$ -eV in these samples, in satisfactory agreement with other estimates.[15]

Acknowledgements

This work was done under the auspices of the Indo-US STI program.

After conclusion of this work, our attention has been drawn to measurements on a-Ge:Si:H alloys reported recently by Matsuura *et al.*[16,17]

References

1. Guha, S., *Journal of Non-Cryst. Sol.* **77–78**, 1451 (1988).

2. Mackenzie, K.D., Eggert, J.R., Leopold, D.J., Li, Y.M., Lin, S., and Paul, W., *Phys. Rev.* **B31**, 2198 (1985).

3. Sze, S.M., *Physics of Semiconductor Devices* (Wiley Eastern, India 1979).

4. Rhoderick, E.H., *Metal Semiconductor Contacts*, page 46 (Clarendon Press, Oxford 1978).

5. See page 103 of reference 4.

6. We recognize that n_i is an arbitrarily defined quantity for an amorphous semiconductor. No errors will, however, be incurred by the indefiniteness of its value as long as it is consistently used.

7. Cohen, J.D. and Lang, D.V., *Phys. Rev.* **B25**, 5321 (1982).

8. Roberts, G.I. and Crowell, C.R., *J. App. Phys.* **41**, 1767 (1970).

9. Snell, A.J., Mackenzie, K.D., LeComber, P.G., and Spear, W.E., *Phil Mag.* **B40**, 1 (1979).

10. Abram, R.A. and Doherty, P.J., *Phil. Mag.* **B45**, 167 (1982).

11. Beichler, J., Fuhs, W., Mell, H., and Welsch, H.M., *J. Non-Cryst. Sol.* **35–36**, 587 (1980).

12. Snell, A.J., Mackenzie, K.D., LeComber, P.G., and Spear, W.E., *J. Non-Cryst. Sol.* **35–36**, 593 (1980).

13. Tiedje, T., Wronski, C.R., and Cebulka, J.M., *J. Non-Cryst. Sol.* **35–36**, 743 (1980).

14. Viktorovitch, P. and Jousse, D., *J. Non-Cryst. Sol.* **35–36**, 569 (1980).

15. Mackenzie, K.D., Burnett, J.H., Eggert, J.R., Li, Y.M., and Paul, W., *Phys. Rev.* **B38**, 6120 (1988).

16. Matsuura, H. and Okushi, H., *J. App. Phys.* **62**, 2871 (1987).

17. Matsuura, H. and Tanaka, K. (1988), M.R.S. Symposium Proceedings, Volume 118 (editors A. Madan, M.J. Thompson, P.C. Taylor, P.G. LeComber and Y. Hamakawa) page 647.

Figure Captions

FIG. 1. A plot of $\log J_F/(1-\exp(-qV/kT))$ *vs.* V and $\log J_R/(1-\exp qV_r/2kT)$ *vs.* V_r at two different temperatures.

FIG. 2. A plot of $\log J_F$ *vs.* $10^3/T$.

FIG. 3. A plot of $\log(J_R/(1-\exp(-qV_r/2kT)))$ *vs.* $10^3/T$ for different values of V_r.

FIG. 4. A plot of measured and corrected capacitance as a function of frequency at 300°K.

FIG. 5. A plot of measured and corrected capacitance *vs.* reverse bias.

FIG. 6. Band structure levels *versus* distance from the junction, illustrating the distance x_e at which E_t (the deepest level responding at frequency w) intersects the Fermi level.

FIG. 7. A plot of $1/C^2$ *vs.* V at room temperature at 8 Hz.

FIG. 8. Temperature dependence of capacitance at zero bias and at $1V$ reverse bias for $f = 8$ Hz.

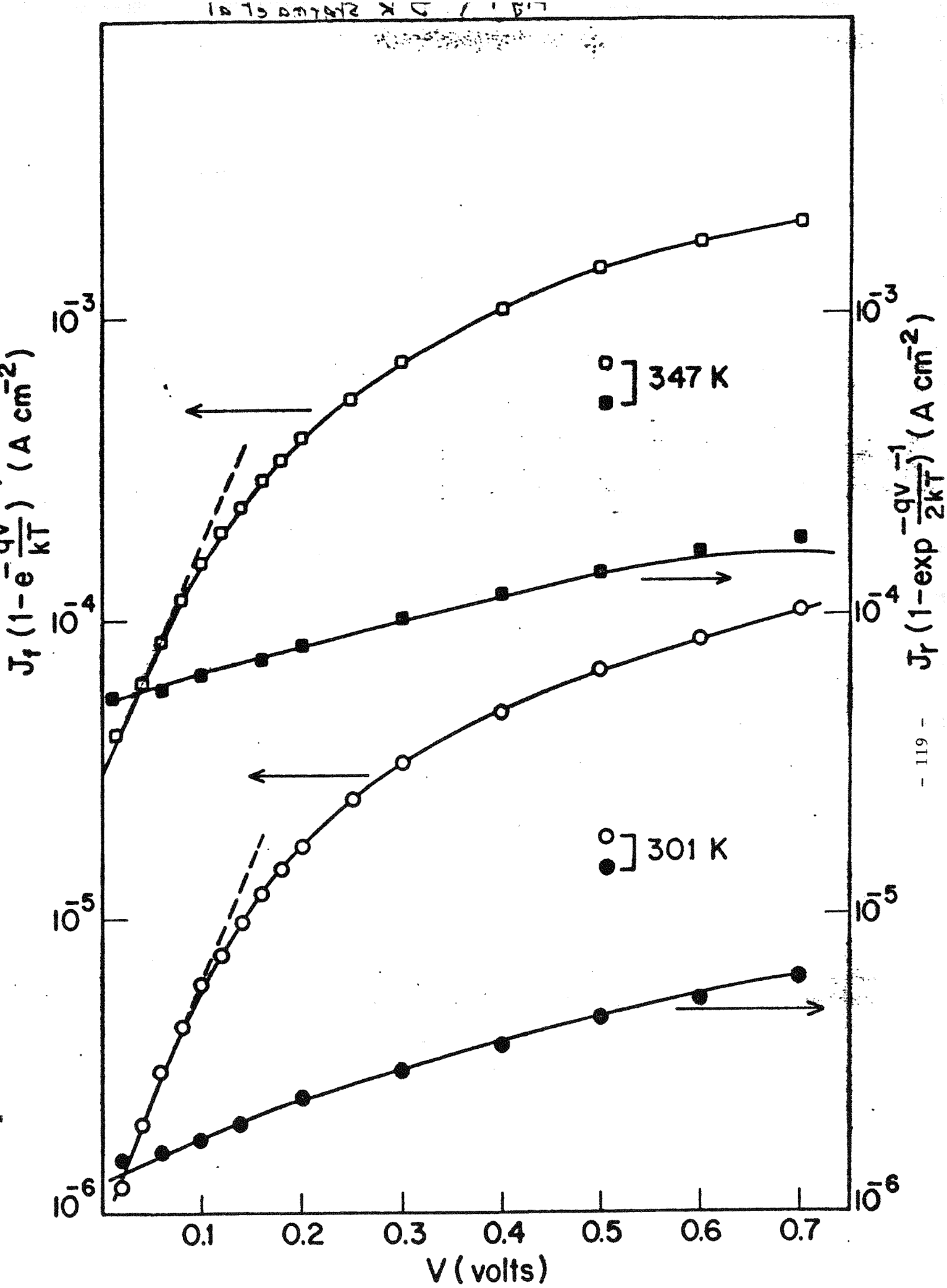
$J_f\,(1-e^{-\frac{qV}{kT}})^{-1}$ (A cm^{-2})
$J_r\,(1-\exp\frac{-qV}{2kT})^{-1}$ (A cm^{-2})
10^{-3}
10^{-4}
10^{-5}
10^{-6}
347 K
301 K
0.1
0.2
0.3
0.4
0.5
0.6
0.7
V (volts)

10^{-4}
10^{-5}
10^{-6}
J_{FO} (A cm^{-2})
ΔE .67 eV
2.8
3.0
3.2
3.4
$10^3/T$ (K^{-1})

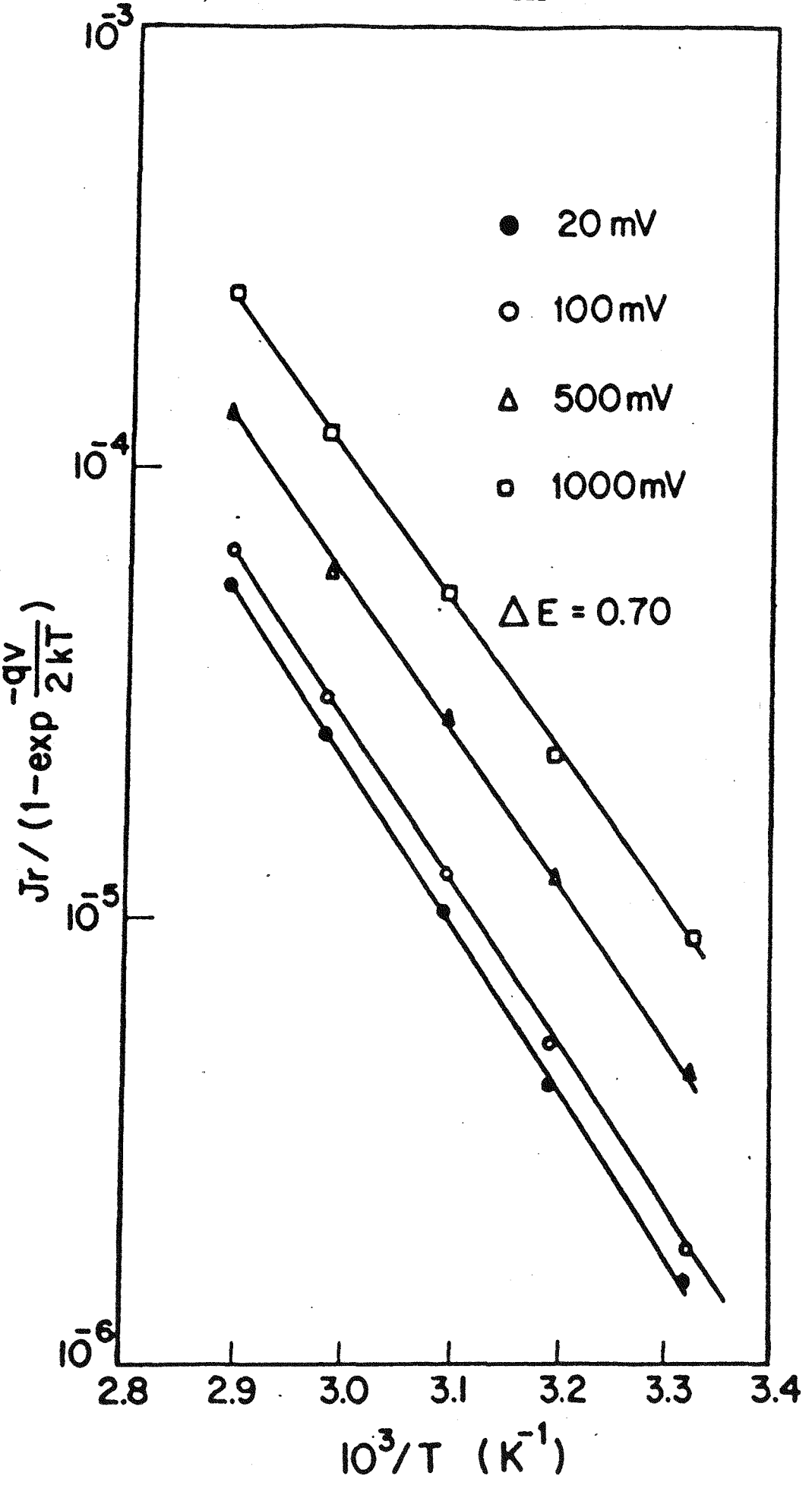
20 mV
100 mV
500 mV
1000 mV
ΔE = 0.70
Jr / (1-exp -qV/2kT)
10^-3
10^-4
10^-5
10^-6
2.8
2.9
3.0
3.1
3.2
3.3
3.4
10^3/T (K^-1)

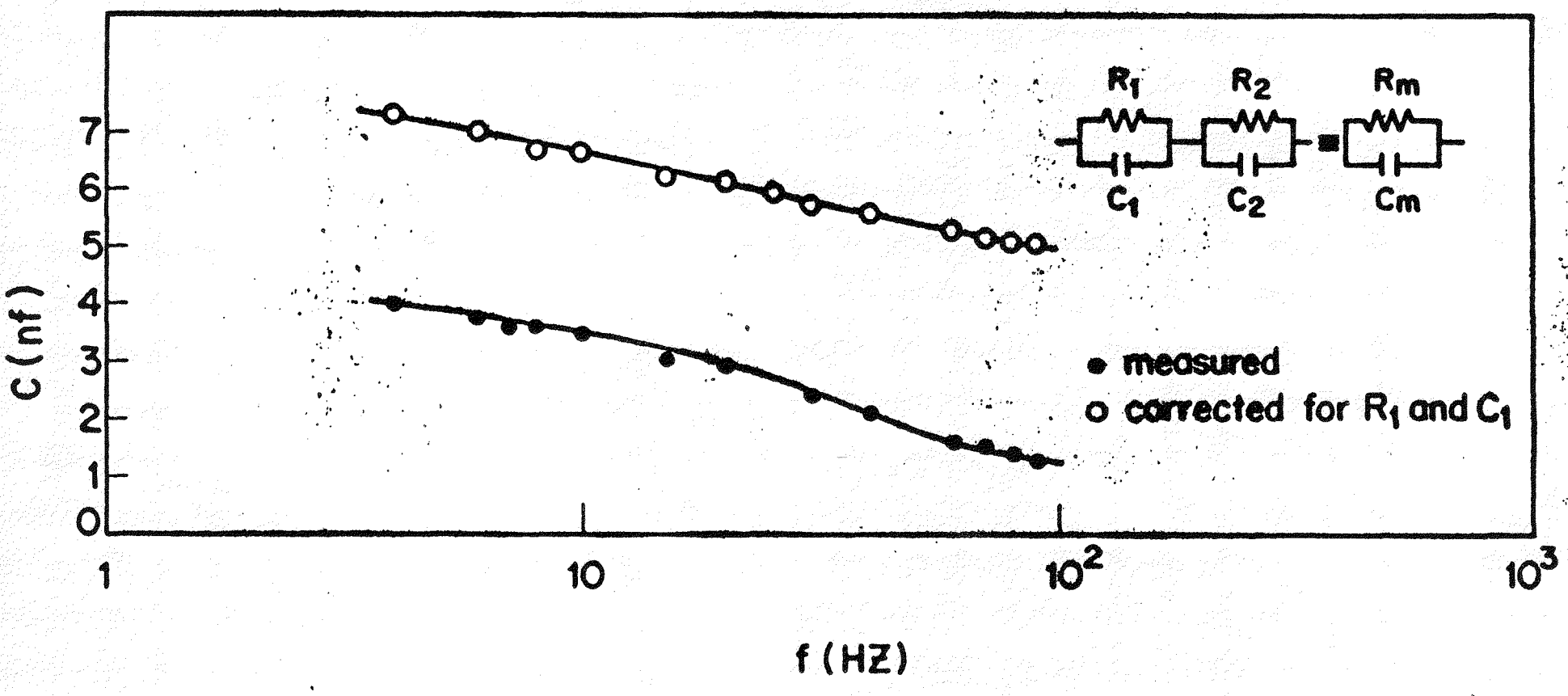
C (nf)
0
1
2
3
4
5
6
7
1
10
10^2
10^3
f (HZ)
R_1
R_2
R_m
C_1
C_2
C_m
• measured
o corrected for R_1 and C_1

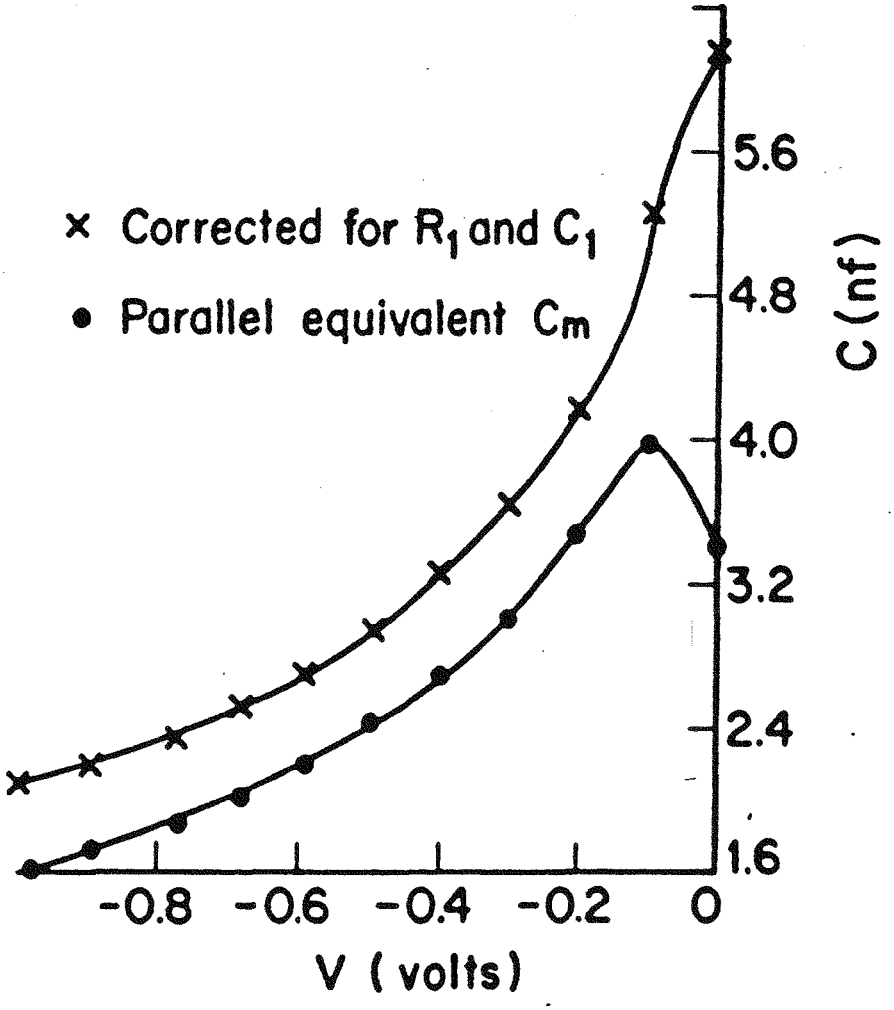
× Corrected for R_1 and C_1
• Parallel equivalent C_m
5.6
4.8
4.0
3.2
2.4
1.6
C (nf)
-0.8
-0.6
-0.4
-0.2
0
V (volts)

D K sharma et al Fig 6.7

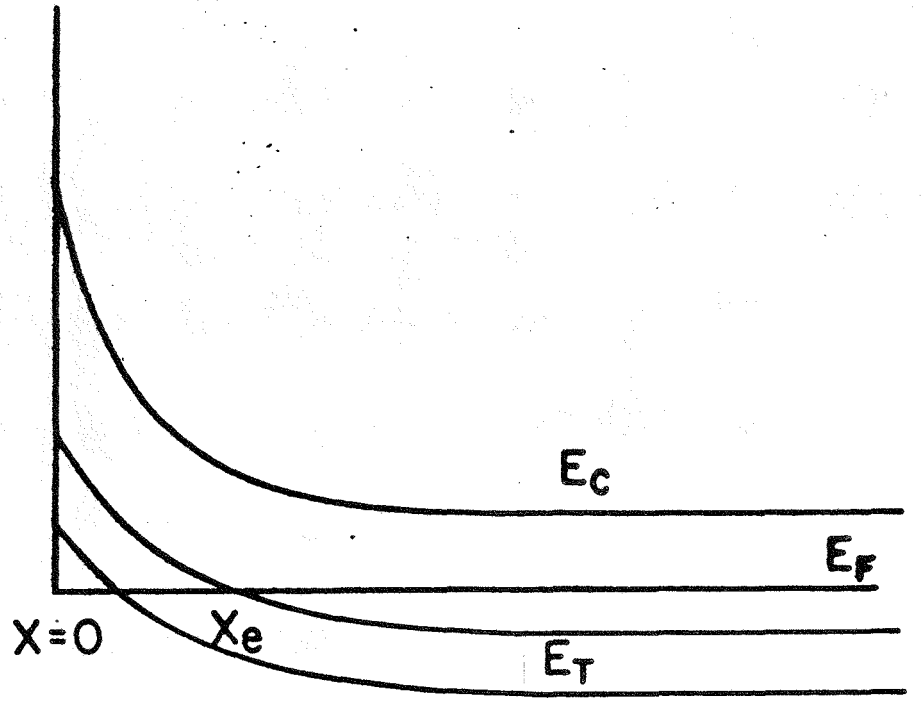

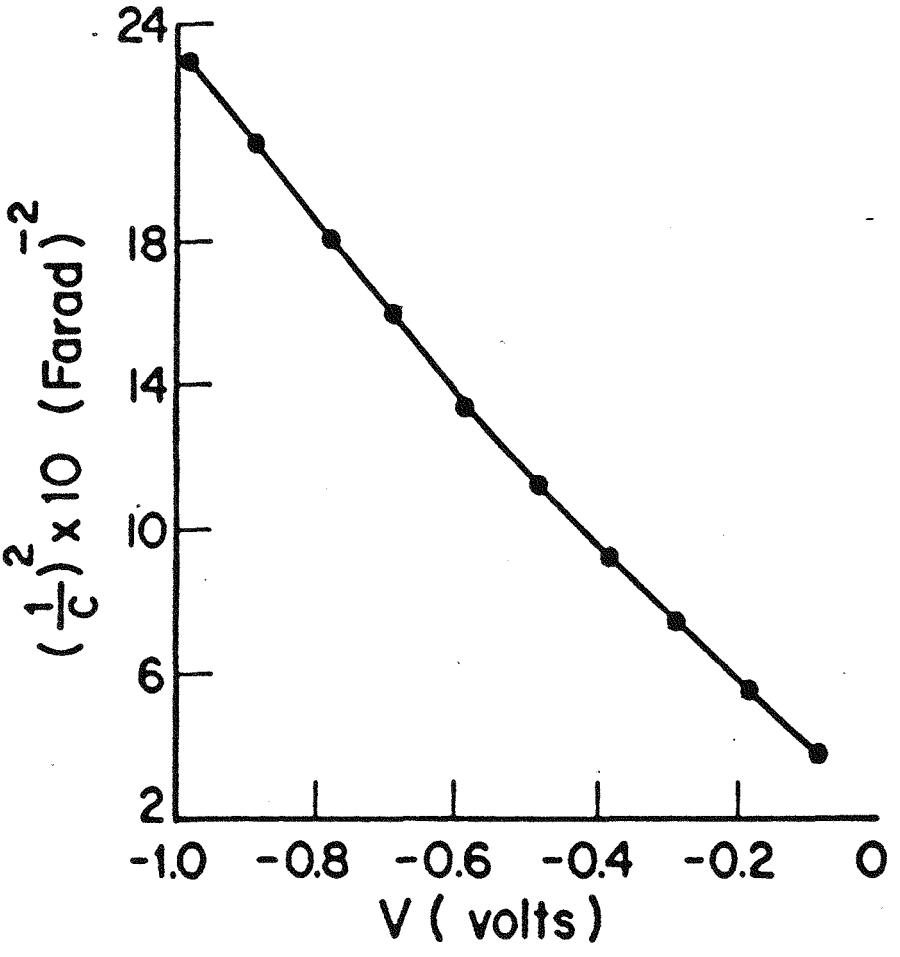

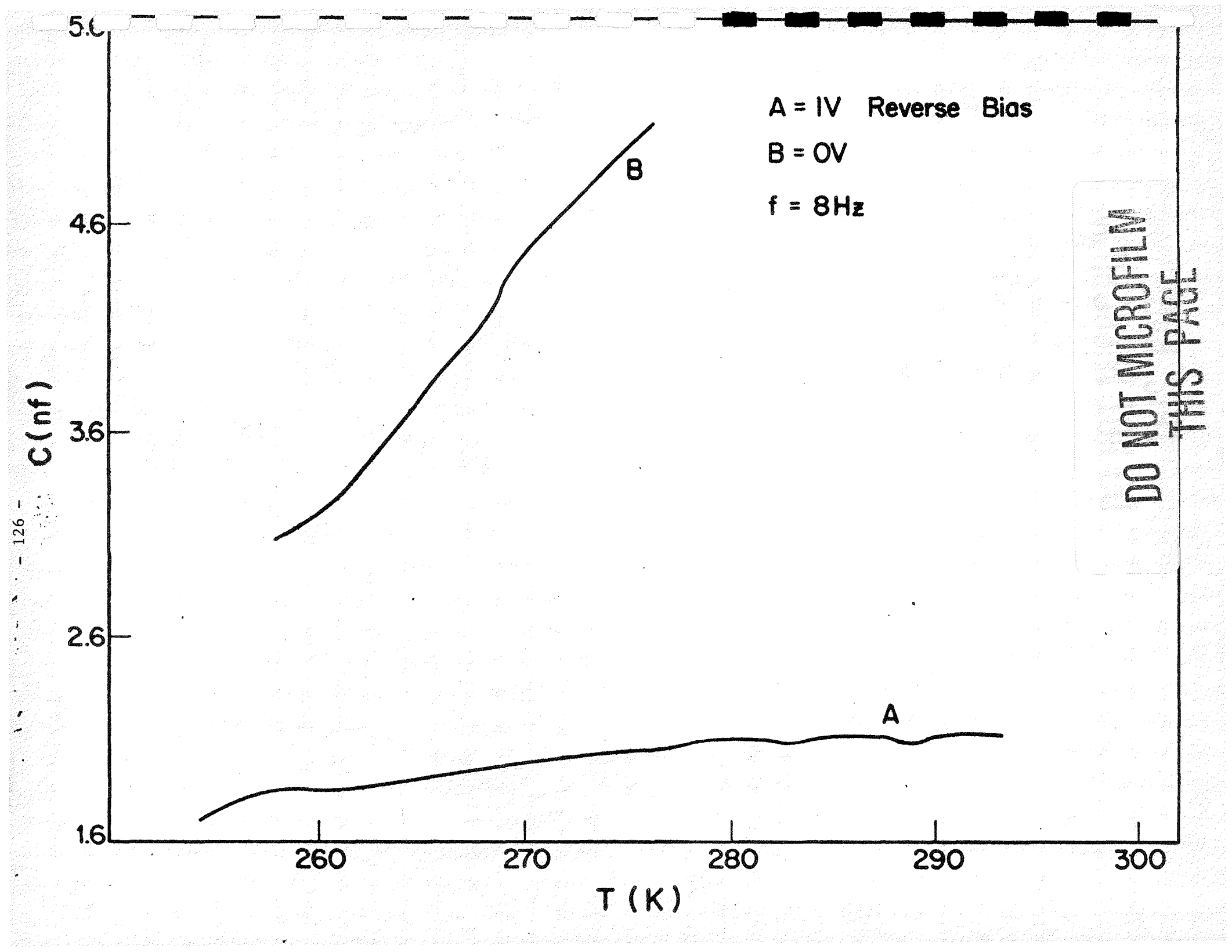

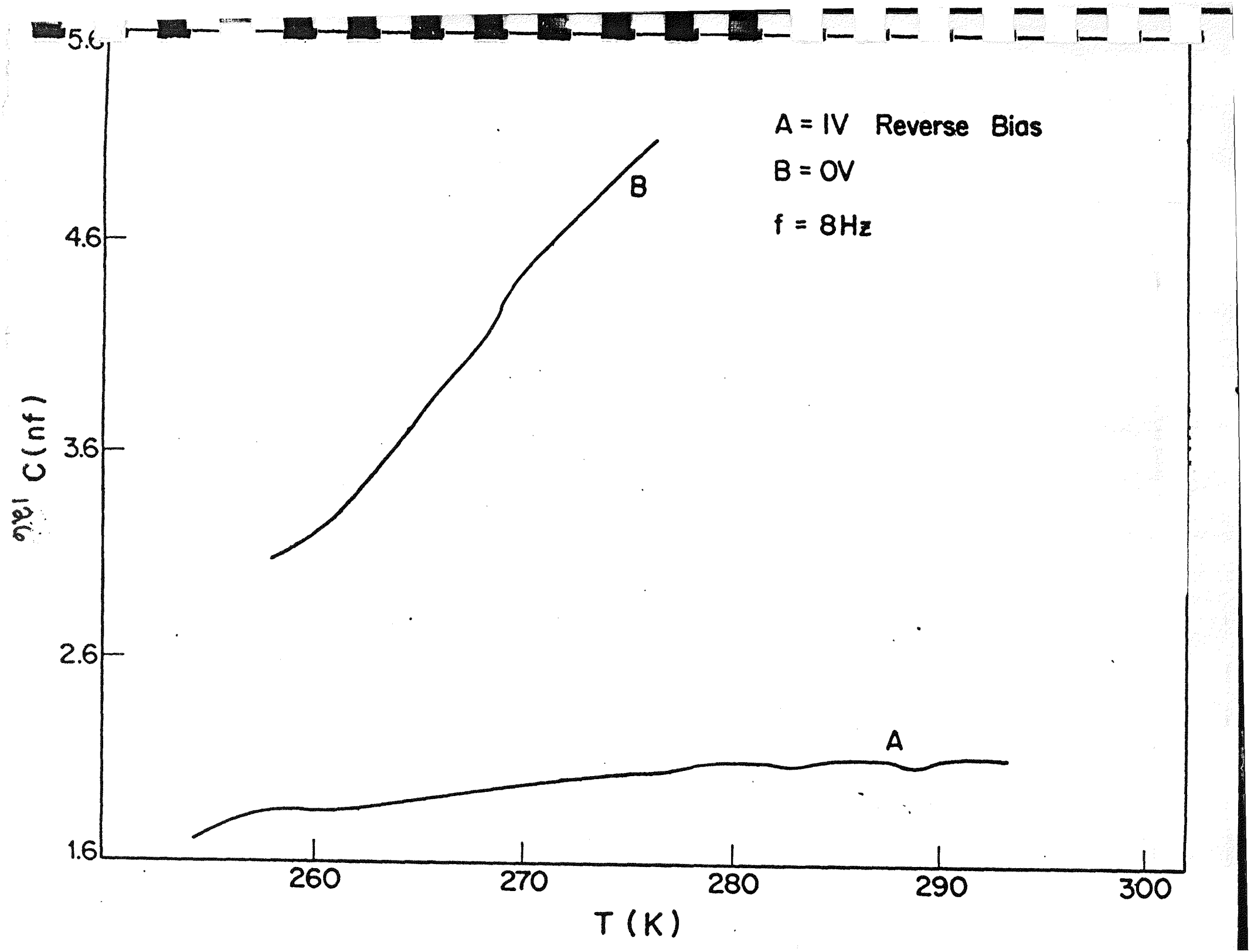
A = IV Reverse Bias
B = 0V
f = 8Hz
B
A
5.6
4.6
3.6
2.6
1.6
C(nf)
260
270
280
290
300
T (K)

APPENDIX C

Comparison of the structural properties of a-Si:H prepared from SiH_4 and $SiH_4 + H_2$ plasmas, and correlation of the structure with the photoelectronic properties

Susanne M. Lee, Scott J. Jones, Yuan-Min Li,
Warren A. Turner and William Paul

Gordon McKay Laboratory, Harvard University, Cambridge, MA 02138 USA

ABSTRACT

The addition of hydrogen gas to silane gas during the deposition of high quality a-Si:H has frequently been reported to improve the optical and electronic responses of the material (Tanaka and Matsuda 1987; Vanier, Kampas, Corderman and Rajeswaran 1984). For our preparations of device-quality a-Si:H(:D) in an r.f. glow-discharge reactor from SiH_4, $SiH_4 + H_2$, and $SiH_4 + D_2$, we find no significant differences between the optical and electronic properties of the as-deposited materials. However, structural examinations by gas evolution and high resolution transmission electron microscopy (HRTEM) reveal marked dissimilarities, the gas evolution being an especially discriminating tool. Moreover, annealing at several temperatures, followed by a full complement of optical, electronic, and HRTEM measurements, demonstrates differences in the optoelectronic properties that can be reasonably correlated with the structural differences.

APPENDIX D

Abstract Submitted
for the New Orleans Meeting of the
American Physical Society
21-25 March 1988

Sorting Category: 23(e)

Rotating Silyl Groups in a-Si:D,H Films.* P. SANTOS, Fh.**, M. P. VOLZ,*** and R. E. NORBERG, Washington U. -- 30 MHz deuteron magnetic resonance (DMR) measurements show a 22 kHz quadrupolar doublet component in some a-Si:D,H films. The doublet is detected between room temperature and 20 K and arises from rotating silyl SiD_xH_{3-x} groups which typically comprise a ≤ 1 at.% deuteron fraction. The 22 kHz doublet emerges from the broad central DMR component as the pulse repetition rate is increased and the longer T_1 components are saturated out. Persistence of the silyl doublet signal to 20 K and below makes it unlikely that the motion reflects a hindered rotation within the Si matrix. The rotors either occur at microvoid surfaces or at interfaces between microcrystals[1] in a non-amorphous component.

*Supported in part by SERI under Subcontract No. XB-7-06055-1 of Contract DE-AC02-83CH10093 with the Department of Energy.
**Lillian Sirovich Predoctoral Fellow/CNPq Brazilian Research Funding Agency.
***Xerox Corporation Predoctoral Fellow.

[1]S. Kaplan, private communication.

R. E. Norberg
Department of Physics
Washington University
St. Louis, Missouri 63130

APPENDIX E

Investigation of surface-related optical absorption in a-Si : H by photothermal deflection spectroscopy

M.L. Thèye, L. Chahed, U. Coscia[x], C. Boccara[+], D. Fournier[+], Y-M. Li* and W. Paul*

Laboratoire d'Optique des Solides, UA CNRS 781, Université Pierre et Marie Curie, 4 place Jussieu, 75252 Paris Cedex 05, France.

[+]Laboratoire d'Optique Physique, Ecole Supérieure de Physique et Chimie, 10 rue Vauquelin, 75005 Paris, France.

*Division of Applied Sciences, Harvard University, Cambridge, MA 02138, USA.

Surface and/or interface contribution to the optical absorption spectra in the absorption edge region of well-characterized undoped and heavily P-doped r.f. glow-discharge a-Si : H films has been investigated in detail by photothermal deflection spectroscopy. Low-frequency experiments performed on identically-prepared films with different thicknesses d ranging from 0.6 to 7.5 μm have shown that the low-energy absorption decreases with increasing film thickness and saturates for $d \gtrsim 3$ μm. On the other hand, high-frequency experiments performed on the thickest samples in different spectral ranges with front and rear surface excitation, have suggested that the main contribution comes from the free surface of the samples. This interpretation has been checked by measurements performed after chemical etching of the film surface.

[x]Permanent address : Laboratory ENEA-FARE/FOTO, Via Vecchio Macello, 80055 Portici, Italy.

Comparison of defect-induced optical absorption in a-Si : H derived from photothermal deflection spectroscopy and photoconductivity.

M.L. Thèye, L. Chahed, Y.M. Li*,
K.D. Mackenzie* and W. Paul*

Laboratoire d'Optique des Solides, UA CNRS 781, Université Pierre et Marie Curie, 4 place Jussieu, 75252 Paris Cedex 05, France.

*Division of Applied Sciences, Harvard University, Cambridge, MA 02138, USA.

The optical absorption spectra of well-characterized r.f. glow-discharge a-Si : H films in the 2.0 to 0.6 eV spectral range have been carefully determined by photothermal deflection spectroscopy (PDS) and photoconductivity (PC) (both by the constant photon flux and constant photocurrent methods), and normalized to optical transmission data at high energies. Care has been taken of surface/interface effects and Staebler-Wronski effects in either case. The PDS and PC - derived optical absorption spectra agree very well in the Urbach edge region, but discrepancies which depend significantly on the type of sample (undoped, P - or B - doped, compensated) are observed at lower energies. These discrepancies are discussed in relation with the defect state density, taking into account the different mechanisms involved in PDS and PC experiments.